Investigations on the transfer of lipophilic drug models from lipid nanoparticles to lipophilic acceptor compartments using different techniques

Dissertation
zur Erlangung des akademischen Grades doctor rerum naturalium
(Dr. rer. nat.)

vorgelegt dem Rat der Biologisch-Pharmazeutischen Fakultät
der Friedrich-Schiller-Universität Jena

von Mohamed Dawoud
geboren am 18.02.1976 in Kairo, Ägypten

Gutachter:

1. Prof. Dr. Alfred Fahr: Chair of Pharmaceutics, Friedrich-Schiller-Universität Jena

2. Prof. Dr. Heike Bunjes: Technische Universität Braunschweig, Institut für Pharmazeutische Technologie

3. Prof. Dr. Thomas Rades: Chair in Pharmaceutical Sciences New Zealand's National School of Pharmacy University of Otago

Tag der öffentlichen Verteidigung: 19.01.2011

Acknowledgements

This work was created under the supervision of Prof. Dr. Heike Bunjes and Prof. Dr. Alfred Fahr at the Department of Pharmaceutical Technology, Friedrich-Schiller-Universität Jena.

I would like to express my sincere gratitude to Prof. Dr. Heike Bunjes, for her valuable scientific guidance, constant support and great help during the course of this study. I would like to thank her for offering me the opportunity to do research in this exciting field and for the knowledge acquired from her.

I refer my appreciation to Prof. Dr. Alfred Fahr for the opportunity to work at the Department of Pharmaceutical Technology, Friedrich-Schiller-Universität Jena after the transition of Prof. Dr. Heike Bunjes. I would like to express my deepest thanks to him for the constructive criticism, constant help and supervision.

I would like to thank the Egyptian government fir the financial support during the four years of my work.

My special thanks to my friends and colleagues at the department for their encouragement. I appreciated the help of Dr. Judith Kuntsche at the beginning of this work. I am grateful to all technical and scientific staff of the department who guided my first steps in my work. I would like to thank Dr. Guenther for assistance with the NMR measurements and for his advices.

Last but not least, I give my deepest gratitude to my family especially my wife for her continuous support and encouragement. I express my warm thanks to my parents for their encouragement

Table of contents

Chapter 1: Aim of the work

Parenteral and oral administration of lipophilic drugs is often problematic because of their intrinsic low water solubility. Among other colloidal drug delivery systems, lipid nanoparticle carrier systems are of interest for intravenous drug delivery. These drug delivery systems are often derived from physiological structures and have compositions similar to their physiological counterparts; therefore, physiological acceptance is expected for many of these types of carriers. Physiological lipids are expected to be metabolized rapidly, resulting exclusively in non-toxic breakdown products. Due to the production by high-pressure homogenization lipid nanoparticles can be produced on large industrial scale. These advantages make lipid nanoparticles as one of the most interesting colloidal carrier systems.
In order to rationally design colloidal carrier drug delivery systems and to obtain information on their potential in-vivo performance, it is necessary to fully characterize their drug retention and release properties. For that purpose, a simple and effective in-vitro assay is required. Several methods have been used to measure the drug release from colloidal carrier systems. Many common release methods appear to be of limited suitability to draw conclusions to the in-vivo performance of colloidal carriers. This is due to the binding of some drug to the filter material and the use of aqueous release media like ordinary buffer solutions. Also methodological problems like the blockage of the applied filter by the colloidal particles can be a problem. In order to approach in-vivo conditions, the buffered media are sometimes supplemented for example with albumin [1-2]. Nevertheless, these conditions are not representative for the situation in the bloodstream, which would, however, be highly desirable. Furthermore, the low aqueous solubility of many of the drugs of interest complicates their analysis in aqueous media.

The aim of this study was focused on overcoming these problems and finding more realistic release conditions with special attention to intravenous administration. To approach this, the transfer from lipid nanoparticles into lipophilic acceptor compartments was measured by different techniques. The lipophilic acceptor compartments are intended to mimic lipophilic compounds present in the blood, e.g. lipoproteins or cellular structures and thereby present a compartment in which the released lipophilic substance is soluble. Determination of the factors, which affect the drug transfer from the lipid nanoparticles into the different lipophilic acceptors, was an important goal of the study. Another important aim of the study was the comparison between the different techniques, which were used to measure the transfer from lipid nanoparticles into lipophilic acceptor compartments, to find the most suitable one for evaluating the drug release behaviour of such lipid nanoparticles and to determine the limitations of each technique.

Three techniques were employed to study the drug transfer from lipid nanoparticle carrier systems to lipophilic acceptor particles with different particle sizes and compositions. Factors affecting the drug transfer from these carrier systems, such as composition and particle size of the acceptor particles as well as drug lipophilicity were studied using these techniques.

The first technique was based on the use of ion exchange columns which was described in detail by Fahr and co-workers [3]. The transfer kinetics of three drug models with different degrees of lipophilicity, porphyrin, Nile red and DiI was investigated in this study. Under the selected conditions, these three drug models are transferred from negatively charged donor lipid nanoparticles to different lipophilic neutral acceptor nanoparticles. Three different lipophilic acceptor particles were used. The first type of acceptor consisted of unilamellar vesicles [4], the second one of a Miglyol nanoemulsion and the third type of acceptor particles were monoolein dispersions in the form of vesicles or cubic particles. This technique depends on the use of charged donor particles, which can be retained by the ion exchange column.

The second technique was based on centrifugation where the transfer kinetics of the same three drug models were investigated. The transfer of these drug models was measured from various lipid nanoparticles to three different lipophilic acceptors, multilamellar vesicles (MLV), o/w emulsion and cubic particles. Separation of both populations (donor and acceptor) was done by centrifugation. This technique using MLV was first presented by Shabbits and co-workers [5].

The third technique used flow cytometry to detect the drug transferred into the acceptor particles. The transfer kinetics from different donor lipid nanoparticle carrier systems into lipophilic acceptor compartments was measured. Three different types of acceptor compartments in the micrometer size range were compared using this technique, MLV, o/w emulsion and monoolein cubic particles. Only the large acceptor particles can be detected by the flow cytometer (not the small donor nanoparticles) thus no critical separation step has to be included and the transfer mixture can be analyzed in situ after dilution. The use of flow cytometry to measure drug transfer process was described recently [6].

Chapter 2: Background

2.1 Colloidal drug carrier systems

In recent years it has been noticed that the development of new drugs alone is not enough to ensure progress in drug therapy due to the therapeutic failure that was observed with these new drugs. To overcome this problem, it was important to develop suitable drug delivery systems or drug carrier systems [7]. Drug delivery systems have an important role in pharmaceutical sciences because they affect drug transport, absorption, distribution and elimination. These drug delivery systems should show many characteristics to be accepted as beneficial carrier systems. One of the most important characteristics of these systems is to deliver difficult drugs such as lipophiles to the site of action (drug targeting) with a controlled release manner. Other properties such as ease of production, ease of administration and the physiological safety are also required with the different systems [7].

Lipophiles are poorly water-soluble molecules, which have a lot of important roles in different biological processes. Many drugs are lipophilic such as anticancer drugs [8], antifungal agents [9] and antioxidants [10-11]. Most scientists prefer parenteral delivery for the targeting of lipophilic drugs [12] but this requires the use of small particle sizes because the smallest capillary is approximately 5 μm in diameter so parenteral delivery systems must be colloidal in nature.

O/w emulsions were the first commercial colloidal delivery carriers of lipophilic drugs. This colloidal carrier exhibits several disadvantages, which are related to the oil and to the properties of the emulsion as a carrier system [7, 13]. Oils that can be used medically show low solubility for most drugs. In addition to this problem emulsions exhibit drug burst release phenomena due to their liquid state. Due to these limitations or disadvantages, it was important to develop other colloidal carrier systems to overcome the disadvantages that were encountered with the emulsion system. Colloidal carriers such as liposomes, cubic particles and lipid nanoparticles have attracted increasing attention during recent years [7, 13].

2.1.1 Liposomes

Liposomes are spherical vesicles, which consist of one or more phospholipid bilayers. Lipophilic drugs can be entrapped in the vesicle bilayer or partition between the bilayer and the aqueous phase while hydrophilic drugs are entrapped in the inner aqueous core [14]. A wide variation of lipids can be used to prepare vesicles. Phospholipids, which are the main component of biological membranes, have a high tendency to aggregate and to form vesicles. Phosphatidylcholine (PC) has been used as the major component for the preparation of liposomes [14]. The properties of liposomes such as rigidity and permeability of the bilayer depend on the type and quality of PC and other bilayer lipids used. Cholesterol

is highly used in the preparation of liposomes and increases the rigidity of the bilayer. Due to the molecular shape and solubility properties of cholesterol, it fills in empty spaces among the phospholipid molecules, thereby increasing the strength of the bilayer. Liposomes are classified as large multilamellar vesicles (MLV, > 0.5 μm), large unilamellar vesicles (LUV, > 100 nm), small unilamellar vesicles (SUV, 20-100 nm), oligolamellar vesicles (OLV, 0.1-1 μm) and multivesicular vesicles (MVV, > 1 μm). This classification depends on size, the number of bilayers and the existence of inner vesicles in a vesicle [14-15].

Liposomes as drug carriers can be used for the intravenous administration of different lipophilic drugs. Liposomes show a high physiological acceptance due to the use of biological phospholipids in their preparation. Liposomes have been used as model membranes and as carriers of drugs, DNA and enzymes. Despite of their high physiological safety, there are many disadvantages of using liposomes as colloidal carriers such as the chemical and physical stability problems which may cause their aggregation during storage [14]. In addition to these chemical and physical problems the production costs of liposomes are very high in comparison with other colloidal systems.

2.1.2 Cubic particles

Another important colloidal drug delivery system is particles with cubic internal structure. Monoolein water mixtures form different lyotropic liquid crystalline structures in dependence on concentration and temperature [16]. In the presence of excess water, a bicontinuous cubic phase is formed at room and body temperature. It consists of a pair of interpenetrating but non-contacting water channels separated by a single, highly curved continuous lipid bilayer. This bilayer structure extends in three dimensions with a high specific bilayer/water interfacial area [17] as illustrated in figure 2.1 [18-19]. Due to its unique structure the cubic phase can host lipophilic as well as amphiphilic and hydrophilic substances and has thus often been used to incorporate and slowly release different types of drugs, e.g acyclovir and somatostatin [20-21]. Furthermore, the cubic phase was used for determining the lipid bilayer/water partition coefficient of drug compounds [17]. In addition to the above studies, colloidal dispersions of cubic particles named cubosomes [22-23] were used to study the release of somatostatin, insulin and cyclosporin [24]. As the bicontinuous cubic phase is stable in excess water, dispersions of cubic particles (often called “cubosomes”) can be prepared. They are typically made by applying high shear (e.g., using high pressure homogenization or sonication) to disrupt a coarse dispersion of the very viscous cubic phase into small, often submicron-sized particles in the presence of surfactants like poloxamer [16, 25]. However, high pressure homogenization and sonication result not only in the desirable size reduction of cubic phase particles but also in the formation of vesicles. Heat treatment of the homogenized dispersions results in improved properties of

cubic phase dispersions such as more uniform size distributions due to the transformation of vesicles into cubic particles.

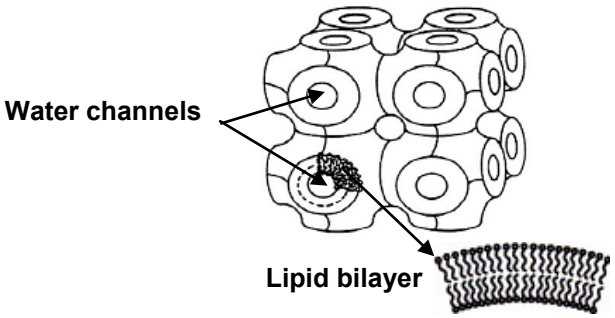

Figure 2.1: Schematic representation of the bicontinuous cubic phase illustrating the non-contacting water channels separated by a continuous lipid bilayer (adapted from [18-19]).

2.1.3 Lipid nanoparticles

The first lipid nanoparticles used in the pharmaceutical field were the lipid nanoemulsions, which were used for parenteral nutrition. These lipid nanoemulsions are usually composed of about 10-20% fatty vegetable oils or medium chain triglycerides as the lipid phase and usually are stabilized with phospholipids. In addition to the use of lipid nanoemulsions for parenteral nutrition, it has been observed that these lipid nanoparticles might also be used as carrier vehicles for many lipophilic drugs [26-31]. Toxicological safety and the possibility of large-scale production by high-pressure homogenization [32-34] are advantages of lipid nanoparticles. The toxicological safety of these nanoparticles was related to the use of lipids, which have a high physiological acceptance [35-36]. A major drawback of the lipid nanoemulsions is the difficulty to obtain controlled drug release due to the small size and the liquid state of the carrier. For most drugs, a rapid release of the drug will be observed [2, 37-38]. To overcome this major problem, solid lipids instead of liquid oils were used to obtain controlled drug release, because drug movement in a solid lipid should be less than in liquid oil. The same advantages of the lipid nanoemulsion were also observed with the solid lipid nanoparticles in addition to the controlled release, which was expected from the solid state of the lipid [39-40]. The controlled drug release expected with the solid lipid nanoparticles is due to the solid nature of the lipid and to keep this important advantage upon administration the melting point of the lipid must exceed body temperature [7]. Lipids of different melting point were employed in the preparation of solid lipid nanoparticles such as triglycerides, fatty acids and waxes. Different surfactants were used, especially phospholipids, which were often used in this field but it was reported that the use of phospholipids as the only surfactant is accompanied by instability and gel formation after solidification of the lipid [39, 41]. To overcome this problem a co-emulsifier (ionic co-emulsifier, e.g. glycocholate or non-ionic surfactant, e.g. tyloxapol) should be used. Westesen and co-workers observed the presence of spherical small particles in the solid lipid

nanoparticles stabilized with excess phospholipids. These spherical small particles were identified as small unilamellar vesicles from the excess phospholipid emulsifier used [39].

2.1.3.1 Preparation of lipid nanoparticles

Many methods were used for the preparation of lipid nanoparticles. Most of these methods rely on two steps for the preparation of lipid nanoparticles. The first step is the preparation of an o/w nanoemulsion, which is the precursor of the solid lipid nanoparticles [7]. The second step is the solidification of the dispersed lipid phase. In order to prepare solid lipid nanoparticles in the nanometer size range, which is the suitable size for parenteral administration, with an acceptable size distribution of the particles (polydispersity), it is important to subject the precursor emulsions to high mechanical forces such as, high pressure homogenization (HPH). Two types of HPH were developed [7]. The first type is the hot HPH, which works at a temperature above the lipid melting point. After the high temperature homogenization, the nanoemulsion must be cooled to a certain temperature to ensure the solidification of the lipid nanoemulsion droplets. This temperature of solidification of the lipid nanoemulsion droplets differs from the recrystallization temperature of the bulk lipid material due to the colloidal size of the lipid nanoemulsion droplets [36, 42] and should therefore be determined carefully. Major drawbacks of the hot HPH are the degradation of thermo labile drugs and the partitioning of the drug into the aqueous phase, which may be related to the increase of drug hydrophilicity with increasing temperature. To avoid these drawbacks of the hot HPH, the second type of HPH, which is the cold HPH technique, was developed. This technique generally produces larger particle sizes and broader particle size distributions. It was reported that high homogenization temperatures produce smaller particle sizes due to the decreased dispersed phase viscosity [43]. Although cold HPH avoids the partitioning of the drug into the aqueous phase, the stability problems and drug degradation were still present due to the high mechanical forces applied during the preparation of the nanoparticles. Another drawback of both types of the HPH is the reduction of the molecular weights of polymers and the degradation of DNA and albumin [43].

2.2 Drug release from colloidal carrier systems

In order to assess colloidal carrier systems such as lipid nanoparticles, it is necessary to fully characterize their drug retention and release properties. For this purpose, it is important to find a simple and effective in-vitro assay to evaluate the drug release behaviour of such particles and to obtain information on their potential in-vivo performance. Many methods have been described to investigate the in vitro drug release of colloidal drug delivery systems.

2.2.1 Sample and separate method

This method depends on the filtration or centrifugation to separate the particles from the release media at different time points followed by drug determination in the release medium [2, 44-47]. Common problems that were observed with this method are the blockage of the filters by the colloidal particles, binding of drugs to the filter material and instabilities of the investigated colloidal systems due to the application of energy during the filtration or centrifugation step [48]. In addition, the high centrifugal force, which is required to separate the small colloidal particles (less than 300 nm) from the release media, will often lead to an increase in the drug release rate [49].

2.2.2 Dialysis based assay

This method is one of the most commonly used methods and it depends on dialyzing the colloidal particles against large volumes of buffer. The excess buffer serves as a sink as an approach to mimic the conditions in the blood and this sink condition increases the drug release from the colloidal particles. After drug release from the colloidal carrier, free drug crosses the dialysis membrane and accumulates in the buffer system. In some cases the dialysis buffer systems were supplied with serum to more closely mimic the physiological environment, which the colloidal carriers encounter in-vivo. Different factors can affect this dialysis assay such as the size of the membrane surface area as well as the presence or absence of different additives in the dialysis buffer medium [50-52]. The main disadvantage of this assay is the absence of a real sink condition since the encapsulated drug will be in equilibrium with the drug in the continuous phase thus the partition coefficient not the release rate is often measured [52-53]. In spite of this disadvantage the dialysis assay has been reported to be successfully used for studying the shelf life of liposomes and drug systems with respect to drug retention [54].

2.2.3 Continuous-flow method

This method depends on the continuous circulation of the colloidal carrier particles with the release buffer medium in special cells. At one end of the cell samples of the release medium are taken and filtered to obtain the free drug while at the other end fresh release buffer medium is introduced into the cell to keep the volume of the buffer constant all over the experiment. The same disadvantages as for the previous two methods are also observed with this method such as the blockage of the filter, which alters the flow rate of the buffer and slows the release medium replacement and thus modifies the release kinetics [48, 52, 55]. All these three methods encounter the same problem because the conditions of measuring the drug release are unlike the conditions in the bloodstream, which would be highly

desirable. Another problem is the insolubility of many interesting lipophilic drugs in the aqueous release medium employed. To overcome the problems encountered with the common methods of measuring the drug release from colloidal carrier systems, other in vitro methods were developed. These methods depend on measuring the drug transfer from the colloidal carrier systems into lipophilic acceptor particles instead of measuring the drug release into an aqueous phase. Some of the most important in vitro methods are summarized in the following paragraphs.

2.2.4 MLV based assay

The MLV method is an in vitro assay which measures the transfer of lipophilic drug molecules from colloidal carrier systems as donor particles to multilamellar vesicles (MLVs) containing 300 mM sucrose, which serve as acceptor particles and are added in excess with regard to the donor nanoparticles. Egg phosphatidyl choline (EPC) and cholesterol were chosen for MLV formulation, since they represent an unsaturated and uncharged bilayer that is similar to many physiological membranes [5]. Following incubation at 37°C, the two particle populations (donor and acceptor) are separated by centrifugation [5]. The amount of drug in the MLV pellet reflects the degree of drug release from the donor to the acceptor liposomes. The MLV-based drug release assay showed a better prediction of *in vivo* drug transfer than the dialysis based assay [5]. A schematic illustration of this method is given in figure 2.2.

2.2.5 Ion-exchange column based assay

The ion-exchange mini-column model is an in vitro system for measuring the transfer of lipophilic drug molecules from colloidal carrier systems to different liposomal formulations, which mimic the membrane binding sites in the body. This assay depends on the use of a negatively or positively charged donor colloidal carrier system. Neutral liposomes (mostly PC-liposomes) are used as acceptor medium at excess in relation to the donor particles to measure the drug release from these donor colloidal carrier systems [56]. After mixing the two populations (donor and acceptor), samples are taken at different time points and passed over an ion exchange column, which allows only the neutral (acceptor) liposomes to be eluted. This model was first presented by Hellings and co-workers [57] and was afterwards modified by van den Besselar and co-workers [58]. The principle of the method is illustrated in figure 2.3.

2.2.6 Flow cytometry assay

In this method, the transfer of fluorescent model substances from lipid nanoparticles into lipophilic acceptor compartments is studied using flow cytometry [6]. The acceptor

droplets are intended to mimic lipophilic compounds as present in the blood. This assay relies on the use of large acceptor particles (> 1 µm) in order to enable the detection of the acceptor particles by flow cytometry [59-61]. O/w emulsion droplets with particle sizes in the micrometer size range were used as acceptor particles to measure the drug transfer from different lipid nanoparticles [6]. The important advantage obtained by this method is the good time resolution, which is often a problem with other techniques [6]. Since only the large acceptor particles are detected by the flow cytometer without significant interference of the small donor lipid nanoparticles, no critical separation step between the donor and acceptor is required and the transfer mixture can be analyzed in situ after dilution. Thus the flow cytometry assay is suitable for the investigation of very rapid drug transfer processes [6]. A drawback of the flow cytometric method is the need for fluorescent substances that can be detected. Moreover, the size of the acceptor particles should be in the µm-range whereas the donor particles size need to be smaller than 500 nm to avoid an interference with the acceptor particles in terms of detection.

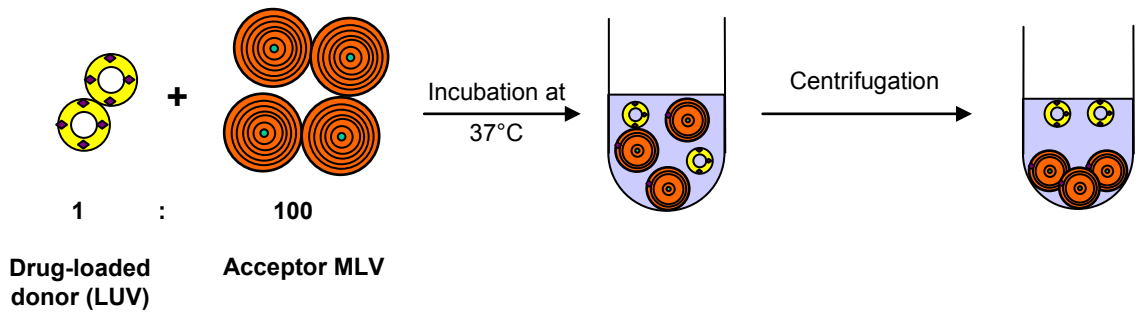

Figure 2.2: Schematic illustration of the centrifugation based in vitro drug release assay procedure using MLV as acceptor particles.

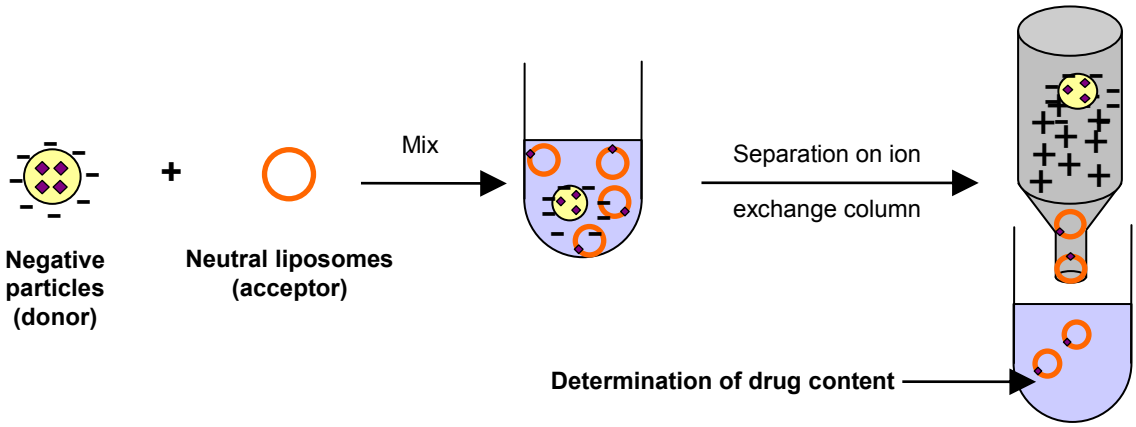

Figure 2.3: Schematic illustration of the in vitro ion exchange column based assay.

Chapter 3: Materials and methods

3.1 Materials

Table 3.1 shows the different materials, which were used in the experiments, and their suppliers.

Table 3.1: Materials used in the experiments and their suppliers

Substance name	Suppliers
Triglycerides trimyristin (D114, Dynasan 114), tristearin (D118, Dynasan 114) and Miglyol 812	Condea Chemie (D-Witten)
Monoolein (GMOrphic-801)	Eastman Chemical Company (Kingsport, TN)
Poloxamer 188 (F68, Lutrol F68) and poloxamer 407 (Lutrol F127)	BASF AG (D-Ludwigshafen)
Polyvinyl alcohol, sodium glycocholate (SGC), cholesterol, Trizma 7.4 pre-set crystals, sucrose, 5,10,15,20-tetrakis (4-hydroxyphenyl)-21H, 23H-porphine, and 1,1-dioctadecyl- 3,3,3,3-tetramethylindocarbocyanine perchlorate (DiI)	Sigma-Aldrich (D-Steinheim)
Partially hydrolyzed poly (vinyl alcohol) (PVA; Mowiol 3-83)	Clariant (D- Frankfurt/Main)
Diethylaminoethyl (DEAE) Sepharose CL-6B	Amersham Biosciences AB (S-Uppsala)
Egg phosphatidyl choline (EPC), Lipoid S75 and Lipoid S75-3	Lipoid GmbH (D- Ludwigshafen)
Nile red	Acros Organics
Glycerol	Solvay GmbH (D-Rheinberg)
Thiomersal	Caesar and Loretz (D-Hilden)
Methanol, tris and scintillation cocktail	Carl Roth GmbH (D-Karlsruhe)
Acetonitrile, ethanol and chloroform	VWR International (D-Darmstadt)
Tetrahydrofurane (THF)	Fisher Scientific (D-Nidderau)
Hepes and sodium chloride	AppliChem GmbH (D-Darmstadt)
sodium azide	Sigma-Aldrich (D-Seelze)
Praseodym (III)-chloride ($PrCl_3$)	Sigma-Aldrich GmbH (D-Schnelldorf)
Purified water was prepared by filtration and deionization/reverse osmosis	Milli-Q, Millipore (Billerica, MA, USA)
^{3}H-cholesteryl oleyl ether	GE Healthcare (Amersham, radiochemical, Buckinghamshire, UK)

3.1.1 Drug models used in the experiments:

Three fluorescent substances, which have different degrees of lipophilicity, were used as drug models in the transfer experiments. These fluorescent drug models were chosen to fit with the flow cytometric transfer experiment, which requires the use of fluorescent substances.

Porphyrin:

Porphyrins are heterocyclic macrocycles derived from four pyrrole-like subunits. A major area where porphyrins are showing significant potential is in the treatment of a wide range of diseases, including cancer, using photodynamic therapy [62]. The model porphyrin that was used in the transfer experiments is 5,10,15,20-tetrakis (4-hydroxyphenyl)-21H, 23H-porphine (porphyrin) (figure 3.1).

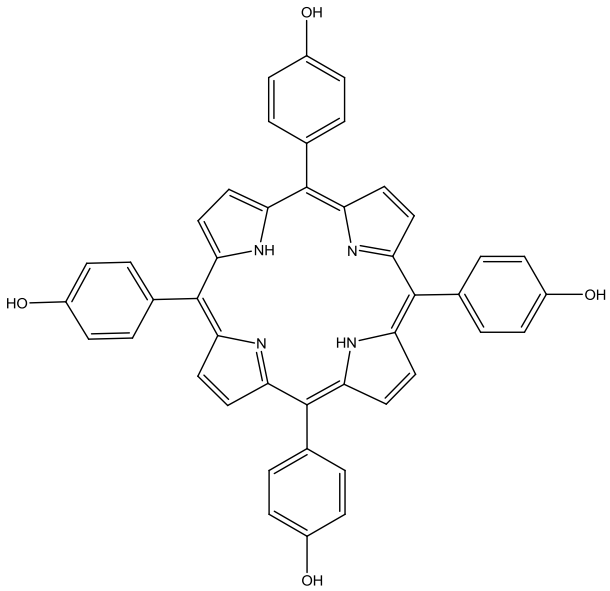

Figure 3.1: 5,10,15,20-tetrakis (4-hydroxyphenyl)-21H, 23H-porphine (porphyrin)

Nile red:

Nile red (figure 3.2) is fluorescent dye, which is more hydrophilic than porphyrin, it has a logP value of about 3.65 [6]. Nile red stains intracellular lipid droplets red and is characterized by a strong yellow-gold emission when in a lipid-rich environment [63]. It excites at 485 nm and emits at 525 nm.

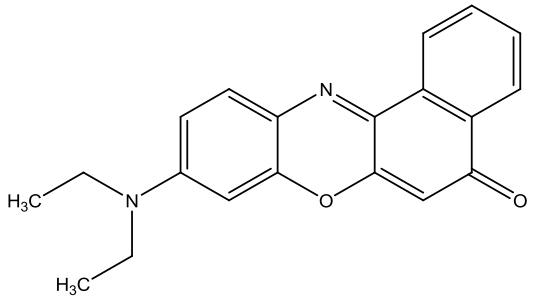

Figure 3.2: Molecular structure of Nile red

DiI:

DiIC$_{18}$(3) (figure 3.3) is a very lipophilic dye, which is employed to analyze membrane structures. Its high lipophilicity was attributed to its two long alkyl chains, which lead to a very high logP value (about 20) [64].

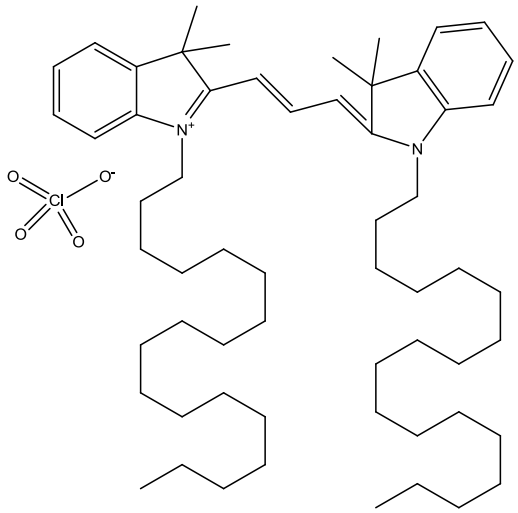

Figure 3.3: Structure of DiI (DiIC$_{18}$(3) 1,1-dioctadecyl- 3,3,3,3 tetramethylindocarbocyanine perchlorate).

3.2 Preparation of the donor particles

3.2.1 Preparation of the trimyristin (D114) nanoparticles

The donor solid lipid nanoparticles (SLN) were prepared by the hot homogenization technique. Four formulations of lipid nanoparticles from trimyristin (D114, 5% w/w) were prepared as described before [65]. The matrix lipid and the aqueous phase containing the surfactant as described in table 3.2 were heated to 70 °C. After melting of the triglyceride, the aqueous phase was poured to the molten lipid and the mixture was pre-homogenized for one minute (Ultra-Turrax T8, IKA Labortechnic, Germany). This crude emulsion was transferred to the 70 °C warm high-pressure homogenizer Microfluidizer M-110S (Microfluidics, US-Newton) and treated for 5 min at 500 bar except for the FS75 formulation, which was homogenized at 600 bar. The dispersions were either stored at room temperature, thereby retaining the liquid state of the trimyristin droplets or the droplets were crystallized into platelet-like particles by storage of the dispersion at refrigerator temperature (2-8 °C) [36]. To separate the solid trimyristin nanoparticles from the excess emulsifier S75, 5 ml samples of the nanosuspensions of FS75/SGClow, FS75/SGChigh and FS75 were subjected to ultracentrifugation (XL-80 ultracentrifuge, rotor type SW55 Ti, Beckman Coulter Inc., US-Fullerton) for 1 hour at 35000 rpm and 15°C.

Table 3.2: Concentration of the different emulsifiers used in the preparation of the four lipid nanoparticle formulations containing 5% trimyristin in an aqueous phase containing 2.25% glycerol and 0.01% thiomersal

Formulation	Percentage of the emulsifier	Preparation of the aqueous phase
FS75/SGClow	1.2% S75 and 0.3% SGC	S75 and SGC were dispersed/dissolved in the aqueous phase by magnetic stirring over night
FS75/SGChigh	1.8% S75 and 0.45% SGC	
FS75	3.2% S75	
Fpoloxamer/DCP	4% poloxamer 188 and 0.3% DCP	Poloxamer was dissolved in the aqueous phase and DCP was melted with the triglyceride

After removing the aqueous supernatant containing the excess emulsifiers the pellet was scraped from the tube bottom, resuspended in 5 ml of aqueous phase and sonicated for 10 minutes at 60°C (followed by filtration through a 0.45 µm membrane filter for FS75/SGClow). The resuspended nanoparticles were stored at room or refrigerator temperature. Loading of porphyrin (0.5 mg/ml) was carried out to the original nanoemulsion (before cooling and crystallization). A stock solution from porphyrin was prepared in methanol (10 mg/ml) and from this stock solution 500 µl was added to 10 ml of the nanoemulsion. Shaking of the samples was done for 2 days at 25°C in a shaking water bath followed by solidification and ultracentrifugation. Loading of Nile red (0.15 mg/ml) was carried out by evaporation of an ethanolic dye stock solution (0.75 mg/ml) in a glass vial leaving behind a thin film of Nile red followed by addition of 5 ml of the nanoemulsion FS75/SGChigh and shaking at 25°C for 2 days followed by solidification. DiI (0.15 mg/ml) was added to the nanoemulsion FS75/SGChigh. A stock solution of DiI was prepared in ethanol (3 mg/ml). 500 µl from this stock solution was added to 10 ml of the nanoemulsion. Shaking of the samples was done for 3 days at 25°C followed by solidification. Small fractions of these nanoparticles were stored at room temperature and the remaining fractions were stored at refrigerator temperature.

3.2.2 Preparation of the tristearin (D118) nanoparticles

Two formulations from 5% D118 and different stabilizers were prepared by hot homogenization. The first one was prepared with 1.8% Lipoid S75-3 and 0.45% sodium glycocholate (SGC) while the second one contained 4% Mowiol 3-83. For the nanoparticles stabilized with phospholipid S75-3, the phospholipid and SGC were dispersed/dissolved in the aqueous phase (containing 2.25% glycerol and 0.01% thiomersal) by magnetic stirring over night. The stabilizer mixture was transiently heated to about 60°C to facilitate dispersion.

After complete dispersion, the mixture was heated to about 90°C. The oil phase containing porphyrin was prepared by adding 500 µl from a methanolic stock solution (10 mg/ml) of porphyrin to the molten lipid and stirring at high temperature till the smell of methanol had disappeared. The hot aqueous phase was poured to the molten lipid and the mixture was pre-homogenized for one minute (Ultra-Turrax T8, IKA Labortechnic, Germany). This crude emulsion was transferred to the 90 °C warm high-pressure homogenizer Microfluidizer M-110S (Microfluidics, US-Newton) and treated for 5 min at 700 bar. The hot colloidal emulsion was allowed to cool to 4°C. The second formulation from D118 was prepared as described above but by using 4% Mowiol, which was dissolved in the aqueous phase. According to these preparation conditions nanoparticles in the α-form will be obtained [66-67]. These lipid nanoparticles in the α-form were stored at refrigerator temperature. In an attempt to transform the particles to the β-form, the nanoparticles of the two formulations were placed in a shaker water bath (Grant OLS 200, Cambridge, England) for 8 hours at 50°C with 100 shakes/minute followed by storage at 23°C.

3.2.3 Preparation of Miglyol 812 nanoemulsions

Nanoparticles from 5% Miglyol 812 and 4% poloxamer 188 were prepared by homogenization at room temperature. Poloxamer 188 (1.2 g) was dissolved in the aqueous phase containing 2.25% glycerol and 0.01% thiomersal (27.3 g). The aqueous phase containing the surfactant was added to the oil phase (1.5 g Miglyol oil) and the mixture was pre-homogenized for 1 minute with an Ultra-Turrax (Ultra-Turrax T8, IKA, Germany) followed by homogenization with a Microfluidizer M-110S (Microfluidics, US-Newton) for 5 minutes at 600 bar. The drug free nanoemulsion was used as acceptor in the transfer experiments with the ion exchange column technique. Loading with porphyrin (0.5 mg/ml) was conducted by direct addition of a methanolic stock solution (2.5 mg/ml) to the nanoemulsion followed by shaking for 24 hours at 25°C at 100 shakes/minute. This nanoemulsion was stored at room temperature. In order to obtain nanoemulsions with different zeta potential, five formulations of Miglyol nanoemulsion were prepared with different ratios between S75 and EPC (table 3.3). S75 and EPC were dispersed in the aqueous phase (containing 2.25% glycerol and 0.01% thiomersal) by magnetic stirring over night. The aqueous phase containing the surfactant was added to 10% Miglyol oil (3 g) and the mixture was pre-homogenized for 1 minute with an Ultra-Turrax (Ultra-Turrax T8, IKA, Germany) followed by homogenization with a Microfluidizer M-110S (Microfluidics, US-Newton) at 600 bar for 5 minutes at room temperature. Loading with porphyrin (0.5 mg/ml) was done as described for the trimyristin donor nanoparticles.

Table 3.3: Composition of Miglyol nanoemulsions prepared with different ratios between Lipoid S75 (S75) and egg phosphatidyl choline (EPC). The total emulsifier concentration was 2% (0.6 g) (all concentrations w/w)

Samples	S75	EPC
10% Miglyol oil (3 g) and 88% aqueous phase (26.4 g)		
MigS75/EPC1	1.5% (0.45 g)	0.5% (0.15 g)
MigS75/EPC2	1.25% (0.375 g)	0.75% (0.225 g)
MigS75/EPC3	1% (0.3 g)	1% (0.3 g)
MigS75/EPC4	0.75% (0.225 g)	1.25% (0.375 g)
MigS75/EPC5	0.5% (0.15 g)	1.5% (0.45 g)

3.3 Preparation of the acceptor particles

3.3.1 Preparation of the acceptor unilamellar vesicles

Acceptor unilamellar vesicles were prepared using EPC and cholesterol in a molar ratio of 8:2 (EPC: cholesterol) [3, 68]. An EPC stock solution was prepared by dissolving 1.52 g in 20 ml chloroform, a cholesterol stock solution by dissolving 0.194 g in 20 ml chloroform. The two lipid solutions (1 ml each) were mixed in a small bottom flask and dried to a thin film under vacuum (200 mbar for 2 hours followed by 30 mbar for 1 hour (Büchi Rotavapor R-114, D-Essen)). The lipid film was rinsed with nitrogen and checked for the absence of any odour of solvent. The resulting thin film was hydrated by vortexing for 10 minutes with 1 ml tris buffer saline (10 mM tris, 140 mM NaCl, pH 7.4) to yield a lipid suspension with a concentration of 85 mg/ml. The lipid suspension was extruded through a 200 nm and then through a 100 nm polycarbonate membrane (Liposofast, Avestin, Canada) for 21 cycles. Unilamellar vesicles from Lipoid S75 (20 mg/ml) were prepared and extruded as described for the EPC and cholesterol vesicles. Radiolabeled unilamellar vesicles from EPC and cholesterol (8:2) were prepared using ^{3}H-cholesteryl oleyl ether at a concentration of 0.1 µCi/mg of the total vesicle lipids (8.5 µCi/ml) [56]. All these vesicles were stored at refrigerator temperature.

3.3.2 Preparation of the acceptor multilamellar vesicles (MLV)

MLV liposomes were prepared as described before [5]. 1 ml EPC chloroform stock solution (76 mg) was added to 1 ml cholesterol chloroform stock solution (9.68 mg) in a small bottom flask (the ratio between EPC and cholesterol being 8:2 mol/mol). The mixture was dried to a thin film under vacuum (200 mbar for 2 hrs to remove organic solvent and then 30

mbar for 1 hr). The lipid film was rinsed with nitrogen for complete removal of the solvent. The lipid film was hydrated with 1 ml warm 300 mM sucrose solution under vortexing to yield MLV liposomes, which were transferred to a plastic Eppendorf tube. The mixture was centrifuged at 1600 xg for 10 min. After centrifugation, the MLV appeared as supernatant layer with the sucrose solution below. An 18G needle syringe was used to pierce the Eppendorf tube and to withdraw the sucrose solution. 0.5 ml of HBS pH 7.4 (20 mM Hepes, 150 mM NaCl adjusted to pH 7.4 with 1 M NaOH) was added to the remaining MLV. The sample was vortexed and centrifuged at 1600 xg for 10 min, after that the MLV appeared as a pellet. The HBS supernatant was decanted and the pellet was washed twice with 0.5 ml HBS. The pellet was finally resuspended in fresh HBS (1 ml) and stored at refrigerator temperature.

3.3.3 Preparation of the acceptor o/w emulsion droplets

The acceptor o/w emulsion was composed of 5% (w/w) liquid medium chain triglycerides (Miglyol 812) stabilized with 3% (w/w) polyvinyl alcohol in an aqueous phase containing 2.25% glycerol and 0.01% thiomersal [6]. The emulsion was prepared at room temperature using an Ultra-Turrax (T8, IKA Labortechnic, Germany) for 15 minutes. The emulsion was stored at room temperature and used directly after preparation. For calibration of the flow cytometer, small fractions of the emulsions were loaded with different amounts of the investigated fluorescent dyes in the same way as described for the donor lipid nanoparticles.

3.3.4 Preparation of the acceptor monoolein dispersions

Six different monoolein dispersions with different amphiphile (monoolein + poloxamer) concentrations were prepared (table 3.4). Corresponding amounts of monoolein (MO) and poloxamer 407 were mixed in the melt and the molten mixture was added dropwise to water under stirring at room temperature [69]. The resulting coarse dispersions were equilibrated under magnetic stirring and protected from light for at least about 1 day at room temperature before homogenization in a microfluidizer M-110S (Microfluidics, US-Newton) at 350 bar for 15 min at 40°C. After homogenization, fractions of the dispersions were autoclaved at 121°C in a laboratory autoclave (Varioklav, 65T, D-Oberschleissheim) for 15 min plus an equilibration time of 5 min. Autoclaving was used to transform vesicular structures potentially present in the dispersions into particles of cubic structure and to obtain particles of different sizes [18, 69].

Table 3.4: Composition of the monoolein dispersions

Amphiphile concentration	% Monoolein (MO)	% Poloxamer 407
12 % poloxamer in amphiphile mixture and aqueous phase to 100%		
5%	4.4	0.6
7%	6.2	0.8
10%	8.8	1.2
15%	13.2	1.8
8 % poloxamer in amphiphile mixture and aqueous phase to 100%		
10%	9.2	0.8
15%	13.8	1.2

For calibration of the flow cytometer, stock solutions of the investigated fluorescent dyes were prepared in methanol in case of porphyrin or in ethanol in case of DiI. Different amounts from these stock solutions were added to different amounts from the acceptor cubic particles. Calibration curves between the concentration of the fluorescent dyes in the cubic particles and the fluorescence intensity were constructed.

3.4 Characterization of the donor and acceptor particles

3.4.1 Photon correlation spectroscopy (PCS)

Particle sizes were measured by photon correlation spectroscopy (PCS) in a Zetasizer Nano (Malvern Instruments Ltd., UK-Worcestershire) after diluting the samples with filtered purified water at 25 °C and at a scattering angle 173°. Three consecutive measurements of 5 min duration after 5 minutes of equilibration were recorded and the resulting z-average and polydispersity index (PDI) were averaged. The polydispersity index (PDI) presents an indication of the homogeneity of the samples.

3.4.2 Laser diffraction (LD)

The size of the different particles was determined using a laser diffractometer with PIDS technology (polarization intensity differential scattering), the Coulter LS 230 Particle Sizer (Beckman Coulter, D-Krefeld,). 8 consecutive measurements of 90 s (recorded without stirring) were averaged. The applied evaluation model used the Mie theory with a refractive index of 1.332 for water and 1.45 for the sample. The volume distributions of the samples were calculated and the results are given as the mean particle sizes.

3.4.3 Zeta potential measurements

The zeta potential was measured with a Zetasizer Nano (Malvern Instruments Ltd., UK-Worcestershire) after diluting the samples with 10 mM tris buffer pH 7.4. The results of three consecutive measurements each consisting of 20 runs were averaged.

3.4.4 Differential scanning calorimetry (DSC) of the donor particles

The physical state of the matrix lipid in the donor lipid nanoparticles was investigated in a DSC Pyris 1 (Perkin Elmer). Approximately 10 µl of the donor FS75/SGClow, FS75/SGChigh and FS75 before and after ultracentrifugation were measured at a scan rate of 5°C/min. An empty crucible was used as a reference. DSC of the supernatant layer (liposomal layer) after ultracentrifugation was also carried out. The measurements consisted of two heating runs and one cooling run ((1) 20°C to 65°C, (2) 65 to –10°C, (3) -10 to 65°C). Between heating and cooling an isothermal phase of 5 min was entered.

The physical state and the polymorphic form (α-form or β-form) of the matrix lipid in the donor lipid nanoparticles, which were prepared from tristearin (D118), were investigated with the same sequences as the trimyristin nanoparticles except that the heating run was performed to 110°C.

3.4.5 Cryo transmission electron microscopy (Cryo-TEM)

Cryo-TEM images were performed by Dr. Frank Steiniger at the electron microscopic centre of the Friedrich Schiller University. A few microliters of the original nanoparticles (before ultracentrifugation), resuspended nanoparticles (after ultracentrifugation) and liposomal layer (supernatant layer after ultracentrifugation) of FS75/SGClow and FS75/SGChigh were placed on a holey grid (Quantifoil Micro Tools, Jena, Germany) and excess of liquid was removed with filter paper (the samples were used without dilution). The samples were cryofixed by rapid immersing into liquid ethane cooled to −170 °C to −180 °C in a cryobox (Carl Zeiss NTS GmbH, Oberkochen, Germany). Excess ethane was removed by blotting in the cold. The samples were transferred with a cryotransfer unit (Gatan 626-DH) into the pre-cooled cryoelectron microscope (Philips CM120, Netherlands) operated at 120 kV and viewed under low dose conditions.

3.4.6 ^{31}P- spectroscopy of the donor particles

In order to investigate the existence of liposomes (small unilamellar vesicles) due to the presence of excess S75 in addition to the real triglyceride nanoparticles, ^{31}P-NMR spectroscopy was carried out for the original nanoparticles (before ultracentrifugation), the resuspended nanoparticles (pellets after ultracentrifugation) and supernatant layer (excess

S75) of FS75/SGChigh and FS75 [70-72]. The ^{31}P-NMR measurements were carried out by Dr. Wolfgang Günther at the institute of organic and macromolecular chemistry of the Friedrich Schiller University. The samples (500 µl) were analyzed by high-resolution ^{31}P nuclear magnetic resonance (NMR) in a Bruker Avance 400 apparatus (Bruker, D-Karlsruhe) operating at a temperature of 30°C before and after the addition of an aqueous praseodymium chloride ($PrCl_3$) solution (1 mg/ml). Deuterium oxide (D_2O) was used as an external reference in a Wilmad NMR reference tube (2 mm), which was placed inside a 5 mm NMR sample tube containing the sample. In the paramagnetic shifted samples, praseodymium chloride solution was added in 1:5 (v/v) portions (100 µl praseodymium chloride and 400 µl sample). As a confirmatory experiment, ^{31}P-NMR spectroscopy for unilamellar vesicles prepared from Lipoid S75 was performed.

3.4.7 Determination of the lipid content by HPLC

The amount of D114 in the original lipid nanoparticles (before ultracentrifugation), resuspended nanoparticles (after ultracentrifugation) and supernatant layer of FS75/SGClow, FS75/SGChigh and FS75 was determined using reversed-phase HPLC and evaporative light scattering detection (Varex MKIII ELSD, Alltech GmbH, D-Unterhaching). The analysis was performed with a 25 cm x 3 mm LiChrocart column packed with LiChrospher 100-5 RP 18 (Merck KgaA, D-Darmstadt) in a System Gold 126 HPLC (Beckman Coulter GmbH, D-Krefeld). Acetonitrile-tetrahydrofurane 55:45 (v/v) was used as mobile phase and the isocratic flow-rate was set at 1 ml/min. For the evaporation of the mobile phase, the temperature of the detector was adjusted at 91°C and the pressure was 2.2 l/min. These conditions were used all over the HPLC analysis. Standard solutions of D114 were prepared and the mean area under the curve was calculated to obtain a HPLC calibration curve for D114. To determine the amount of D114 in the nanoparticles a small amount of FS75/SGClow, FS75/SGChigh, FS75 and Fpoloxamer/DCP was dissolved in acetonitrile-tetrahydrofurane 20:80 (v/v) to prepare 1 µl/ml samples and 100 µl of these solutions were injected into the HPLC for analysis. The amount of D114 in the samples was determined from the calibration curve.

3.4.8 Drug content

Since porphyrin was added to the D114 formulations before solidification and ultracentrifugation some drug was lost into the supernatant layer (excess S75) after ultracentrifugation. The amount of the drug in 20 µl ultracentrifuged and resuspended nanoparticles (pellets) and supernatant layer (for FS75/SGClow, FS75/SGChigh and FS75) was determined after diluting the samples to 5 ml with a mixture of acetonitrile-tetrahydrofurane 20:80 (v/v) and measuring the UV absorbance at 421 nm.

3.4.9 Small angle diffraction of the acceptor monoolein dispersions

To confirm the presence or absence of cubic particles in the different monoolein/poloxamer dispersions before and after autoclaving, small-angle X-ray diffractograms were recorded in a capillary sample holder for 1-2 h with a SWAX camera based on a Kratky collimator system (Hecus M. Braun, Optical Systems GmbH, Graz, Austria) with an Iso-Debyeflex 3003 60 kV generator (Seifert-FPM D-Freiberg), an X-ray tube (copper anode) FK 61-04 × 12 and equipped with two position sensitive detectors (PSD-50M, M. Braun, Garching, Germany).

3.5 Drug transfer studies with the column method

3.5.1 Calibration curves of the drug models in the different solvents

For the calibration curve of porphyrin in ethanol, a stock solution of porphyrin was prepared by adding 1.02 mg porphyrin to 100 ml ethanol (10 µg/ml). 0.1, 0.2, 0.5, 1, 2, 3, or 5 ml of this solution were diluted with ethanol to 25 ml to prepare solutions of 0.04, 0.08, 0.2, 0.4, 0.816, 1.224 and 2.04 µg/ml. The absorbance of these solutions was measured at 421 nm (Beckman, Du 640, U.S.A.).

In the case of an acetonitrile-tetrahydrofurane mixture as solvent, a stock solution of porphyrin was prepared by adding 1.5 mg porphyrin to 100 ml of a mixture of acetonitrile-tetrahydrofurane 20:80 (v/v). 15, 20, 50, 75, 150 or 175 µl of this solution were diluted with the solvent mixture to 10 ml to prepare solutions of 0.022, 0.03, 0.075, 0.112, 0.225 and 0.27 µg/ml. The absorbance of these solutions was measured at 421 nm.

In the case of Nile red, a stock solution was prepared by adding 0.4 mg Nile red to 50 ml ethanol (8 µg/ml). 5, 10, 20, 30, 50, 100, 200, 300, 400, 500 or 600 µl of this solution were diluted with ethanol to 1 ml to prepare solution of 0.04, 0.08, 0.16, 0.24, 0.4, 0.8, 1.6, 2.4, 3.2, 4 and 4.8 µg/ml. The absorbance of these solutions was measured at 548 nm. The Nile red calibration curve in the acetonitrile-tetrahydrofurane mixture was constructed as that in ethanol. A calibration curve for DiI was constructed in acetonitrile-tetrahydrofurane as described for Nile red but at wavelength 550 nm. Linear calibration curves with good correlation coefficients ($R^2 \geq 0.999$) were obtained in all cases (see appendix A.1).

3.5.2 Preparation of the ion exchange columns

A total of 50 ml of DEAE-Sepharose CL-6B was washed twice with a 3-fold excess of tris buffer saline (10 mM tris, 140 mM NaCl, pH 7.4). After each washing, the tris buffer was carefully decanted off and finally the gel was washed with a 3-fold excess of sucrose buffer (290 mM sucrose, 10 mM Trizma 7.4 pre-set crystals, 0.02% sodium azide, pH 7.4) and then

diluted 1:1 (v/v) with sucrose buffer, which was also used for the elution of the columns [3]. The column length was 5 cm with an inner diameter of 0.5 cm. An example of these columns is illustrated in figure 3.4. Some glass wool was placed at the bottom of the columns. About 1 ml ion exchange suspension (DEAE-Sepharose) was filled in the column and the column was eluted with 2 ml sucrose buffer for packing and the eluate was discarded. The columns were lipid saturated (to reduce non-specific adsorption and to improve the recovery of acceptor particles) by applying 20 µl of the respective acceptor dispersion and eluting with 1.5 ml sucrose buffer [56]. This eluate was also discarded. In all experiments, the elution of the columns was performed using 1.5 ml sucrose buffer.

Figure 3.4: Column used in the transfer experiments

3.5.3 Validation of the column method

3.5.3.1 Acceptor recovery with radiolabeled unilamellar vesicles

10 µl of the crystalline donor particles of FS75/SGClow, FS75/SGChigh and FS75 before and after ultracentrifugation was added to Eppendorf tubes containing 100 µl of the radiolabeled unilamellar acceptor vesicles and 390 µl sucrose buffer. The Eppendorf tubes were incubated in a shaking water bath at 37°C. At appropriate time intervals (2, 4 and 24 hours) 200 µl of the incubation mixture was placed on a mini-column containing DEAE-Sepharose CL-6B. The eluent containing the radiolabeled unilamellar vesicles (1.5 ml) was diluted with 7 ml scintillation cocktail. The amount of radioactivity in the eluent was measured and the percentage of the eluted radiolabeled acceptor liposomes was determined.

3.5.3.2 Charge transfer from the donor to the acceptor

50 µl of the crystalline donor particles of FS75/SGChigh before and after ultracentrifugation was added to 500 µl of the acceptor neutral unilamellar vesicles (EPC: cholesterol 8:2) and the volume was completed to 2 ml with sucrose buffer. Ultracentrifugation (XL-80 ultracentrifuge, rotor type SW55 Ti, Beckman Coulter Inc., US-Fullerton) of these mixtures was carried out at 35000 rpm, 15°C for 1 hour to separate the acceptor unilamellar vesicles (supernatant) from the crystalline donor particles (pellets). The zeta potential of both the supernatant (unilamellar vesicles) and the pellets (crystalline donor particles) was measured after diluting the samples with 10 mM tris buffer pH 7.4.

3.5.3.3 Retention of the donor particles

10 µl of the porphyrin loaded donor crystalline or liquid particles of FS75/SGClow, FS75/SGChigh and FS75 before and after ultracentrifugation was placed on the column after saturation of the column with 20 µl acceptor unilamellar vesicles. The columns were eluted with 1.5 ml of sucrose buffer. The eluate was collected directly into Eppendorf tubes and diluted to 5 ml with a mixture of acetonitrile-tetrahydrofurane 20:80 (v/v) and the UV absorbance was measured at 421 nm.

3.5.4 Determination of the suitable zeta potential range for the column method

10 µl of the five Miglyol formulations, which were prepared with different concentrations of EPC and S75 and loaded with porphyrin, was placed on the column after saturation of the columns with 20 µl Miglyol nanoemulsion free from porphyrin. The columns were eluted with 1.5 ml of sucrose buffer. The eluate was collected directly into Eppendorf tubes, diluted to 5 ml with ethanol and the UV absorbance was measured at 421 nm.

3.5.5 Transfer of the different drug models to the acceptor unilamellar vesicles

All transfer experiments to the different acceptors were carried out on the resuspended particles (after ultracentrifugation) in a crystalline or liquid form, which was prepared by melting the crystalline one. The transfer experiments from the crystalline and liquid donor particles of FS/75/SGClow, FS75/SGChigh and FS75 after ultracentrifugation to the acceptor unilamellar vesicles were carried out with molar ratios of 1:25 and 1:100 with different total lipid concentrations in the aqueous phase (transfer mixture). Different amounts of the donor particles were added to Eppendorf tubes containing different amounts of unilamellar vesicles and sucrose buffer (table 3.5). The Eppendorf tubes were incubated at 37°C. At appropriate time intervals 200 µl of the incubation mixture was placed on the ion exchange columns and eluted with sucrose buffer. The eluate was dissolved with a mixture of acetonitrile-tetrahydrofurane 20:80 (v/v) and the UV absorbance was measured at 421 nm. To evaluate the effect of the lipid concentration on the drug transfer, the transfer of porphyrin from the resuspended nanoparticles of FS75/SGChigh to the acceptor unilamellar vesicles was also investigated at a low lipid concentration (5 mg/ml) and with a molar ratio of 1:100. 20 µl donor was added to a glass vial containing 800 µl SUV and 9180 µl sucrose buffer (total volume of the mixture was 10 ml). The glass vial was incubated in a shaking water bath for the intended times at 37°C and the remaining steps were continued as before.

The transfer of Nile red and DiI from the resuspended nanoparticles of FS75/SGChigh to the acceptor unilamellar vesicles was done with a molar ratio of 1:100. 600 µl of the acceptor unilamellar vesicles and 385 µl of sucrose buffer were mixed in Eppendorf tubes,

then 15 µl of the crystalline donor particles was added to the mixture. The remaining steps were completed as described with porphyrin but the UV absorbance was measured at 548 nm for Nile red and 550 nm for DiI.

Table 3.5: Amounts of the different donors (loaded with porphyrin) and acceptors in the transfer experiments, lipid molar ratios and the total lipid concentrations in the transfer mixture

Donor volume (µl)	Acceptor volume (µl)	Sucrose buffer volume (µl)	Lipid molar ratios*	Total lipid concentration (mg/ml)*
FS75/SGClow donor and acceptor unilamellar vesicles				
10	95	395	1:25	17
10	380	110	1:100	65
FS75/SGChigh donor and acceptor unilamellar vesicles				
10	100	390	1:25	18
10	400	90	1:100	68
60	600	340	1:25	50
15	600	385	1:100	50
FS75 donor and acceptor unilamellar vesicles				
10	95	395	1:25	17
10	380	110	1:100	65
FS75/SGChigh donor and acceptor monoolein dispersions (5% amphiphile) in the form of vesicles or cubic particles				
100	1000		1:25	48
FS75/SGChigh donor and acceptor Miglyol nanoemulsion				
20	1000		1:100	50

*referring to the ratio between the trimyristin (calculated after ultracentrifugation by HPLC) and the different lipid in the acceptors excluding the surfactants (e.g. lipoid S75, SGC and poloxamer)

3.5.6 Transfer to the acceptor monoolein dispersions and Miglyol nanoemulsion

The transfer of porphyrin from the resuspended nanoparticles of FS75/SGChigh to the acceptor monoolein dispersions (molar ratio 1:25) and the Miglyol nanoemulsion (molar ratio 1:100) was also studied. The acceptor monoolein dispersions used in these studies were prepared with 5% amphiphile (monoolein and poloxamer) without and with autoclaving. As a preliminary experiment, the recovery of the acceptor particles was measured by adding

200 µl of the acceptor that was loaded with porphyrin, to the ion exchange columns. The eluate was dissolved by using a mixture of acetonitrile-tetrahydrofurane 20:80 (v/v) and the UV absorbance was measured at 421 nm.
For the transfer experiments, different amounts (table 3.5) of the donor nanoparticles were added to Eppendorf tubes containing 1 ml of the acceptor particles (monoolein dispersions and Miglyol nanoemulsion) and the remaining steps were done as described with the acceptor unilamellar vesicles.

DiI transfer from the resuspended nanoparticles of FS75/SGChigh to the acceptor cubic nanoparticles, which were prepared from 5% amphiphile, was investigated with molar ratios of 1:25 and 1:100. Different amounts of the donor nanoparticle dispersions (25 and 100 µl for the molar ratio 1:100 and 1:25, respectively) were added to Eppendorf tubes containing 1 ml of the cubic nanoparticles. The remaining steps were done as described with porphyrin.

3.5.7 Porphyrin affinity to monoolein dispersions and unilamellar vesicles

To compare the affinity of porphyrin to the acceptor monoolein dispersions before or after autoclaving (5% amphiphile, vesicles or cubic particles) and the acceptor unilamellar vesicles, 4 ml of the respective acceptors was added to glass vials each containing 10.7 mg of porphyrin (porphyrin in excess). At different time points, 500 µl dispersion from each glass vial was filtered through 0.45 µm filters. 50 µl of the filtrate was dissolved in a mixture of acetonitrile-tetrahydrofurane 20:80 (v/v) and the UV absorbance was measured at 421 nm.

3.6 Drug transfer studies with the centrifugation method

3.6.1 Transfer of different drug models to the acceptor multilamellar vesicles (MLV)

The transfer of porphyrin was studied from the donor resuspended nanoparticles in the liquid form, which was prepared by melting the crystalline form of FS75/SGClow, FS75/SGChigh, FS75 and from the original lipid nanoparticles of Fpoloxamer/DCP to the acceptor MLV particles. Different amounts of the donor (table 3.6) were added to Eppendorf tubes containing 600 µl of the acceptor MLV and different amounts of HBS (the total volume was 1 ml). The samples were incubated in a shaking water bath at 37 °C. Samples were taken at specific times, vortexed and centrifuged (3MK centrifuge, Sigma, D-Osterode) at 5300 rpm (1600 x g) for 10 min to separate the nanoparticles from the pellet MLV liposomes. The supernatant (nanoparticles) was collected by decantation and the absorbance was measured at 421 nm after dilution with a mixture of acetonitrile-tetrahydrofurane 20:80 (v/v) to 5 ml.

Table 3.6: Amount (µl) of the different donor particles mixed with 600 µl MLV acceptor to obtain different lipid molar ratios in the transfer experiments with the centrifugation method. The total lipid concentration in the transfer mixtures was 50 mg/ml

Donor	Donor volume (µl)	Lipid molar ratios
FS75/SGClow	64	1:25
	32	1:50
	16	1:100
FS75/SGChigh	60	1:25
	30	1:50
	15	1:100
FS75	64	1:25
	32	1:50
	16	1:100
Fpoloxamer/DCP	40	1:25
	20	1:50
	10	1:100

The MLV containing pellet was washed twice with 250 µl HBS, vortexed and centrifuged (the centrifugation time for each washing was 10 min). The first and second washings were combined and the absorbance was measured at 421 nm after dilution with the same solvent mixture to 5 ml. The amount of drug detected in the supernatant and washes was combined to obtain an overall supernatant amount. The percent drug retained in the nanoparticles was [(Amount of drug in supernatant)/ (total amount of drug in the donor at time = 0)] × 100.

The amount of drug at time zero was determined by diluting the respective amount of the donor dispersion to 5 ml with a mixture of acetonitrile-tetrahydrofurane 20:80 (v/v) and measuring the UV absorbance at 421 nm. The amount of the drug in the MLV was determined by dissolving the MLV pellets in ethanol, diluting to 5 ml and measuring UV absorbance at 421 nm. The percent drug transferred was [(Amount of drug in MLV pellets)/ (total amount of drug in the donor at time = 0)] × 100.

The porphyrin transfer from Fpoloxamer/DCP to the acceptor MLV in the presence of 3% PVA was studied by adding 10 µl of the donor particles to Eppendorf tubes containing 385 µl HBS and 600 µl MLV acceptor with 3% PVA. The Eppendorf tubes were incubated in a shaking water bath at 37°C. The other steps of the transfer experiment were performed as described before. The transfer of Nile red from the resuspended liquid nanoparticles of FS75/SGChigh to the acceptor MLV was studied with a molar ratio of 1:100. 15 µl donor particles were added to Eppendorf tubes, which contained 385 µl HBS and 600 µl MLV. The

transfer procedures were done as described before with porphyrin and the UV absorbance was measured at 548 nm.

3.6.2 Transfer of different drug models to the acceptor o/w emulsion

The transfer of porphyrin from the resuspended crystalline nanoparticles of FS75/SGChigh and the original crystalline nanoparticles of Fpoloxamer/DCP to the acceptor o/w emulsion was studied with a molar ratio of 1:25. Different amounts of the crystalline loaded donor particles (80 µl of FS75/SGChigh and 60 µl of Fpoloxamer/DCP) were mixed with 1 ml of the acceptor o/w emulsion in Eppendorf tubes. The Eppendorf tubes were incubated in a shaking water bath at 37°C. After shaking, the samples were diluted with 3 ml purified water into an ultracentrifugation tube. The samples were ultracentrifuged (XL-80 ultracentrifuge, rotor type SW55 Ti, Beckman Coulter Inc., US-Fullerton) for 30 minutes at 45000 rpm to separate the crystalline donor from the acceptor emulsion. After removing the cream layer and aqueous supernatant the pellet was scraped from the tube bottom, resuspended in 250 µl of water and sonicated for 2 min. The suspension was transferred into glass vials and the centrifugation tube was rinsed with 250 µl water, which was added to the glass vials. The pellet suspension was dissolved in 3 ml of a mixture of acetonitrile-tetrahydrofurane 20:80 (v/v) and the UV absorbance was measured at 421 nm.

The transfer of Nile red from the resuspended crystalline nanoparticles of FS75/SGChigh to the acceptor o/w emulsion was studied with a molar ratio of 1:100. 20 µl of the donor particles was mixed with 1 ml of the acceptor o/w emulsion in Eppendorf tubes. The other steps of the transfer experiment were done as before and the UV absorbance of Nile red was measured at 548 nm.

3.6.3 Transfer of different drug models to the acceptor cubic particles

The transfer of porphyrin from the resuspended nanoparticles of FS75/SGChigh to the acceptor cubic particles with different particle sizes was investigated with a molar ratio of 1:25. 100 µl of the donor was mixed with different amounts of the acceptor (1 and 0.5 ml in case of cubic particles prepared with 5 and 10% amphiphile, respectively) in Eppendorf tubes and shaken at 37°C (100 shakes/minute). After shaking, the donor and acceptor were separated as described before with the acceptor o/w emulsion. The UV absorbance of the pellets (dissolved in a mixture of acetonitrile-tetrahydrofurane) was measured at 421 nm.

The DiI transfer from the resuspended nanoparticles of FS75/SGChigh to the acceptor cubic particles, prepared from 5% amphiphile, was studied with molar ratios of 1:25 and 1:100. 100 or 25 µl of the donor particles were mixed with 1 ml of the acceptor cubic particles in Eppendorf tubes to achieve molar ratios of 1:25 and 1:100, respectively. The other steps

of the transfer experiment were done as before and the UV absorbance of DiI was measured at 550 nm.

3.7 Drug transfer studies with the flow cytometry method

3.7.1 General procedure

The measurements were performed in a similar way as described previously [6]. To select the conditions for the fluorescence measurements, the acceptor particles (cubic particles, o/w emulsion and MLV) were measured (without drug) in the flow cytometer (Epics XL MCL, Beckman Coulter Inc., US-Fullerton). Different amounts of the acceptor dispersions were diluted with purified water in a measurement tube and subsequently measured by flow cytometry. The right amount of the acceptors was achieved when a count rate of approximately 250 events per second was reached. After the detection of 10,000 events the measurements were stopped. The emitted fluorescence of porphyrin and Nile red was detected at the photomultiplier tube number 4 (FL4) with a wavelength range of 665-685 nm while the emitted fluorescence of DiI was detected at FL2 (565-585 nm). The flow cytometer was calibrated by measuring the fluorescence intensity of acceptor samples, which had been loaded with defined amounts of the drug models and the fraction of drug transferred was calculated from the resulting calibration curves. Between the measurements, cleaning steps were introduced to avoid mixing with residual particles of preceding samples.

3.7.2 Calibration curves of the drug models with the different acceptors

In case of the acceptor MLV, 6 samples of the MLV acceptor containing porphyrin were prepared with the same procedures as used for the preparation of the MLV without drug except that small amounts of stock solution of porphyrin in methanol were added to the chloroform solution of the EPC and cholesterol. Due to the loss of some drug during the preparation of MLV, the final amount of the drug in the MLV was determined by UV spectroscopy after dissolving the MLV in ethanol. 3-5 µl of these porphyrin loaded MLV formulations were diluted with 1 ml water and measured by flow cytometry. A calibration curve between the porphyrin concentrations in the MLV acceptor and the fluorescence intensity was constructed.

With the acceptor o/w emulsion, a stock solution of porphyrin (10 µg/ml) was prepared in ethanol. Different amounts of this stock solution were taken and added to different amounts of acceptor emulsion to prepare emulsion loaded with different amounts of drug (0.1 to 1 µg/ml) followed by shaking in a shaker water bath at 25°C for 1 day. 10-15 µl of these mixtures were diluted with 1 ml water and measured by flow cytometry. The calibration curves of the other dyes in the different acceptors were performed as described for porphyrin

with the acceptor emulsion. For all drug models and acceptor under investigation, linear calibration curves with good correlation coefficients ($R^2 \geq 0.997$) were obtained (see appendix A.2).

3.7.3 Porphyrin and Nile red transfer to the acceptor MLV

The transfer of porphyrin was investigated by adding different amounts of the loaded donor particles of Fpoloxamer/DCP in the liquid form (40, 20 and 10 µl for molar ratios of 1:25, 1:50 and 1:100 respectively) to Eppendorf tubes containing 600 µl MLV acceptor dispersion and different amounts of HBS (total mixture volume was 1 ml). The tubes were subsequently incubated in a water bath shaker at 37 °C. Samples were collected at different time points after mixing. 3 to 5 µl of the mixture were diluted in 1 ml purified water and subsequently measured at the flow cytometer.

The transfer of Nile red from the resuspended crystalline nanoparticles of FS75/SGChigh to the acceptor MLV was studied as described for porphyrin by mixing 15 µl of the loaded donor particles with 600 µl MLV acceptor and 385 µl HBS in Eppendorf tubes (molar ratio 1:100).

3.7.4 Porphyrin and Nile red transfer from different donors to the o/w emulsion

The transfer of porphyrin and Nile red was investigated by mixing different amounts of the loaded donor particles (specified in table 3.7) with 1 ml of the acceptor o/w emulsion in Eppendorf tubes. The other steps of the transfer experiment were performed as described with the acceptor MLV except that 10 to 15 µl of the transfer mixture were diluted in 1 ml purified water and subsequently measured at the flow cytometer.

3.7.5 Porphyrin and DiI transfer to the acceptor cubic particles

The transfer of porphyrin and DiI from the resuspended crystalline nanoparticles of FS75/SGChigh to two acceptor cubic particles with different particle sizes was studied with a molar ratio of 1:25 in case of porphyrin while with DiI the molar ratio was 1:25 and 1:100. The experiments were done with the acceptor cubic particles (after autoclaving), which were prepared from 15 % amphiphile with 12 and 8% poloxamer (particle size > 1 µm). Different amounts of donor particles (125 and 31 µl of the donor particles loaded with DiI and 125 µl of porphyrin donor particles) were added to Eppendorf tubes containing 400 µl acceptor cubic particles and different amounts of water (total mixture volume was 1 ml). The other steps of the transfer experiment were performed as described with the acceptor MLV except that 10 to 15 µl of the transfer mixture were diluted in 500 µl purified water and subsequently measured at the flow cytometer.

Table 3.7: Amount (µl) of the different donor particles mixed with 1 ml acceptor o/w emulsion to obtain different lipid molar ratios in the transfer experiments with the flow cytometric method. The total lipid concentration in the transfer mixtures was 50 mg/ml

Donor	Volume of the donor (µl)	Molar ratios
Resuspended crystalline nanoparticles of FS75/SGChigh loaded with porphyrin	80	1:25
	40	1:50
	20	1:100
Fpoloxamer/DCP in the liquid or crystalline form loaded with porphyrin	60	1:25
	30	1:50
	15	1:100
Miglyol nanoemulsion loaded with porphyrin	10	1:100
Resuspended crystalline tristearin nanoparticles in the different physical forms loaded with porphyrin	18	1:100
Monoolein vesicles (5% amphiphile) loaded with porphyrin	10	1:100
Monoolein cubic particles (5% amphiphile) loaded with porphyrin	10	1:100
Resuspended crystalline nanoparticles of FS75/SGChigh loaded with Nile red	20	1:100

3.8 Transfer kinetics

The data points of the percental transferred amount of the different drug models to the different acceptors with the three transfer methods were exponentially fitted using Microcal Origin 6.0 software (OriginLab Corporation, US-Northampton) and the exponential function:

$$A_{acc} = A_{final} - A \times e^{-k \times t} \qquad [1]$$

A_{acc} is the percental amount of fluorescent dye transferred to the acceptor particles at time t, A_{final} is the final percental transferred amount of dye and marks the height of the plateau, A is a pre-exponential coefficient and K is the rate constant of the transfer. All transfer kinetics values (transfer rate constant and the final percent transferred) were obtained from the fitted curves and the equilibrium time was determined by calculating the time at which 99% of the plateau was reached.

Chapter 4: Results and discussion

4.1 Characterization of the donor particles

4.1.1 Particle size and zeta potential of D114 nanoparticles

Figure 4.1 shows the particle size of the D114 nanoparticles stored at room and refrigerator temperature. The nanoparticles stored at refrigerator temperature had a higher particle size because the recrystallization of the colloidally dispersed trimyristin is accompanied by the formation of platelet-like colloidal crystals. These anisometric particles have a larger hydrodynamic diameter in PCS compared with the corresponding spherical nanoemulsion particles [35, 42, 73].

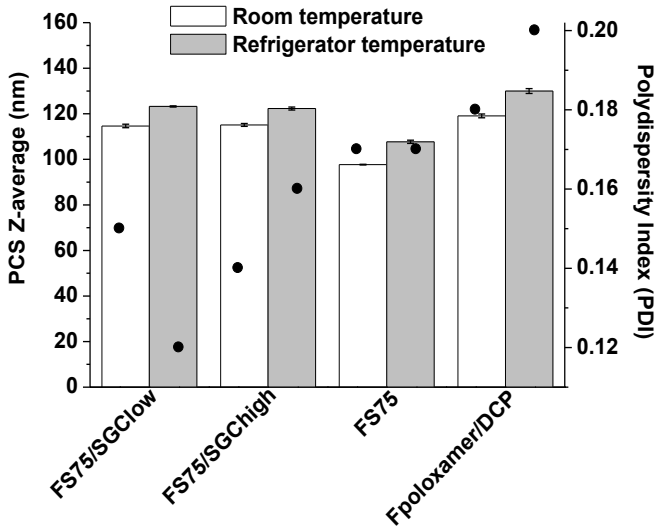

Figure 4.1: PCS z-average mean particle size (bars) and polydispersity indices (PDI, circles) of the four D114 formulations stored at room and refrigerator temperature (n = 3).

It was reported earlier [39] that colloidal emulsions and lipid nanoparticles that were prepared by the homogenization process and with phospholipids as emulsifier contain a significant amount of small unilamellar vesicles (SUV) due to the excess emulsifier (phospholipid) used. The transfer experiments were intended to be done from the lipid nanoparticles to the different acceptors. According to this requirement, it was important to separate the lipid nanoparticles from the excess phospholipid. Thus, after crystallization of the lipid nanoparticles, the formulations that were prepared with the emulsifier Lipoid S75 were treated by ultracentrifugation in an attempt to remove excess phospholipid into the

supernatant [70-72]. The ultracentrifugation process was carried out on FS75/SGClow, FS75/SGChigh and FS75 only. Figure 4.2 illustrates the particle size of the resuspended lipid nanoparticles (pellets after ultracentrifugation). The dispersions had an acceptable PDI, which indicates the homogeneity of the resuspended nanoparticles. The particle size of the resuspended nanoparticles (pellets) was larger than that of the original nanoparticles (before ultracentrifugation) and this could be explained by the loss of the excess S75 emulsifier, which might lead to the aggregation of the nanoparticles. The particle size and PDI of the resuspended nanoparticles containing the drug models was nearly the same as without (figure 4.3).

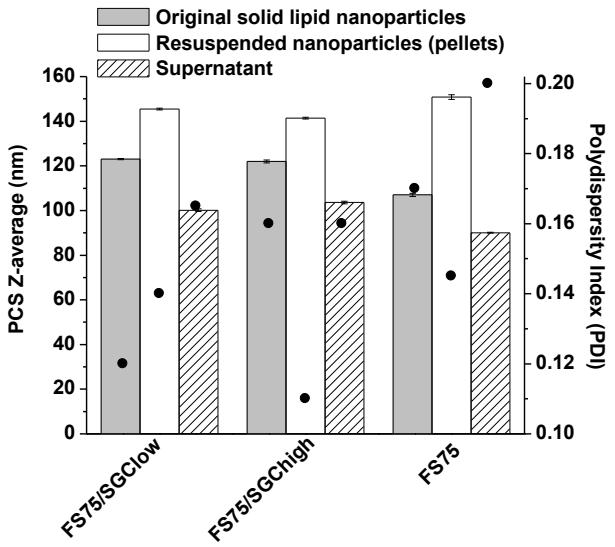

Figure 4.2: PCS z-average mean particle size (bars) and polydispersity indices (PDI, circles) of the three D114 formulations before and after ultracentrifugation (n = 3).

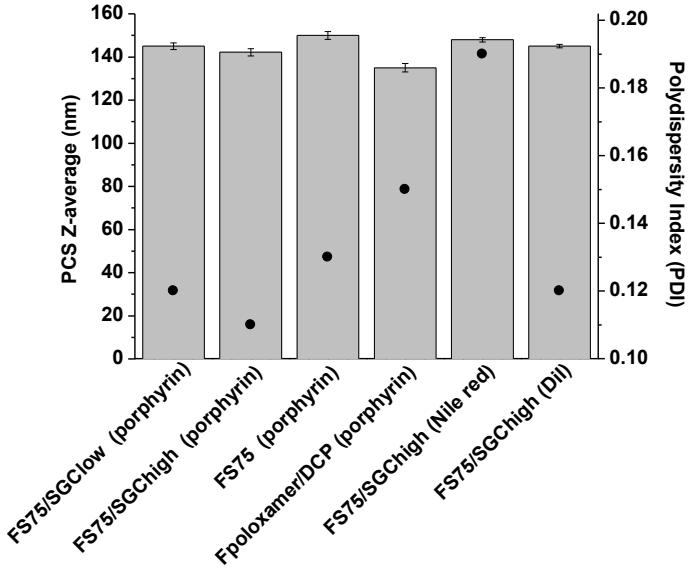

Figure 4.3: PCS z-average mean particle size (bars) and polydispersity indices (PDI, circles) of resuspended D114 lipid nanoparticles (crystalline nanoparticles after ultracentrifugation) loaded with the drug models porphyrin, Nile red and DiI (n = 3).

Figure 4.4 shows the particle size of FS75/SGClow, FS75/SGChigh and FS75 before and after ultracentrifugation as obtained from LD-PIDS measurements. There were no particles in the micrometer (μm) size range and all crystalline lipid nanoparticles before and after ultracentrifugation were located in the nanometer (nm) size range with a good homogeneity. Only the resuspended nanoparticles of FS75 contained a very small fraction of microparticles. These small amounts of large particles did not appear in the original formulation before ultracentrifugation indicating that they were formed during the ultracentrifugation/redispersion process. The LD-PIDS results confirmed the PCS data where a slight increase in the particle size after ultracentrifugation was observed.

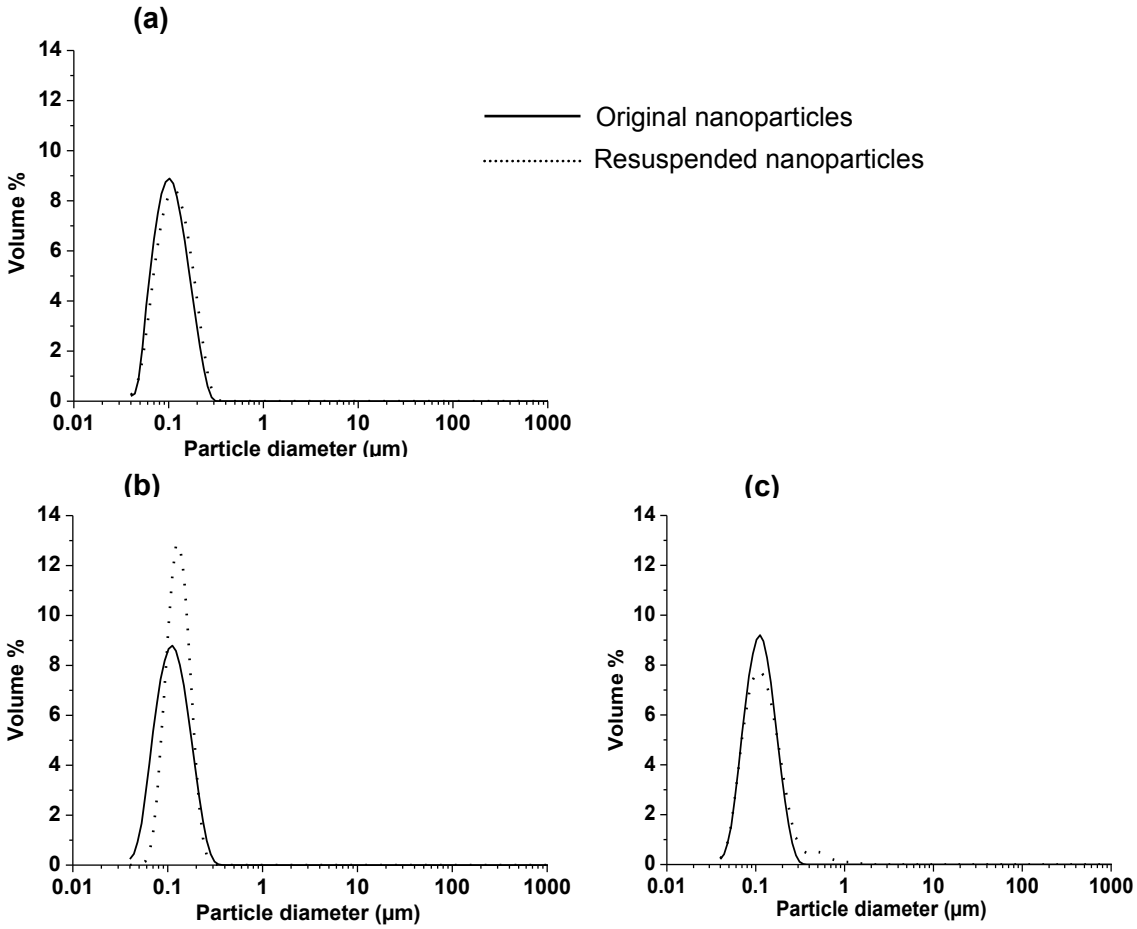

Figure 4.4: LD-PIDS particle size distributions of the original crystalline nanoparticles (before ultracentrifugation) and the resuspended crystalline nanoparticles (pellets after ultracentrifugation) a) FS75/SGClow, b) FS75/SGChigh and c) FS75.

Also the zeta potential of the four formulations was determined. As shown in figure, 4.5, the zeta potential of Fpoloxamer/DCP was low (-14 mV). This low zeta potential may be due to the presence of poloxamer on the surface of the nanoparticles so that DCP molecules could probably not reach the interface in the required position in order to obtain negatively charged nanoparticles. In other words, the presence of poloxamer hindered the localization of DCP in the surface of the nanoparticles and thus DCP molecules could not give a negative

charge to the nanoparticles. Negatively charged donors were, however, important for the nanoparticles to be suitable for the transfer experiments with the column technique. The high zeta potential of FS75/SGClow, FS75/SGChigh and FS75 could be attributed to the presence of S75. In spite of the neutral charge of Lipoid S75, the negative potential can be attributed to the presence of fatty acids in its composition [74]. As a confirmatory experiment, the zeta potential of small unilamellar vesicles prepared from S75 only was measured and it was –50 mV ± 2.1. This result was in agreement with the high zeta potential that was observed with FS75, which was prepared from Lipoid S75 only. The zeta potential of FS75/SGClow and FS75/SGChigh was higher than that of FS75 and this may be due to the presence of the anionic emulsifier SGC in these formulations.

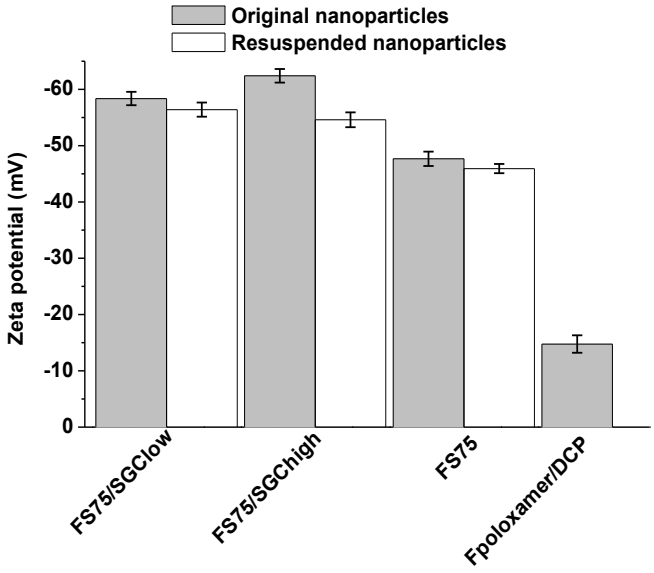

Figure 4.5: Zeta potential of the four D114 formulations before (original nanoparticles) and after (resuspended nanoparticles) ultracentrifugation (n = 3).

4.1.2 DSC of D114 nanoparticles

The objective of this study was concerned with the release and transfer behaviour of different drug models from the lipid nanoparticles, especially those in the crystalline form. From this point of view, monitoring of the crystalline status was a crucial point and was carried out by DSC measurements. Another important aim of these DSC measurements was to determine the effect of the ultracentrifugation/redispersion process on the crystalline lipid nanoparticles. Figure 4.6 shows the DSC melting curves of FS75/SGClow, FS75/SGChigh and FS75 before and after ultracentrifugation. The DSC curves of the resuspended nanoparticles indicated that these particles were in a crystalline form. For more detailed evaluation, sum curves of the resuspended nanoparticles and supernatant layer curves were

constructed for FS75/SGClow, FS75/SGChigh and FS75. By comparing these sum curves with the melting curves of the original crystalline nanoparticles before ultracentrifugation a

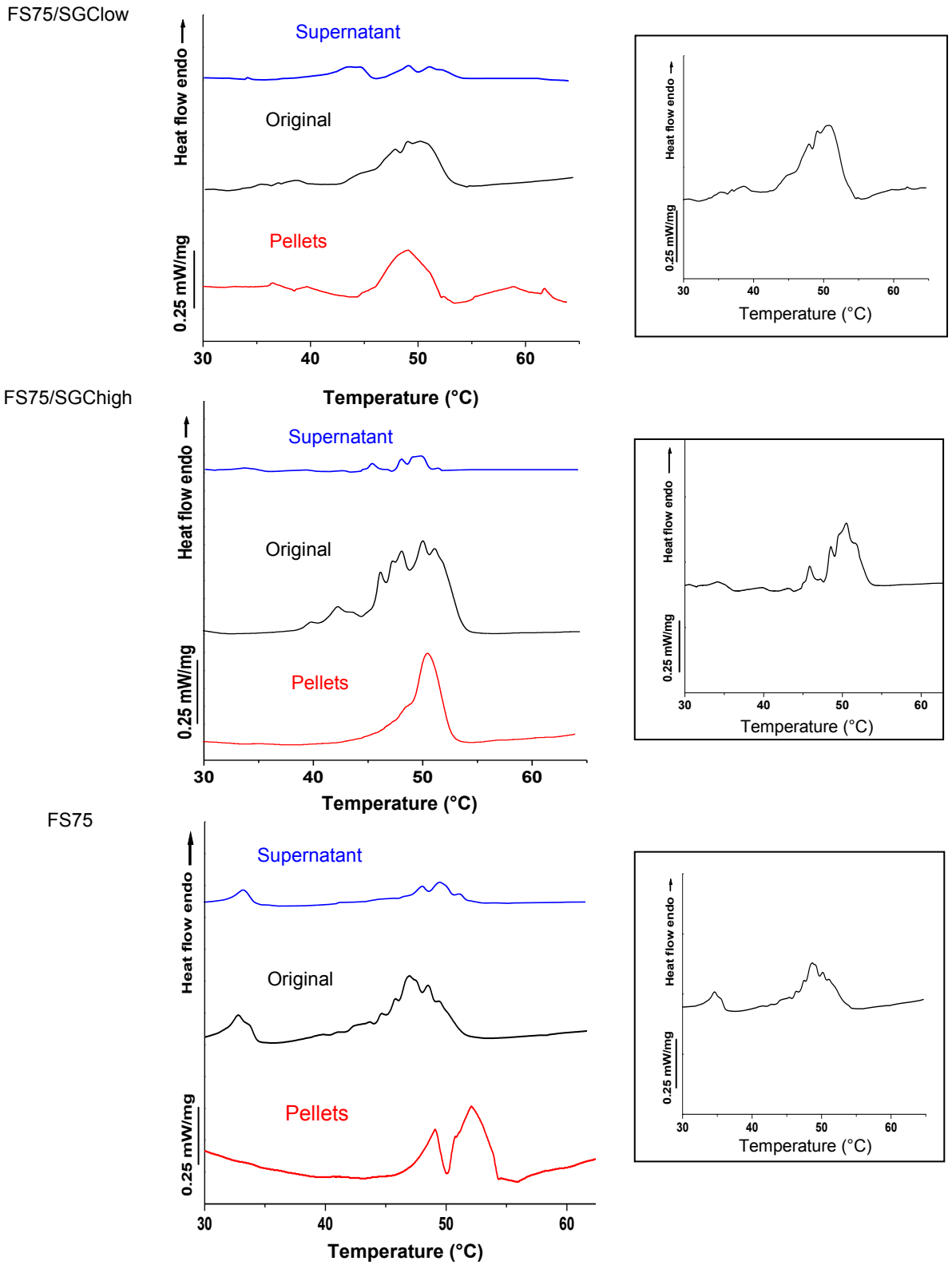

Figure 4.6: DSC heating curves of the original crystalline lipid nanoparticles before ultracentrifugation; resuspended nanoparticles after ultracentrifugation (pellets) and the supernatant layer of FS75/SGClow, FS75/SGChigh and FS75 stored at refrigerator temperature. The small right panel graphs are the sum curves of the resuspended nanoparticles and supernatant curves of FS75/SGClow, FS75/SGChigh and FS75.

high similarity was observed. This similarity indicated that there was no change in the nanoparticles after ultracentrifugation. DSC of the supernatant layers was carried out to determine if these layers contain crystalline trimyristin lipid nanoparticles or not. According to figure 4.6, these supernatant layers did contain crystalline particles. Obviously, these particles were very small because the melting transition was broadened and displayed several melting maxima [42] as compared to the melting curves of the resuspended nanoparticles. These small particles could not be separated into the pellets during the ultracentrifugation process. The graphs displayed in figure 4.6 are a good illustration of the fact that the melting behaviour of triglyceride nanoparticles strongly depends on particle size [42]. Particles in coarser dispersions melted in a single transition with a maximum slightly below that of the bulk material reflected in the melting behaviour of the crystalline resuspended nanoparticles (particle size was about 140-145 nm). On contrary to the resuspended nanoparticles, the melting curves of the original crystalline nanoparticles before ultracentrifugation (particle size was about 115-120 nm) and the melting curves of the supernatant layers (particle size was about 90-100 nm) displayed several distinct melting maxima (stepwise melting) according to figure 4.6. This stepwise melting is most probably due to the subsequent melting of classes of particles with different platelet heights (different particle thicknesses) [42, 75-77].

4.1.3 Cryo transmission electron microscopy (Cryo-TEM) of D114 nanoparticles

Figure 4.7 shows cryo-TEM images of the crystalline lipid nanoparticles of FS75/SGClow and FS75/SGChigh before and after ultracentrifugation. In this figure, the presence of weak circular and ellipsoidal structures, which represent thin platelets in top view, can be observed. If the particles are viewed edge-on, they appear as dark rods or needles since, in this position, the increased thickness of the structures leads to a darker appearance [39, 78]. According to figure 4.7, the presence of these structures could be observed in all investigated samples, including the supernatant layer. These results were in agreement with the DSC data, which illustrated the loss of nanoparticles into the supernatant. A small amount of liposomal structures could be observed in the images of the supernatant layer (figure 4.7 (a)) where they appeared as small spherical structures or ring shaped structures. These liposomal structures could not, however, be observed in figure 4.7 b and c, the images of resuspended nanoparticles (pellets) after ultracentrifugation and the original lipid nanoparticles (before ultracentrifugation). In case of the original nanoparticles, the liposomal structure may not be observable due to the abundance of the crystalline nanoparticles in the medium. In the images of the resuspended nanoparticles, the lack of these liposomal structures might be correlated with their removal after the ultracentrifugation process.

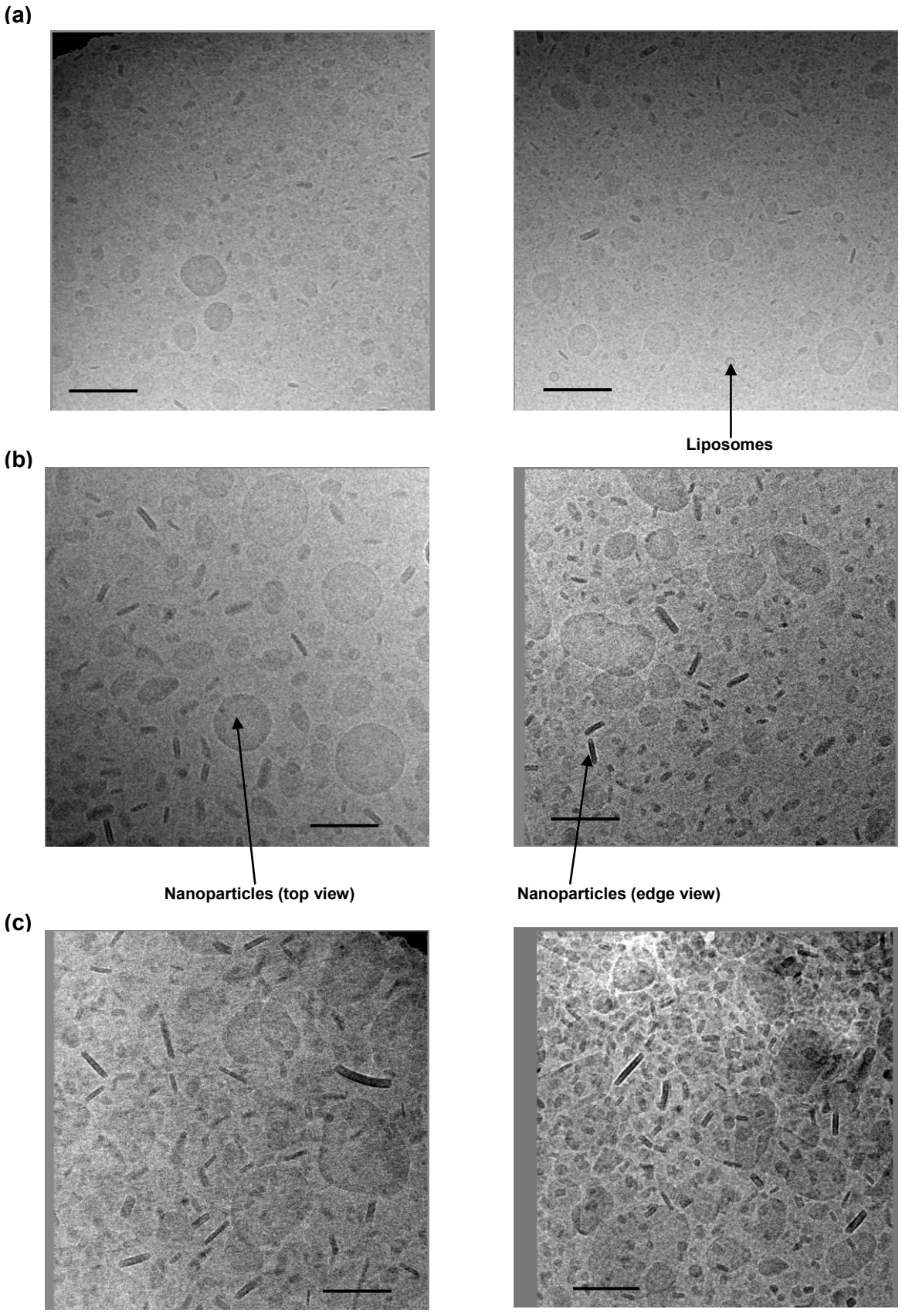

Figure 4.7: Cryo-TEM images of FS75/SGClow (left panel) and FS75/SGChigh (right panel); a) supernatant layer; b) resuspended nanoparticles (pellets) after ultracentrifugation; c) original nanoparticles before ultracentrifugation. The bar represents 200 nm.

4.1.4 ^{31}P- spectroscopic investigation of D114 nanoparticles

^{31}P-NMR spectroscopy was used to confirm the presence of liposomes due to excess S75 in the prepared nanoparticles and to determine the distribution of the phospholipid between the triglyceride nanoparticles and the liposomes. As reported before, small phospholipid-containing structures, such as micelles and sonicated vesicles, lead to relatively narrow, symmetrical ^{31}P-NMR lines [79-80]. Unsonicated phospholipid bilayers (large multilamellar structures or large unilamellar liposomes), on the other hand, exhibit broad, unsymmetrical lines. Figure 4.8 shows the NMR spectra of FS75/SGChigh and FS75 (original nanoparticles before ultracentrifugation, resuspended nanoparticles and supernatant layer). Two signals with different line shapes can be observed in the original nanoparticles (figure 4.8 (a)). A larger and sharper signal (around 0 ppm) was attributed to phospholipid headgroups in a more hydrophilic environment (liposomes formed by the excess S75). The broader zone of resonance (around 5 ppm) was attributed to the phospholipid headgroups in a lipophilic environment, which belong to the phospholipid coat of the trimyristin nanoparticles. The sharp signal at 0 ppm, which represents the phospholipid of the liposomes, was lost after centrifugation and only the broader signal (the phospholipid coat of the trimyristin nanoparticles) was found in the resuspended nanoparticles (figure 4.8 (b)). Both signals (the sharp and the broad one) were observed in the supernatant layer after ultracentrifugation, which indicates the presence of the two populations of the phospholipid (phospholipid coat of the triglyceride particles and phospholipid in liposomes due to the excess S75) (figure 4.8 (c)).

To confirm that the sharp signal corresponds to the liposomes (from excess S75) and the broad signal corresponds to the phospholipid coat of the triglyceride particles praseodymium chloride ($PrCl_3$) was added to the different dispersions as a shifting reagent. $PrCl_3$ only interferes with the accessible phospholipid (phospholipid of the outer liposomes layer and phospholipid coat of the triglyceride nanoparticles) but not with the inner phospholipid layer of liposomes.

^{31}P-NMR measurements in the presence of $PrCl_3$ reveal that the sharp peak was still present in the case of the original formulations before ultracentrifugation but the intensity of this peak was smaller than without $PrCl_3$ (figure 4.8 (a) right panel). This decrease in the intensity was due to the shift of the signal of the accessible phospholipid headgroups and only this sharp peak is related to the inaccessible phospholipid headgroups belonging to the inner phospholipid layer of liposomes. The broad peak was shifted to about 10 ppm. Corresponding results were obtained with the supernatant layer after the ultracentrifugation process, which indicates the presence of triglyceride nanoparticles as well as liposomes in this supernatant layer (figure 4.8 (c) right panel). In case of the resuspended nanoparticles

(pellets) the broad peak related to the phospholipid coat of the triglyceride nanoparticles was shifted to about 10 ppm (figure 4.8 (b) right panel).

The results obtained from ^{31}P-NMR spectroscopy after addition of the shifting reagent confirm the results that were obtained without $PrCl_3$, which indicate that the sharp signal is related to the liposomes while the broad signal is related to the phospholipid coat of the triglyceride nanoparticles. The loss of the sharp signal after ultracentrifugation indicates that the excess S75 liposomes were removed by the ultracentrifugation technique. Although ultracentrifugation is a good technique to separate the excess S75 liposomes from the nanoparticles, it led to the loss of a fraction of triglyceride nanoparticles as observed from the presence of the broad signal in the supernatant layer, which belongs to the phospholipid coat of the triglyceride nanoparticles. NMR data suggest the existence of SUV in addition to the triglyceride nanoparticles in the systems prepared by using S75 as a surfactant. NMR analysis confirmed the results that were observed before with DSC and cryo-TEM, which showed the presence of a fraction the triglyceride nanoparticles in the supernatant layer.

As a confirmatory experiment, ^{31}P-NMR spectroscopy of the small unilamellar vesicles, which were prepared from S75 only, was performed. A sharp signal at about 0 ppm (figure 4.9 (a)) was observed as detected before with the lipid nanoparticle formulations confirming that this sharp signal is due to phospholipid headgroups in a more hydrophilic environment (S75 liposomes). Two signals were observed after mixing the small unilamellar vesicles with the resuspended crystalline nanoparticles of FS75/SGChigh (figure 4.9 (b)). The two signals were the sharp signal belonging to the phospholipid headgroups of the S75 unilamellar vesicles, and the broader signal attributed to the phospholipid headgroups in a lipophilic environment (phospholipid coat of the triglyceride nanoparticles). Shifting of this broader signal in the mixture between the small unilamellar vesicles and the resuspended crystalline nanoparticles was observed after the addition of $PrCl_3$ (figure 4.9 (c)).

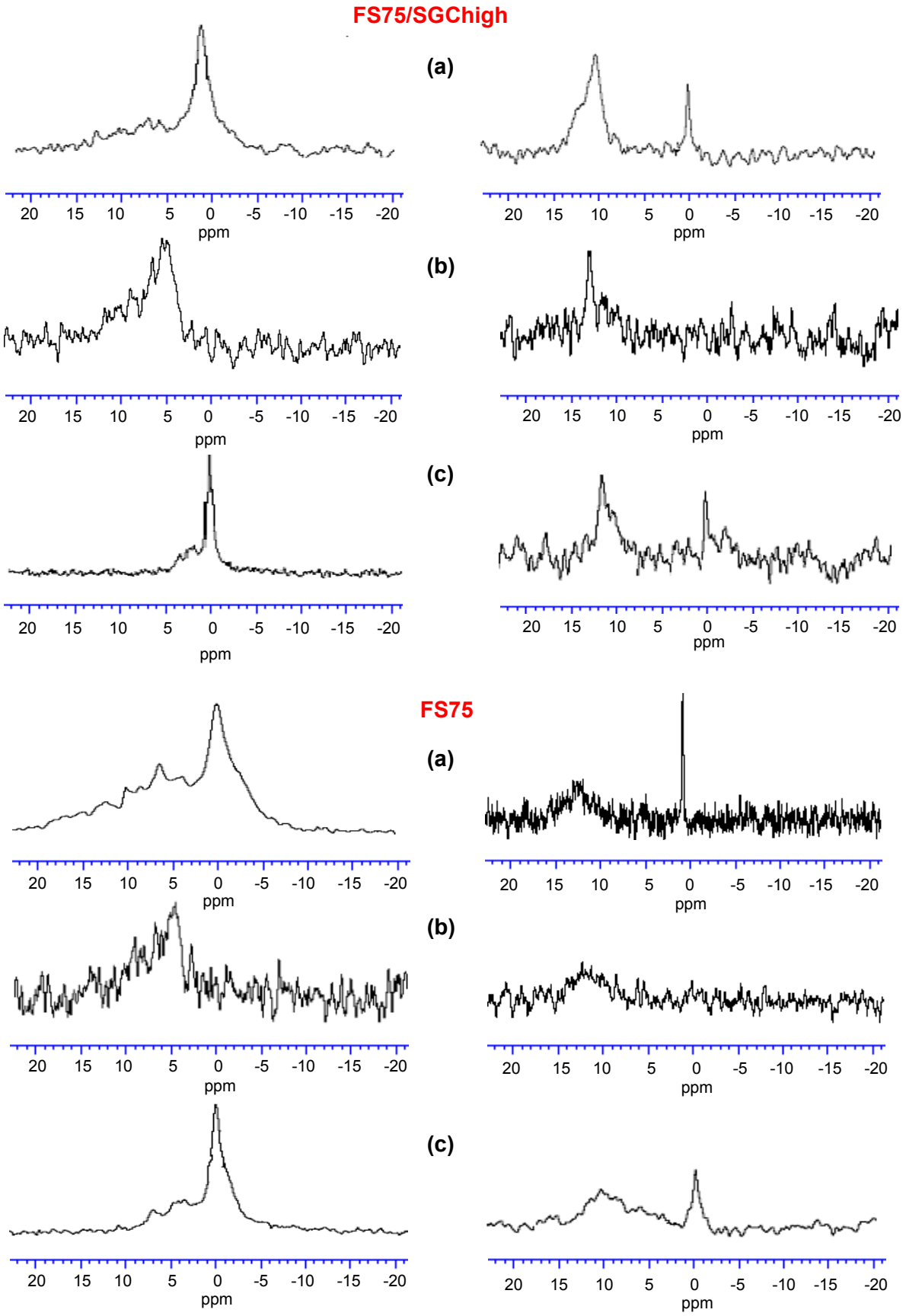

Figure 4.8: ^{31}p-NMR spectra of the crystalline lipid nanoparticles of FS75/SGChigh and FS75; (a) original nanoparticles before ultracentrifugation; (b) resuspended nanoparticles or pellets; (c) supernatant layer; without $PrCl_3$ (left panel) and with $PrCl_3$ (right panel).

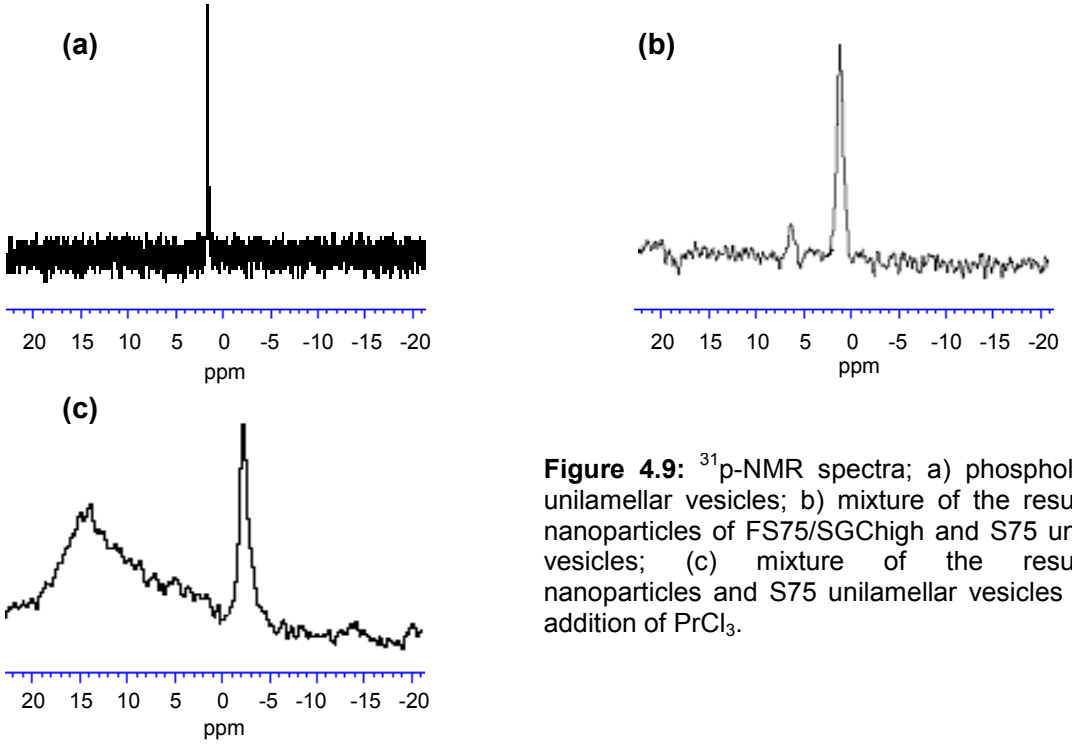

Figure 4.9: ^{31}p-NMR spectra; a) phospholipid S75 unilamellar vesicles; b) mixture of the resuspended nanoparticles of FS75/SGChigh and S75 unilamellar vesicles; (c) mixture of the resuspended nanoparticles and S75 unilamellar vesicles after the addition of $PrCl_3$.

4.1.5 Determination of the lipid content by HPLC

Since the ultracentrifugation process may lead to a loss of triglyceride from the formulations, a determination of the real D114 content in the nanoparticles formulations was performed. Determination of the lipid content in the lipid nanoparticles was carried out by HPLC with an evaporative light scattering detector (ELSD). The HPLC analysis of D114 showed a distinct peak at about 2 minutes (figure 4.10). The plot of the peak area versus sample concentration in double logarithmic coordinates gave a linear correlation, which showed a good correlation coefficient (R^2) = 0.999 (figure 4.11).

The content of trimyristin in FS75/SGClow, FS75/SGChigh, FS75 and Fpoloxamer/DCP before and after ultracentrifugation was determined from the calibration curve. The amount of trimyristin remaining in the redispersed nanoparticle suspensions after ultracentrifugation was 67%, 77% and 72% for FS75/SGClow, FS75/SGChigh and FS75 respectively (table 4.1). The low trimyristin content in FS75/SGClow after ultracentrifugation may be attributed to the filtration of this formulation (the amount before filtration was 37.5 mg/ml and the percentage was 75%). According to the HPLC analysis of the supernatant layers of the three nanoparticle formulations about 20% of the trimyristin was lost into the supernatant during the ultracentrifugation process. This is in agreement with the results of DSC, cryo-TEM and NMR measurements; all showed that the supernatant layer contained a fraction of the crystalline lipid nanoparticles (the very small particles).

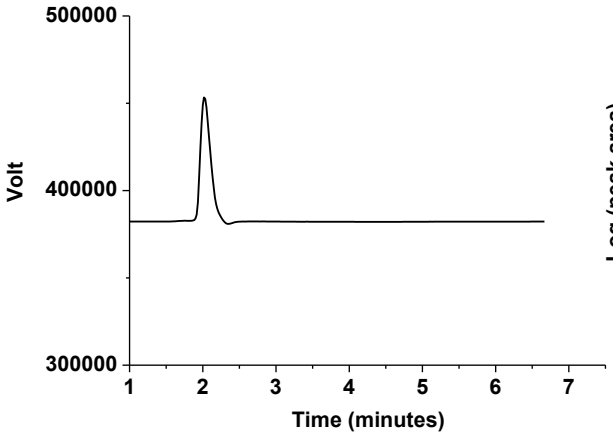

Figure 4.10: HPLC analysis of D114 using evaporative light scattering detection (ELSD) revealing one distinct peak at about 2 minutes.

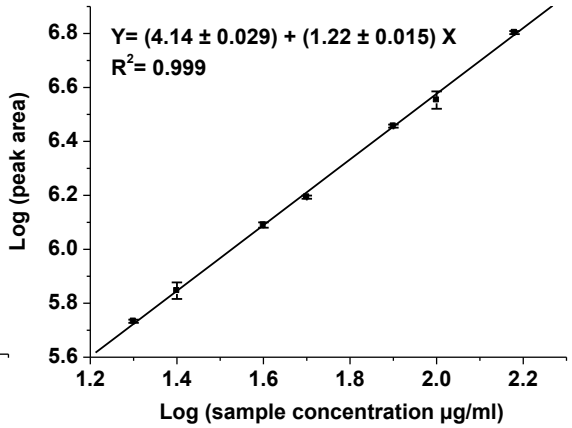

Figure 4.11: HPLC calibration curve for D114 with the evaporative light scattering detector (ELSD).

Table 4.1: Concentration of the matrix lipid trimyristin (D114) in the original samples (before ultracentrifugation), resuspended nanoparticles (pellets) and the supernatant layer of FS75/SGClow, FS75/SGChigh, FS75 and Fpoloxamer/DCP as determined by HPLC

Formula		Concentration of D114 mg/ml	% of D114 in relation to the original samples
Original samples	FS75/SGClow	50.25 ± 0.12	-
	FS75/SGChigh	50.75 ± 0.2	-
	FS75	45.5 ± 0.03	-
	Fpoloxamer/DCP [a]	50.9 ± 0.5	
Resuspended particles (pellets)	FS75/SGClow	33.5 ± 0.15	67%
	FS75/SGChigh	39 ± 0.18	77%
	FS75	32.8 ± 0.11	72%
Supernatant	FS75/SGClow	10.5 ± 0.07	21%
	FS75/SGChigh	9.8 ± 0.045	20%
	FS75	6.8 ± 0.11	16%

[a] Fpoloxamer/DCP was not subjected to ultracentrifugation because it does not contain the phospholipid S75 as emulsifier.

4.1.6 Drug content

Table 4.2 shows the drug distribution between the resuspended crystalline lipid nanoparticles of FS75/SGClow, FS75/SGChigh and FS75 after ultracentrifugation and the corresponding supernatant layers. According to these results the drug affinity is higher for

liposomes (the supernatant layer) than for the resuspended lipid nanoparticles. It has been reported earlier that crystalline lipid nanoparticles exhibit a low drug payload capacity and drug expulsion into the aqueous phase may occur due to the transition into highly ordered lipid particles during lipid crystallization [13, 34, 41].

Table 4.2: Distribution of porphyrin between resuspended crystalline nanoparticles and supernatant layer of FS75/SGClow, FS75/SGChigh and FS75, the percentages refer to the total amount of porphyrin introduced during the preparation

	FS75/SGClow	FS75/SGChigh	FS75
Resuspended nanoparticles (pellets)	26% ± 2.4 (0.13 mg/ml)	35% ± 1.5 (0.17 mg/ml)	32% ± 1.3 (0.16 mg/ml)
Supernatant layer	63% ± 1.7	66% ± 2.1	70% ± 1.9

As observed in the DSC, ^{31}P-NMR spectroscopy, cryo-TEM and the HPLC analysis of the supernatant layer, which contains the excess emulsifier S75, this supernatant layer also contains a certain amount of D114 crystalline nanoparticles and this may increase the drug content in the liposomal layers. The low drug content of the resuspended crystalline lipid nanoparticles of the FS75/SGClow (26%) may be due to the filtration process after sonication, which led to a loss of the drug together with the triglyceride as demonstrated in the HPLC analysis. The highest amount of the drug in the supernatant of FS75 (70%) may be attributed to the highest content of S75 (3.2%) and so the highest amount of liposomes in this formulation.

4.1.7 Particle size of D118 nanoparticles

Figure 4.12 shows the particle size of the two formulations of D118 in the different physical state of the lipid. The particle size of the nanoparticles stored immediately after preparation at 4°C was lower than the particles that were placed in a shaker water bath at 50°C for 8 hours followed by storage at 23°C. This indicates that the particles stored at 4°C may be in the α-form while the particles heated to 50°C for 8 hours may be in the β-form. As reported before [67], the changes in the polymorphic form are accompanied by increase in the particle size, which explains the difference in the particle size between the cold stored particles and the particles heated to 50°C.

The particle size was also measured with LD-PIDS in order to determine if any large particles (µm size range) had formed after heating the nanoparticles to 50°C (figures 4.13 and 4.14). µm-sized particles were not detected and no remarkable difference in the particle size could be observed between the different types of particles of the two formulations.

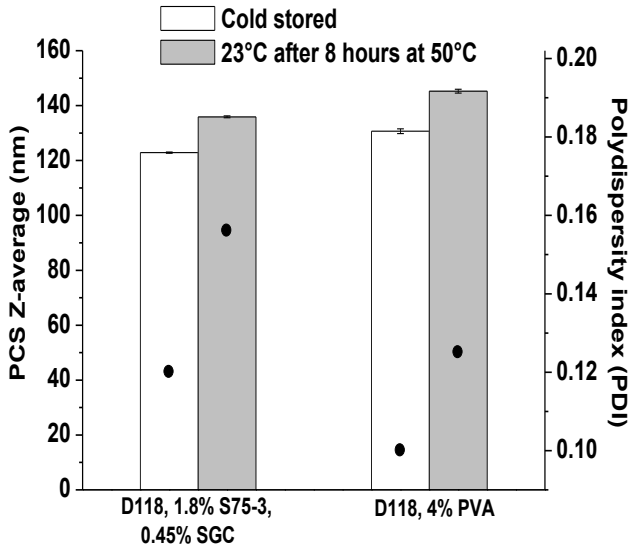

Figure 4.12: PCS z-average mean particle size (bars) and polydispersity indices (PDI, circles) of D118 nanoparticles stored at 4°C immediately after preparation or at 23°C after heating to 50°C for 8 hours (n = 3).

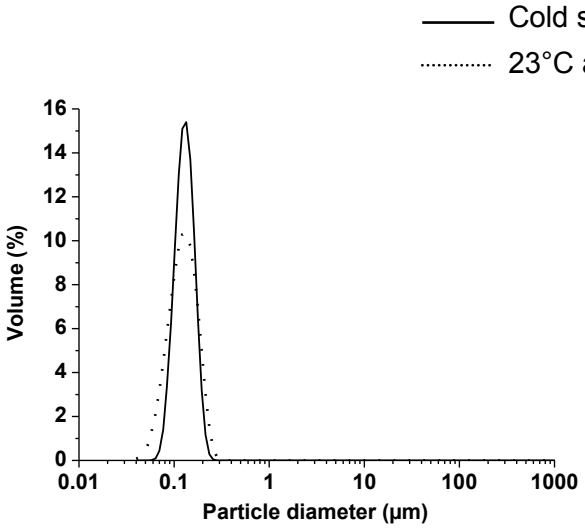

Figure 4.13: LD-PIDS particle size distribution of D118 nanoparticles prepared with 1.8% S75-3 and 0.45% SGC and stored at 4°C immediately after preparation or at 23°C after heating to 50°C for 8 hours.

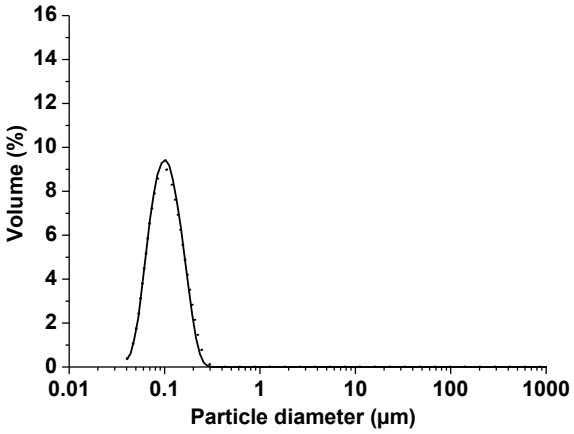

Figure 4.14: LD-PIDS particle size distribution of D118 nanoparticles prepared with 4% PVA and stored at 4°C immediately after preparation or at 23°C after heating to 50°C for 8 hours.

4.1.8 DSC of D118 nanoparticles

In order to confirm the physical states of the donor D118 lipid nanoparticles and to determine their polymorphic form, DSC measurements were performed. Figure 4.15 (a and b) illustrates the DSC melting and cooling curves of D118 nanoparticles stabilized with 1.8% S75-3 and 0.45% SGC. The heating curve of the cold stored D118 nanoparticles displayed a large endotherm around 52°C which points to the presence of α-polymorph (figure 4.15 (a)). Aging the sample at elevated temperatures (50°C for 8 hours) close to the α-melting point transformed the particles into the β-modification (figure 4.15 (b)). The presence of α-

polymorph in case of the sample stored at 4°C could be attributed to the stabilization of tristearin nanoparticles with an emulsifier mixture containing hydrogenated soybean phospholipid (with fully saturated acyl chains) [65-66]. This hydrogenated soybean phospholipid forms a shell of solidified phospholipid in the emulsifier monolayer surrounding the triglyceride core of the nanoparticles. This solidified phospholipid shell could act as a template for surface nucleation causing the increase in the crystallization temperature (about 38°C) and suppresses the polymorphic transformation (figure 4.15 (a, b)).

For tristearin nanoparticles stabilized with 4% PVA and stored at 4°C immediately after preparation, there was no evidence of the presence of β-polymorph because there was no

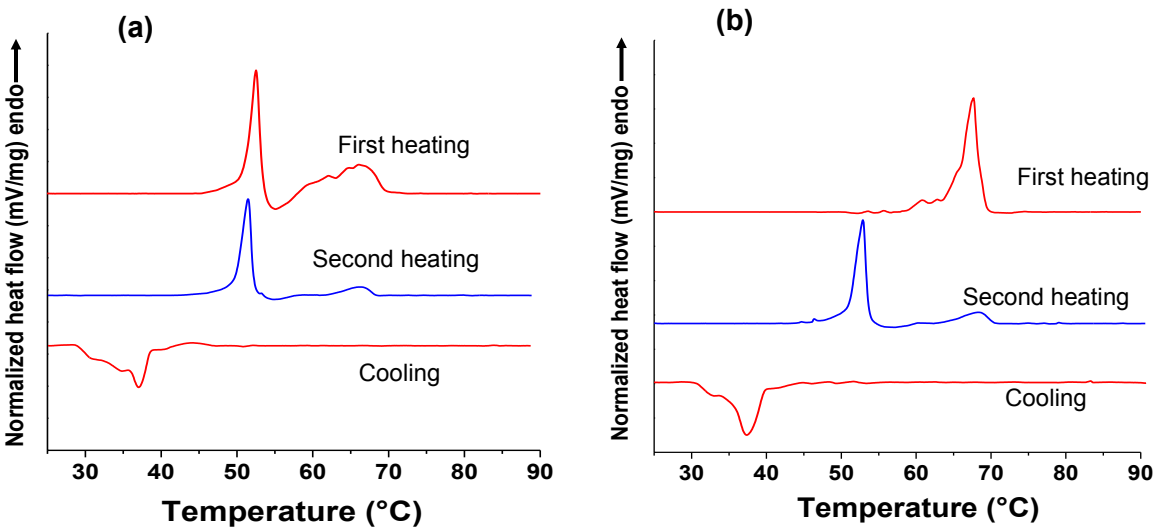

Figure 4.15: DSC melting and cooling curves of D118 nanoparticles prepared with 1.8% S75-3 and 0.45% SGC as stabilizers. a)- Particles stored at 4°C immediately after preparation, b)- Particles heated to 50°C for 8 hours and stored at 23°C.

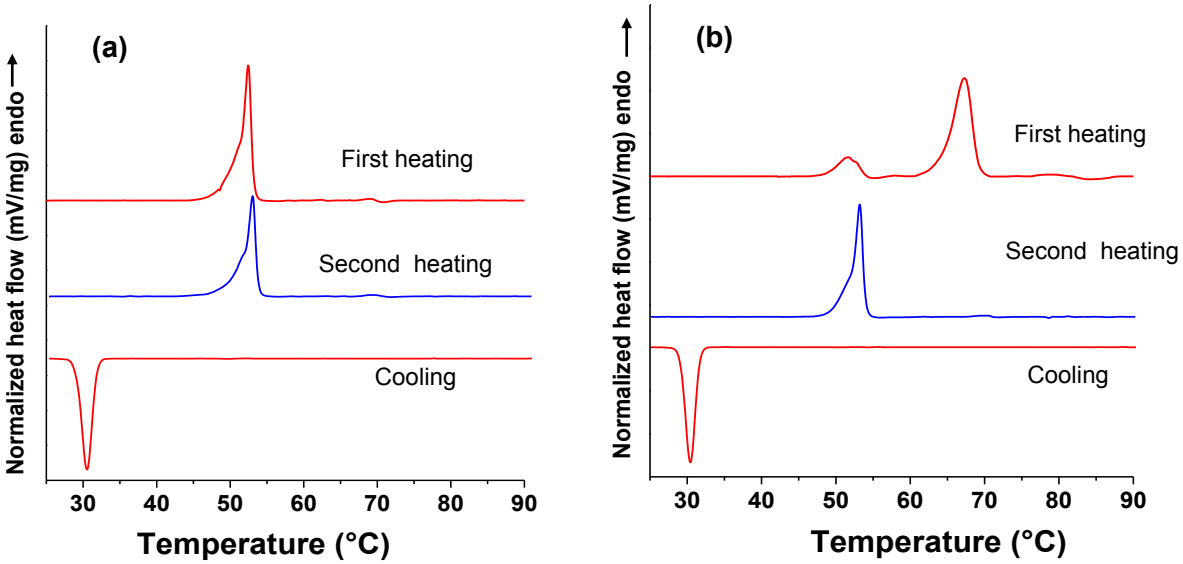

Figure 4.16: DSC melting and cooling curves of D118 nanoparticles prepared with 4% PVA as a stabilizer. a)- Particles stored at 4°C immediately after preparation, b)- Particles heated to 50°C for 8 hours and stored at 23°C.

melting peak in the β-polymorphic region (about 68°C). Only one endothermic peak around 52°C, which points to the presence of α-polymorph, was detected (figure 4.16 (a)). Aging this sample at elevated temperatures (50°C for 8 hours) close to the α-melting point transformed the particles into the β-modification (figure 4.16 (b)). Unlike the particles stabilized with S75-3, which showed complete transformation into β-modification by aging at 50°C, the particles stabilized with 4% PVA did not transform completely under these conditions but a small fraction of the particles remained in the α-form (figure 4.16 (b)). The nanoparticles prepared with PVA showed also a high stability of the α-polymorph. One explanation might be that PVA causes a high viscosity or immobilization of the molecules in the interfacial region and therefore sterically hinders the conversion from α to β as reported before [67]. The crystallization temperature of the particles stabilized with 4% PVA was about 30°C (figure 4.16) while the crystallization temperature of the particles stabilized with 1.8% S75-3 was about 38°C (figure 4.15), which also confirms that the stabilization of the particles with hydrogenated soybean phospholipid increases the crystallization temperature due to the templating action of the solidified phospholipid shell.

4.1.9 Particle size and zeta potential of Miglyol nanoemulsions

Five formulations of Miglyol nanoemulsions were prepared by cold homogenization using different ratios between S75 and EPC as stabilizers. The particle size of the five formulations ranged between 100 and 110 nm with a good PDI ranging from 0.11 to 0.125 (figure 4.17). This small particle size and the low PDI were very useful to check the retention of these particles on the ion exchange column. Any retention of such small particles on the column should be caused by the interaction (ion exchange) between the negatively charged emulsion and the gel inside the column and not due to the blockage of the column by large particles. Different ratios between S75 and EPC were used in the preparation of these emulsions to obtain emulsions with different zeta potential. As expected, the highest negative surface charge (-28 mV) was obtained with the highest S75 content [74] and lowest content of EPC, while the lowest negative surface charge (-13.5 mV) was obtained with the lowest S75 and the highest EPC content (figure 4.18).

The PCS-particle size of the Miglyol nanoemulsion, which was prepared from 5% Miglyol and 4% poloxamer 188, was 115 nm ± 0.8 with a homogenous particle distribution as the polydispersity index (PDI) was 0.14. No significant change in the particle size was observed after addition of porphyrin (z-averge: 120 nm ± 0.54, PDI: 0.15). The zeta potential of this nanoemulsion without porphyrin was –4.6 mV. This Miglyol nanoemulsion was used also as acceptor in the transfer experiments with the ion exchange column technique due to its small particle size and neutral zeta potential.

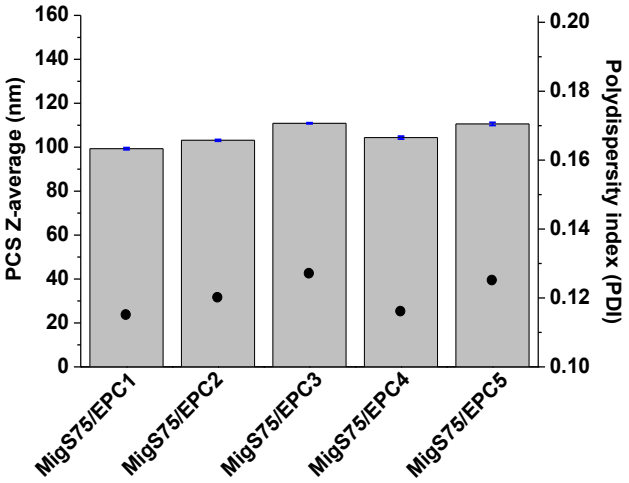

Figure 4.17: PCS z-average mean particle size (bars) and polydispersity indices (PDI, circles) of Miglyol nanoemulsions prepared with different ratios between S75 and EPC.

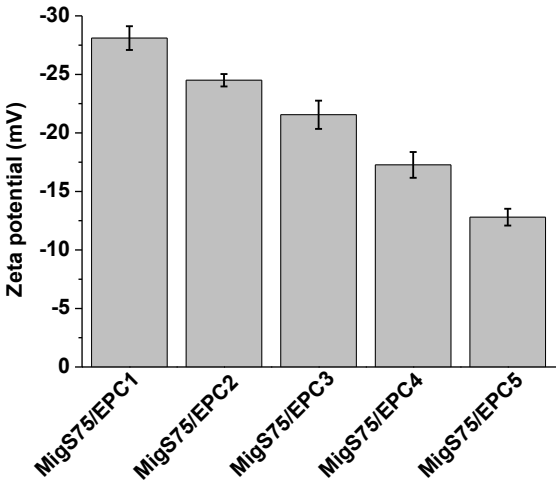

Figure 4.18: Zeta potential of the Miglyol nanoemulsions prepared with different ratios between S75 and EPC.

4.2 Characterization of the acceptor particles

4.2.1 Unilamellar and multilamellar vesicles

The acceptor vesicles (unilamellar or multilamellar) were prepared from egg phosphatidyl choline (EPC) and cholesterol with a molar ratio of 8:2 for EPC/cholesterol. EPC and cholesterol were chosen to mimic the cell membranes and other lipid compartments in the body and to obtain acceptor vesicles with neutral charge to be used on the ion exchange column [3, 56, 68]. The small unilamellar vesicles as an acceptor particles could be prepared from EPC only as described before [57]. Recently, liposomes were utilized for studying drug transfer and uptake [4].

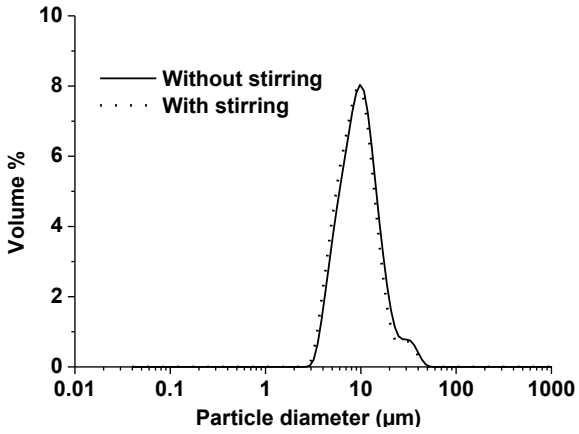

Figure 4.19: LD-PIDS particle size distributions of the acceptor MLV with a molar ratio between EPC/cholesterol of 8:2 measured with and without stirring.

The z-average particle size of the unilamellar vesicles from EPC and cholesterol that had been extruded through a 100 nm membrane filter was 151.3 ± 1.2 nm (PDI 0.07). The zeta potential was –5.34 ± 1.1 mV and thus close to neutrality. The mean particle size of the MLV liposomes was about 10 µm (figure 4.19). LD-PIDS of the MLV liposomes after 4 months of storage at refrigerator temperature showed no alterations in the mean particle size, which indicates the stability of these particles.

4.2.2 Particle size of o/w emulsion droplets

Figure 4.20 illustrates the particle size of the acceptor o/w emulsion, which was prepared by Ultra-Turrax homogenization. The mean particle size was about 6 µm.

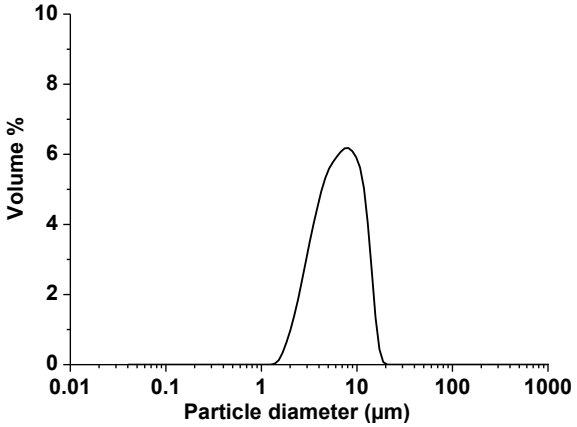

Figure 4.20: LD-PIDS particle size distribution of the o/w acceptor emulsion.

4.2.3 Particle size of monoolein dispersions

As pointed out in an earlier study, coarse glycerol monooleate/poloxamer (GMO/P407) dispersions can be prepared by simple mixing of the components followed by mechanical shaking for prolonged periods of time (12 h) [69]. Such dispersions consist of particles in the size range of 0.2-2 µm and a fraction of larger, visually observable particles of more than 10 µm diameter that tend to accumulate at the surface of the dispersion. It is generally necessary to homogenize GMO-based dispersions in order to get rid of macroscopic particle contaminants and to narrow the particle size distribution. However, the attempts to prepare cubic phase dispersions with small particles and with narrow particle size distributions by high shear energy homogenization usually lead to dispersions consisting of almost only noncubic, vesicular structures. It was reported before [18, 81-83], that heat treatment of monoolein/poloxamer dispersions could be used to transform such vesicular dispersions into dispersions of cubic phase or to improve the cubic/non-cubic particle ratio in dispersions already containing particles with cubic internal structure.

Figure 4.21 illustrates LD-PIDS particle size distributions of the monoolein dispersions prepared with different amphiphile (monoolein + poloxamer) concentrations (5, 7, 10 and 15%) and with 12% or 8% poloxamer (related to the total amphiphile amount) before and after autoclaving. After homogenization, the samples prepared with 5 and 7% amphiphile were translucent homogeneous dispersions with monomodal particle size distributions and mean sizes of about 100 nm. Heat treatment transformed these dispersions into milky fluids

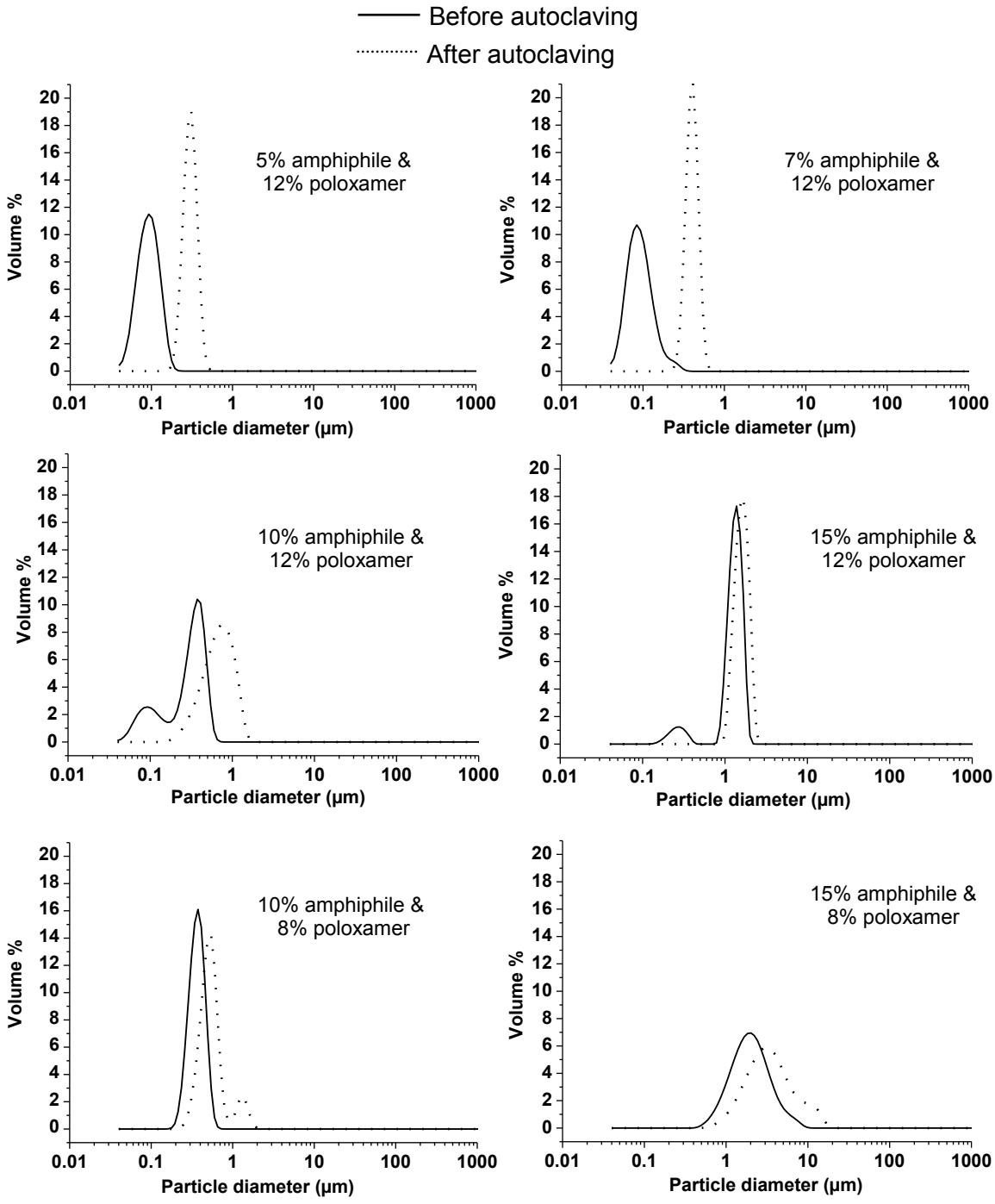

Figure 4.21: LD-PIDS particle size distributions of monoolein/poloxamer nanodispersions prepared with different amphiphile concentrations (monoolein + poloxamer) and with poloxamer concentrations of 12% and 8% (related to the total content of amphiphile) before and after autoclaving.

with a mean particle size of about 320 and 440 nm for the samples with 5 and 7% amphiphile, respectively.

The dispersions prepared with 10 and 15% amphiphile (12% poloxamer) were milky fluids already before autoclaving and characterized by bimodal particle size distributions with mean sizes of about 450 and 790 nm for the dispersion with 10 and 15% amphiphile, respectively. After autoclaving of these dispersions, there was no change in the physical appearance but an increase in the particle size (0.71 and 1.2 µm for the dispersion prepared with 10 and 15% amphiphile, respectively) and a monomodal particle size distribution was obtained. These results were in agreement with earlier observations showing that an increase in the amphiphile concentration leads to an increase in the particle size of the dispersion upon autoclaving [69]. The particle sizes obtained were, however, quite small to be used in the flow cytometric experiments. In order to prepare cubic particles in the micrometer size range to be used for the transfer experiments with the flow cytometric method, two other dispersions were prepared from 10 and 15% amphiphile but with lower concentration of poloxamer (8% related to the total amphiphile amount).

Figure 4.21 shows the particle size distributions of the dispersions prepared from 10 and 15% amphiphile with 8% poloxamer. The dispersions were milky fluids before and after autoclaving. The particle size of about 0.45 and 1.2 µm for the dispersions with 10 and 15% amphiphile, respectively, before autoclaving increased to 0.75 and 2.05 µm after autoclaving. The change in particle size upon heat treatment could be attributed to the particle fusion, which occurred during the heat treatment process. One hypothesis is that fusion is related to the reduced solubility and stabilizing efficiency exhibited by poly (ethylene oxide)-based substances at elevated temperatures [69]. According to the results of the particle size analysis, the autoclaved dispersions prepared from 15% amphiphile with 12 and 8% poloxamer were used as acceptor particles in the flow cytometric transfer experiments (a particle size of 1.2 and 2.05 µm can be detected by the flow cytometer).

4.2.4 Small angle diffraction measurements of monoolein dispersions

The occurrence of corresponding small angle X-ray reflections confirmed the existence of cubic particles in all autoclaved dispersions for all formulations with different amphiphile concentrations (figure 4.22). In contrast, no reflections were observed for the nonautoclaved dispersions prepared with 5 and 7% amphiphile. According to earlier results [18], these dispersions contain predominantly vesicular particles, which do not display any small angle reflections. The dispersions prepared from 10 and 15% amphiphile and different concentrations of poloxamer (8 and 12%) displayed distinct small angle reflections already before autoclaving, which indicates the presence of cubic particles. In all cases, the small angle X-ray reflections observed were characteristic of a P-type cubic phase.

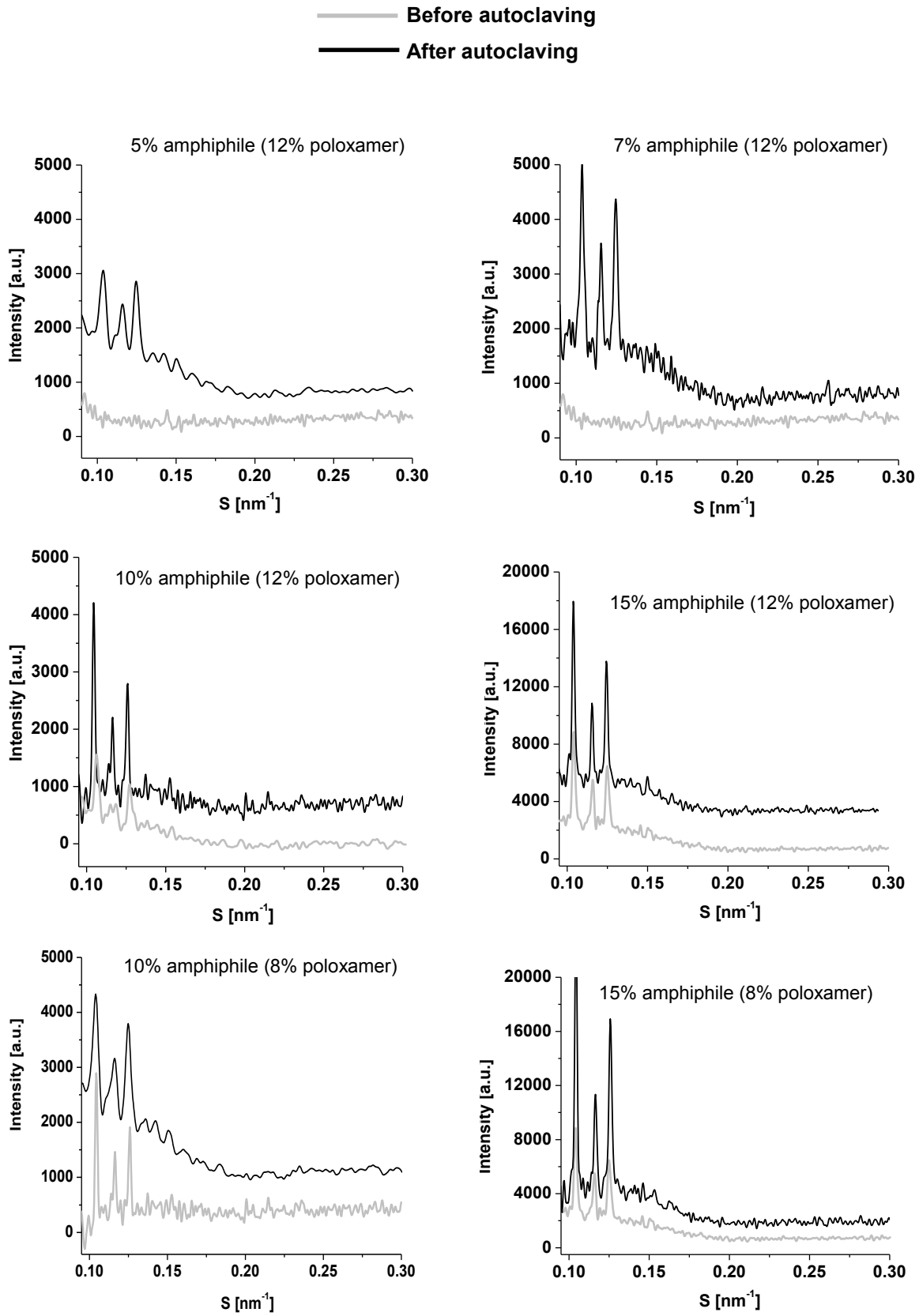

Figure 4.22: Small angle X-ray diffractograms of monoolein/poloxamer dispersions prepared with different amphiphile (monoolein and poloxamer) concentrations and with two poloxamer concentrations before and after autoclaving.
Up to concentrations of 10% amphiphile the intensity scale was adjusted to 5000, for 15% amphiphile the scale was adjusted to 20000

4.3 Transfer studies with the column method

4.3.1 Validation of the column method

Three validation experiments were performed to check the ability of the ion exchange column for the separation between the donor and acceptor particles and to determine if the neutral acceptor particles acquired any charge from the charged donor particles or not.

4.3.1.1 Acceptor recovery with radiolabeled unilamellar vesicles

A transfer experiment with radiolabeled acceptor liposomes was performed to investigate if the neutral acceptor liposomes were completely eluted from the column. Figure 4.23 shows the percent of acceptor vesicles eluted after 2, 8 and 24 hours of mixing with the donor particles of FS75/SGClow, FS75/SGChigh and FS75 (original nanoparticles before ultracentrifugation and resuspended nanoparticles after ultracentrifugation). The results show that with pre-equilibrated columns, 93-97% of the neutral acceptor vesicles were recovered in the eluate at all time points up to 24 hours. There were no differences in the elution of acceptor liposomes incubated with the donor before or after ultracentrifugation. The very low amount of the neutral acceptor vesicles retained on the column (3-7%) may be referred to a small amount of fusion, which may have occurred between the neutral vesicles and donors during incubation [56].The retention of the acceptor liposomes on the column was thus very low and this might indicate that there was no charge transfer from the different charged donors to the neutral acceptor vesicles. For more confirmation of this assumption, a second validation experiment was performed.

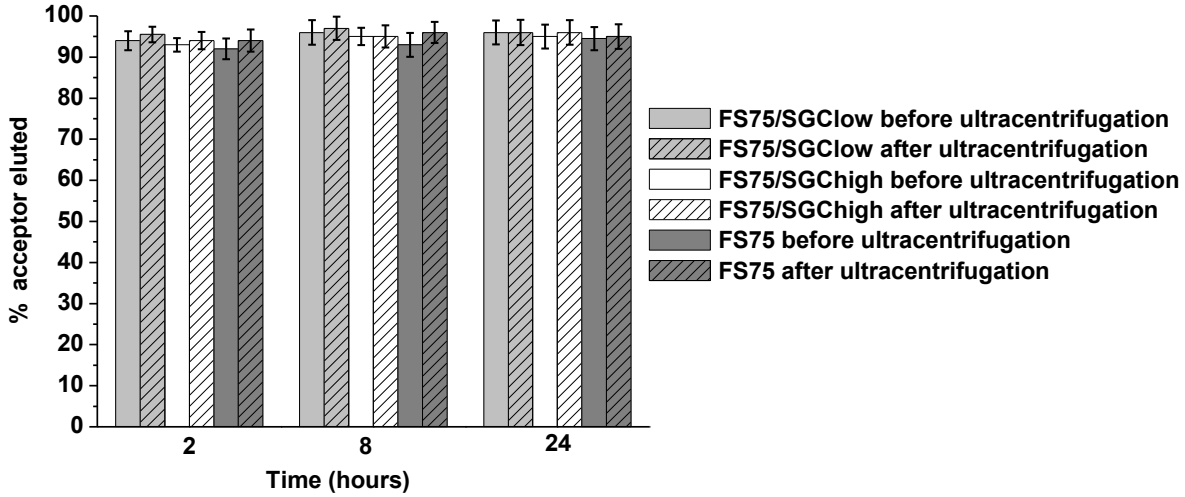

Figure 4.23: Percentage of radiolabeled acceptor liposomes eluted from the column after incubation with the donor for different time intervals (n = 3).

4.3.1.2 Charge transfer from the donor to the acceptor

In order to confirm that there was no charge transfer from the donor to the neutral acceptor particles, mixtures between the crystalline nanoparticles of FS75/SGChigh (original nanoparticles or resuspended nanoparticles) and neutral liposomes were separated by ultracentrifugation. Figure 4.24 (a and b) shows the zeta potential distribution curves of the mixture between the donor and acceptor after separation by ultracentrifugation. There was only one neutral peak observed in the supernatant layer of the mixture between the resuspended nanoparticles and the neutral liposomes (figure 4.24 (a) left panel). In case of the supernatant layer of the mixture between the original nanoparticles and the neutral liposomes, it could be observed that there were 2 peaks, one major peak of the neutral acceptor liposomes (-4 mV) and a minor peak of the unilamellar vesicles from the excess S75 (-45 mV) (figure 4.24 (b) left panel). From the zeta potential distributions of the two supernatant layers it could be concluded that there was no effect of the charged donor particles on the neutral liposomes or by other words there was no charge acquired by the

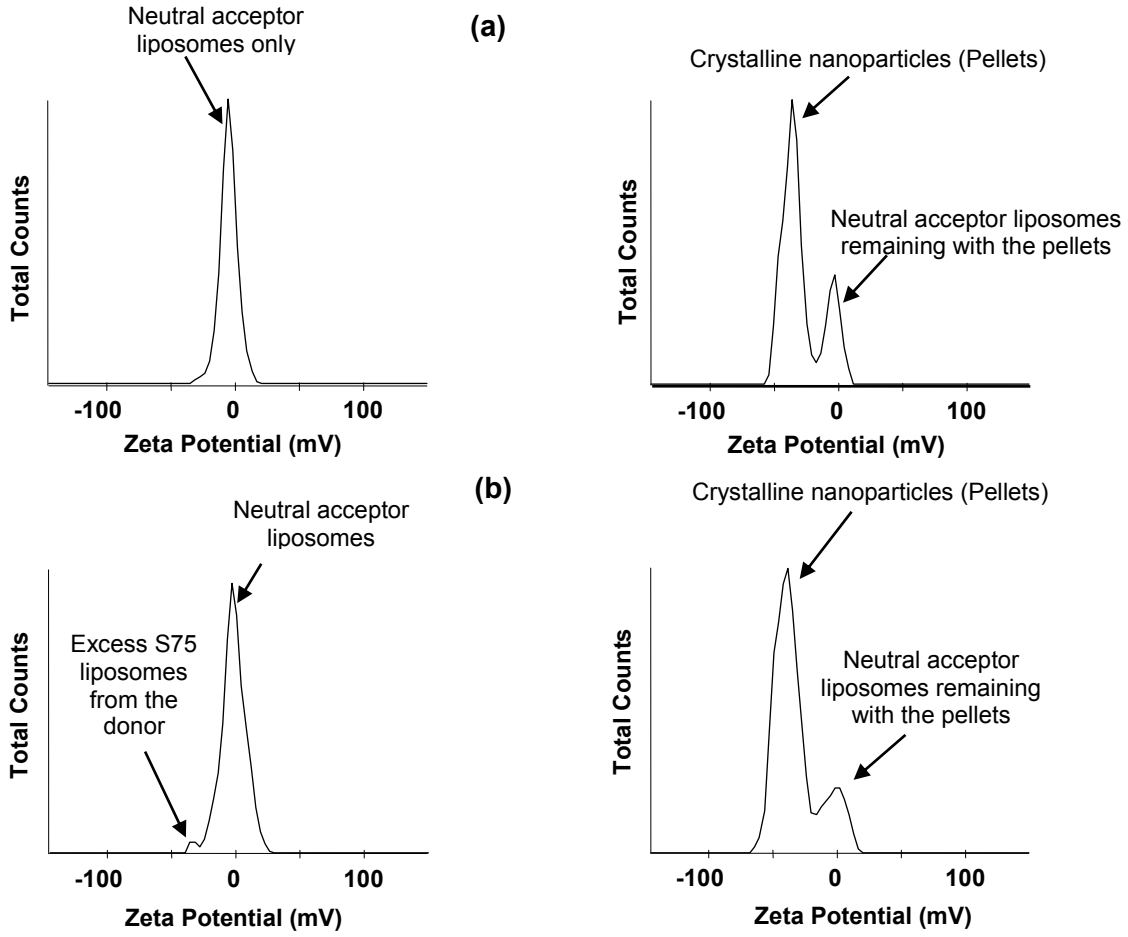

Figure 4.24: Zeta potential distribution of the mixture between the donor and acceptor particles after separation by ultracentrifugation at 35000 rpm for 1 hour; a) mixture between the resuspended crystalline lipid nanoparticles of FS75/SGChigh and the neutral acceptor liposomes; b) mixture between the original crystalline lipid nanoparticles of FS75/SGChigh and the neutral acceptor liposomes; supernatant layer (left panel); crystalline nanoparticles (right panel).

neutral acceptor liposomes from the charged donor. The small peak at neutral zeta potential in the curves of the pellets (figure 4.24 a and b (right panel)) may be attributed to the presence of a small amount of the neutral acceptor liposomes with the crystalline lipid nanoparticles.

4.3.1.3 Elution of the donor particles

Insufficient retention of the donor particles on the column would disturb the experiments. To check that the donor nanoparticles were completely retained on the column, 10 µl of the original samples (before ultracentrifugation), resuspended crystalline particles and resuspended liquid particles (the FS75/SGClow, FS75/SGChigh and FS75) were added to the column. After that, the drug concentration in the eluent was analysed. Less than 1% of the different donors were eluted from the column (table 4.3). These results indicate the good retention property of the DEAE-Sepharose column for the donor particles prepared with S75 due to their negative zeta potential (table 4.3). The same experiment was performed on the Fpoloxamer/DCP nanoparticles where more than 90% of the nanoparticles were eluted from the column (table 4.3). The low charge of these particles (zeta potential -14 mV) obviously does not allow their retention by DEAE-Sepharose.

Table 4.3: Percentage of the different donor particles eluted from the column

Formula		Zeta potential (mV)	Donor eluted from the column (%)
Original samples	FS75/SGClow	-58 ± 1.2	0.85 ± 0.042
	FS75/SGChigh	-62.5 ± 1.2	0.53 ± 0.033
	FS75	-47 ± 1.3	0.68 ± 0.063
	Fpoloxamer/DCP	-14 ± 1.5	92.2 ± 1.12
Resuspended crystalline nanoparticles (pellets)	FS75/SGClow	-56 ± 1.3	0.45 ± 0.021
	FS75/SGChigh	-55 ± 1.4	0.4 ± 0.032
	FS75	-46 ± 0.8	0.61 ± 0.014
Resuspended liquid nanoparticles (prepared by melting the crystalline ones)	FS75/SGClow		0.52 ± 0.025
	FS75/SGChigh		0.43 ± 0.027
	FS75		0.51 ± 0.042

Table 4.4: Elution of the Miglyol nanoemulsions with different zeta potential from the ion exchange column

Sample	Zeta potential (mV)	Nanoemulsion eluted from the ion exchange column (%)
MigS75/EPC1	-28	1.28 ± 1.02
MigS75/EPC2	-25	3 ± 1.05
MigS75/EPC3	-20	18 ± 3.6
MigS75/EPC4	-17	35 ± 4.8
MigS75/EPC5	-13	50 ± 6.3

4.3.2 Determination of the suitable zeta potential range for the column method

As seen from the previous section, the zeta potential had a great effect on the retention of the donor particles on the ion exchange column. According to this effect, it was important to determine the suitable zeta potential range for the donor particles to be used with the column method. To prepare nanoemulsions with different zeta potential, different concentrations of S75 and EPC were used. These experiments were performed on nanoemulsions and not the crystalline nanoparticles because nanoemulsions are stable with these emulsifier mixtures (S75 and EPC) while the crystalline nanoparticles may not stable with these emulsifier mixtures [39]. Table 4.4 illustrates the elution of emulsions with different zeta potential from the column. As expected, the nanoemulsion MigS75/EPC1 with the highest negative charge (-28 mV) shows the lowest percentage of elution from the column (1.28%) while the nanoemulsion MigS75/EPC5 with the lowest negative charge (-13.5 mV) shows the highest percentage of elution (50%). From these results it could be concluded that the emulsion or a donor with a zeta potential of –25 mV and higher can be used for the column method. Particles with a zeta potential of –20 mV and lower can not be used in the transfer experiments employing the column method for the separation between the neutral acceptor and the donor particles because a large fraction of the donor particles will be eluted.

4.3.3 Transfer of the different drug models to the acceptor unilamellar vesicles

The transfer experiments to the acceptor unilamellar vesicles were performed with the nanoparticle formulations FS75/SGClow, FS75/SGChigh and FS75 only because Fpoloxamer/DCP had a low zeta potential and was thus insufficiently retained on the column. Figure 4.25 (a, b and c) shows the porphyrin transfer from the crystalline and liquid donor particles of FS75/SGClow, FS75/SGChigh and FS75. The three formulations showed a rapid initial drug transfer. At a molar ratio of 1:25, 14%, 15% and 15.5% of porphyrin had been

transferred from the crystalline donors of FS75/SGClow, FS75/SGChigh and FS75, respectively, after 2 minutes (first time point of measurements). For the same formulations at a molar ratio of 1:100, the initial drug transfer (after 2 minutes) was 33.5%, 35% and 33% for FS75/SGClow, FS75/SGChigh and FS75. A plateau value was reached after about 40 minutes in all cases with similar equilibrium values (about 40 and 80% with molar ratios of 1:25 and 1:100, respectively) for the three formulations (table 4.5). This observation indicates that the time course of drug transfer did not depend on the lipid ratio between the donor and acceptor and that the lipid ratio only affects the amount of drug transfer (table 4.5).

The final amount of drug transferred from the three formulations at both donor: acceptor molar ratios was much lower than the expected values (theoretical values). Assuming an equal porphyrin distribution between the donor and acceptor, about 99% of the porphyrin was expected in the acceptor unilamellar vesicles at a molar ratio of 1:100 between the donor and acceptor and about 96% of the porphyrin was expected in the acceptor particles used at a molar ratio of 1:25.

These low equilibrium values might be attributed to the localization of the drug at the interface of the acceptor liposomes (porphyrin did not entrapped in the vesicles bilayer) [84], which means that after saturation of this interface the transfer stopped at low values. Additionally, the acceptor unilamellar vesicles were prepared from EPC with the addition of cholesterol, which increases the rigidity of the bilayer [85] and occupies a part of the accessible outer surface and so decreased the amount of drug transfer to the acceptor liposomes.

Increasing the acceptor to donor ratio from 1:25 to 1:100 led to an increase in the final percent of drug transferred (table 4.5, figure 4.25) and this may be attributed to the increase in the number of the acceptor particles relative to the donor particles. This increase in the number of the acceptor particles will lead to an increase in the accessible surface available for drug transfer.

There were no or only slight differences in the transfer between the crystalline and liquid donor for the three formulations at low donor: acceptor ratios (1:25) (figure 4.25). A slightly higher drug transfer from the crystalline donor particles compared to the liquid particles was observed at the higher donor: acceptor ratio (1:100) (figure 4.25). This higher drug transfer from crystalline compared to liquid donor might be attributed to the formation of highly ordered particles in the β modification upon crystallization, which leaves little space for the drug molecules, and so leads to the expulsion of drug to the surface of the crystalline particles [34, 41, 86-87].

Table 4.5: Results of the transfer studies with porphyrin to the acceptor unilamellar vesicles obtained by the column method assuming transfer kinetics according to equation [1]

Donor	Molar ratio	Total lipid concentration (mg/ml)	Transfer rate constant K (min^{-1})	Final % transferred	Equilibrium time (minutes)
FS75/SGClow (liquid)	1:25	18	0.1 ± 0.007	38.5 ± 1.6	40
	1:100	68	0.11 ± 0.011	76 ± 2.2	38
FS75/SGClow (crystalline)	1:25	18	0.1 ± 0.006	40 ± 1.9	38
	1:100	68	0.1 ± 0.01	79 ± 2.7	37
FS75/SGChigh (liquid)	1:25	18	0.1 ± 0.007	41 ± 2.2	38
	1:100	68	0.09 ± 0.008	78 ± 2.4	43
FS75/SGChigh (crystalline)	1:25	18	0.095 ± 0.005	43 ± 1.5	42
	1:100	68	0.1± 0.009	80 ± 1.3	39
FS75 (liquid)	1:25	18	0.1 ± 0.009	41 ± 1.9	38
	1:100	68	0.09 ± 0.011	76 ± 0.9	42
FS75 (crystalline)	1:25	18	0.11 ± 0.008	40 ± 2.1	39
	1:100	68	0.1 ± 0.01	79.5 ± 2.5	39

All kinetics values were obtained from the fitted curves and the equilibrium time was determined by calculating the time at which 99% of the plateau was reached. The same procedure was performed with all transfer data shown in the following tables.

One of the important factors, which affect the drug transfer, is the total lipid concentration of both the acceptor and donor in the transfer mixture [6]. To study the effect of the total lipid concentration on porphyrin transfer, the transfer experiment from FS75/SGChigh (resuspended crystalline nanoparticles) to the acceptor unilamellar vesicles was carried out with different lipid concentrations in the transfer mixture and with the two molar ratios 1:25 and 1:100.

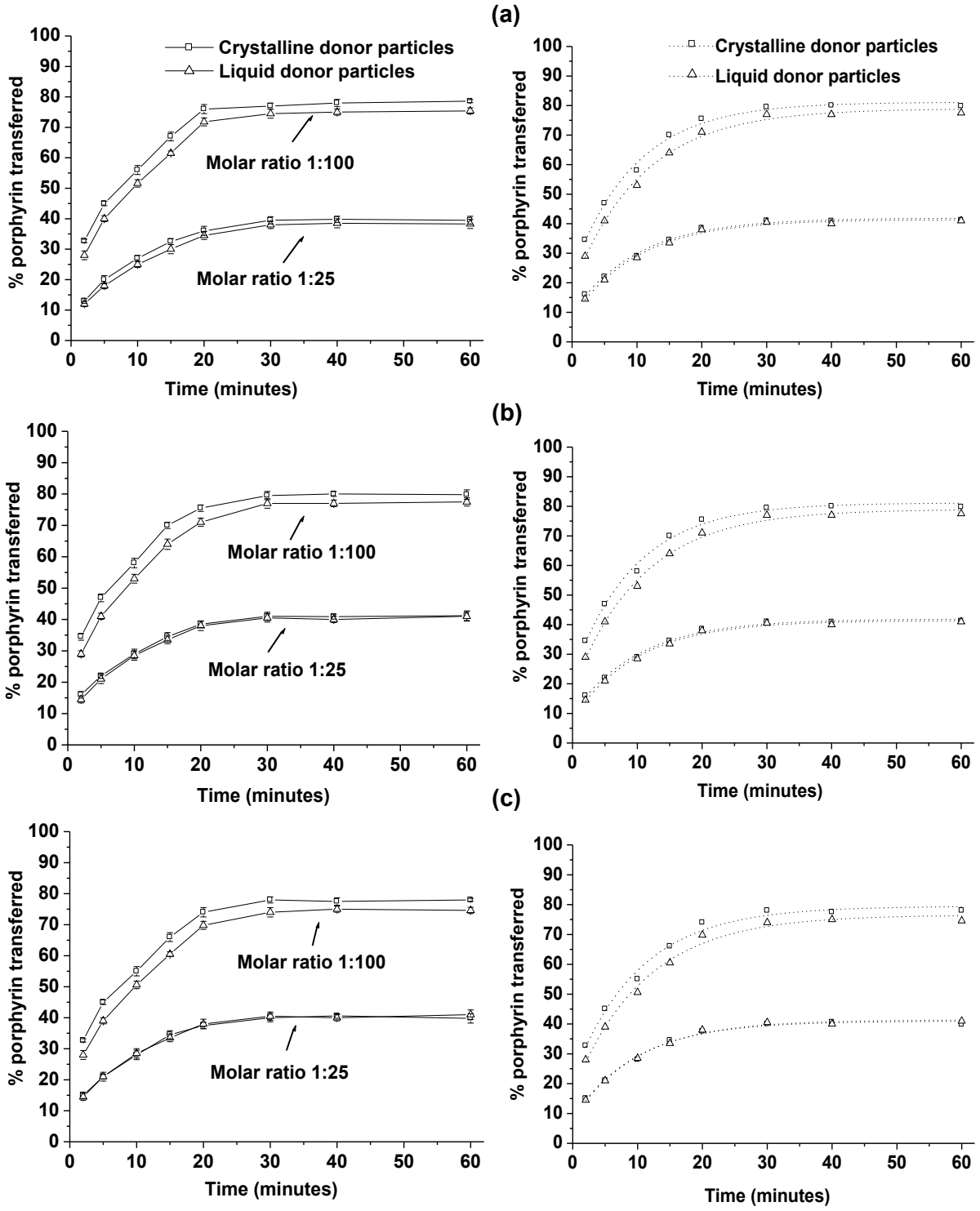

Figure 4.25: Percentage of porphyrin transferred from the crystalline and liquid donor particles to the acceptor unilamellar vesicles with molar ratios of 1:25 and 1:100, a) FS75/SGClow, b) FS75/SGChigh, c) FS75, measurements results (left panel), fitted curves (right panel), n = 3.

By decreasing the total lipid concentration from 50 mg/ml to 5 mg/ml at a molar ratio of 1:100, the transfer rate decreased as expected (figure 4.26, table 4.6). The final amount transferred was about 80, 76 and 72.5% with a transfer rate constant of 0.1, 0.09 and 0.032 min^{-1} for the lipid concentration 68, 50 and 5 mg/ml, respectively. The steady state was reached after 39 and 45 minutes in the case of lipid concentrations of 68 and 50 mg/ml,

respectively, while at a lipid concentration of 5 mg/ml the steady state was reached only after 95 minutes (table 4.6). Transfer occurs either by one of the following two mechanisms or by both mechanisms at the same time [88]. The first mechanism is the collision, which needs a direct contact of donor and acceptor particles in the transfer mixture and this mechanism has been described between colloidal carrier particles and cells [88-89]. The second one depends on the diffusion of the drug through the aqueous phase [90-91]. The increase in the drug transfer rate by increasing the total lipid concentration might be related to the decreasing distance between the donor and acceptor particles inside the transfer mixture. The smaller distance between the donor and acceptor particles at higher lipid concentrations may facilitate the drug transfer from the donor to the acceptor particles by one of the two mechanisms (collision or diffusion) and thus increase the rate of drug transfer. The amount of drug transferred in the equilibrium did not depend much on the lipid concentration. This is expected since the transfer experiments were done with the same molar ratio between the donor and acceptor (1:100). With a molar ratio of 1:25, the final percent of drug transferred was about 43 and 55% with lipid concentrations of 18 and 50 mg/ml, respectively.

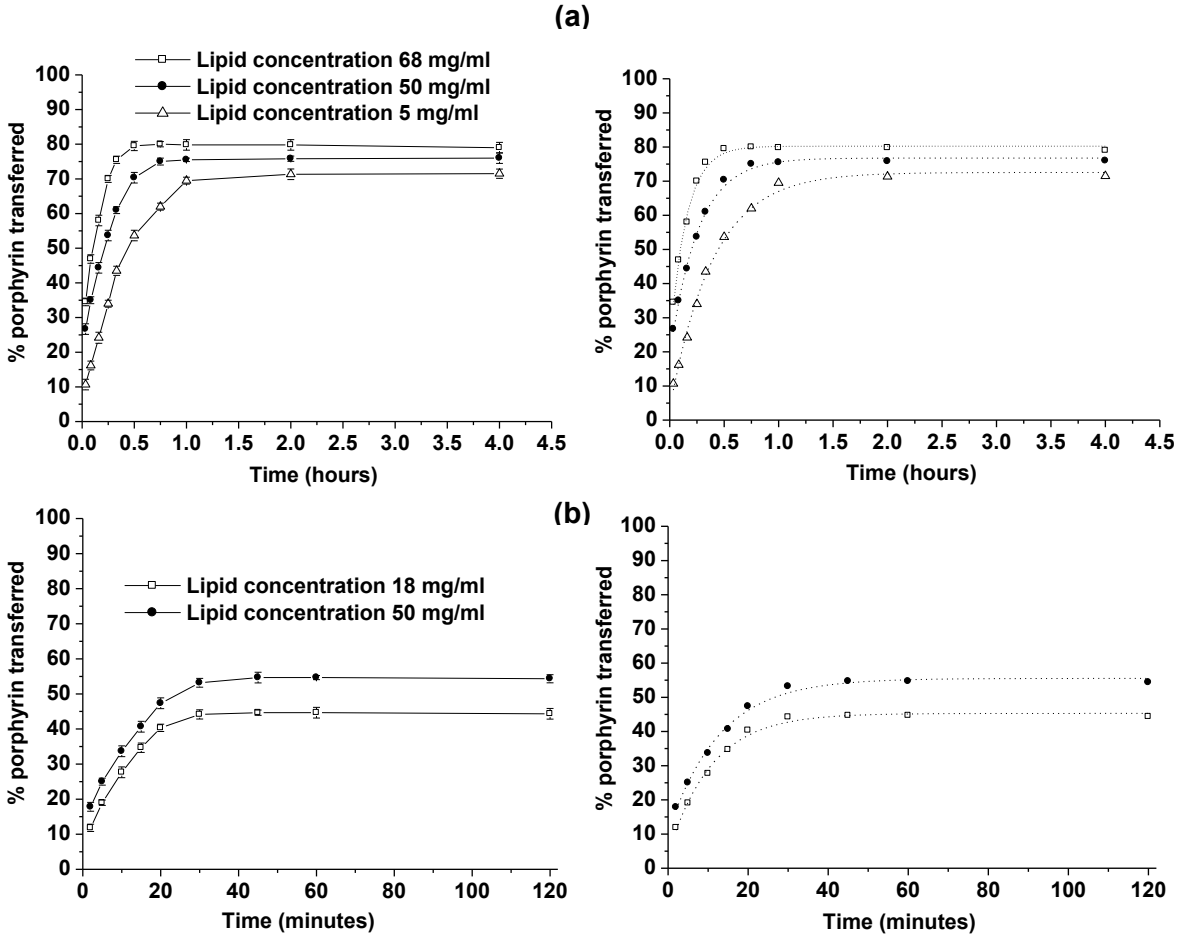

Figure 4.26: Porphyrin transfer (column method) from the resuspended crystalline donor nanoparticles of FS75/SGChigh to the acceptor unilamellar vesicles with different lipid concentrations, a) lipid molar ratio 1:100, b) lipid molar ratio 1:25, measurement results (left panel), fitted curves (right panel), n = 3.

Table 4.6: Results of the transfer studies with porphyrin from the crystalline resuspended nanoparticles of FS75/SGChigh to the acceptor unilamellar vesicles obtained by the column method assuming transfer kinetics according to equation [1]

Molar ratio	Total lipid concentration (mg/ml)	Transfer rate constant K (min^{-1})	Final % transferred	Equilibrium time (minutes)
1:25	18	0.095 ± 0.005	43 ± 1.5	42
	50	0.09 ± 0.002	55 ± 1.1	42
1:100	5	0.032 ± 0.004	72.5 ± 1.5	95
	50	0.09 ± 0.003	76 ± 1.6	45
	68	0.1± 0.009	80 ± 1.3	39

The transfer rate constant was nearly the same with both lipid concentrations (about 0.1 min^{-1}) leading to an equilibrium time of about 42 minutes (table 4.6). The transfer rate constant was thus nearly the same with the different molar ratios and the different lipid concentrations except with a lipid concentration of 5 mg/ml which had a lower transfer rate than the other lipid concentrations (table 4.6). These results were in agreements with previous observations [6], which showed that the transfer rate of Nile red from D114 nanoparticles to acceptor o/w emulsion droplets decreased after the dilution (decreasing the total lipid concentration) of the transfer mixture.

The lipophilicity of the drug model used is considered as one of the most important factors, which affect the drug transfer [6]. For that reason, the transfer of Nile red (logP 3.65) [6], which is less lipophilic than porphyrin (logP 9) [6], and DiI, which is more lipophilic than porphyrin (logP 20) [64], to the acceptor unilamellar vesicles was measured for comparison. The transfer of Nile red was very rapid and seemed to be completed already after 1 minute (figure 4.27). Assuming an equal distribution of Nile red between the donor and acceptor, about 99% of the Nile red would be expected in the acceptor particles at equilibrium. The drug transfer at equilibrium corresponded to the expected value, which indicates that all of the Nile red must have transferred from the donor to the acceptor particles. Large differences were thus observed between the transfer of porphyrin and Nile red. Porphyrin transfer reached equilibrium values lower than expected with a molar ratio of 1:100 while Nile red transfer reached the expected equilibrium value (table 4.7). By comparing the transfer of Nile red and porphyrin to the acceptor unilamellar vesicles, it may be assumed that porphyrin transfer occurred to the outer surface of the acceptor particles and that porphyrin has low or

no ability to get inside the inner interface layers of the acceptor particles. However, Nile red has the ability to get inside the inner interface of the acceptor particles due to its lower lipophilicity and consequently its higher diffusion than porphyrin. Contrary to Nile red transfer, the DiI transfer to the acceptor unilamellar vesicles was very slow. The amount of DiI transferred after 5 days was about 3.8% (figure 4.28) with a very low transfer rate constant (0.4 day^{-1}) (table 4.7). This very slow transfer rate to the acceptor unilamellar vesicles was nearly the same as in previous results of DiI transfer to an acceptor emulsion [6]. This very slow DiI transfer to the acceptor unilamellar vesicles could be attributed to the very high lipophilicity of DiI (due to its long alkyl chains), which decreases the diffusion of the drug molecule through the aqueous phase to a very high extent.

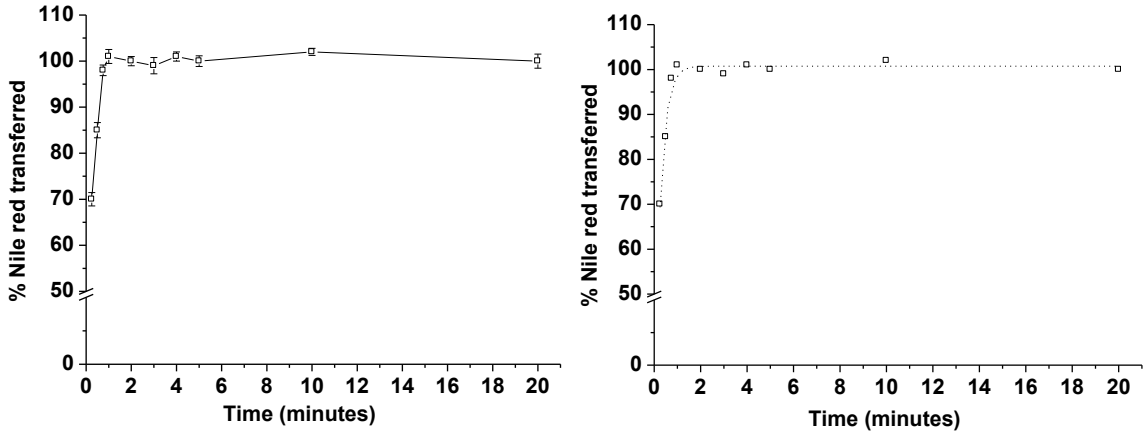

Figure 4.27: Nile red transfer from the resuspended crystalline nanoparticles of FS75/SGChigh to the acceptor unilamellar vesicles with a molar ratio 1:100, measurement results (left), fitted curve (right), n = 3.

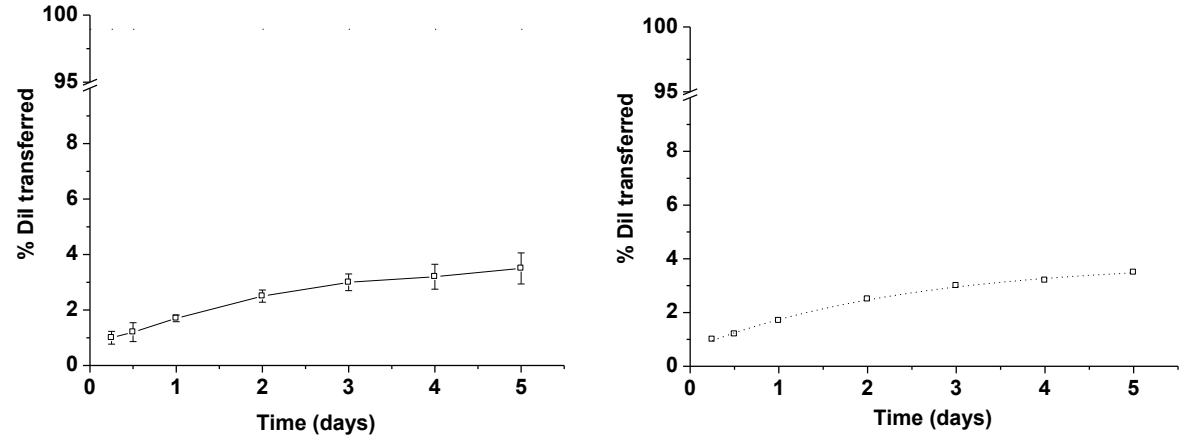

Figure 4.28: DiI transfer from the resuspended crystalline nanoparticles of FS75/SGChigh to the acceptor unilamellar vesicles with a molar ratio 1:100, measurement results (left), fitted curve (right), n = 3.

Table 4.7: Results of the transfer studies for the different drug models to the acceptor unilamellar vesicles with a donor: acceptor molar ratio of 1:100 and a total lipid concentration of 50 mg/ml obtained by the column method assuming transfer kinetics according to equation [1]

Donor	Transfer rate constant K (min^{-1})	Final % transferred	Equilibrium time (minutes)
FS75/SGChigh (porphyrin)	0.09 ± 0.003	76 ± 1.6	45
FS75/SGChigh (Nile red)	3.6 ± 1.34	100 ± 2.6	1
FS75/SGChigh (DiI)	$2.7 * 10^{-4} \pm 0.27 * 10^{-4}$ ($0.4\ day^{-1}$)	3.8 ± 0.14	7200 (5 days)

4.3.4 Porphyrin transfer to monoolein dispersions and a Miglyol nanoemulsion

In order to investigate the effect of the acceptor lipid composition and structure on the transfer of porphyrin, the transfer of porphyrin to acceptor monoolein dispersions and a Miglyol nanoemulsion was studied. As a first step the suitability of monoolein/poloxamer nanodispersions (vesicular and cubic particles) and the Miglyol nanoemulsion as acceptors for transfer experiments with the column method was tested. Drug loaded samples were prepared to measure the recovery of the acceptor from the column. The fraction of the different acceptor particles that was retained on the ion exchange column was always less than 2% (table 4.8). These results indicate the suitability of these acceptor nanodispersions for transfer experiments with the ion exchange column. Although the size of the monoolein cubic particles was large in comparison with the monoolein vesicles and the Miglyol nanoemulsion, their retention on the column was comparable with that of monoolein vesicles and the Miglyol nanoemulsion. With the three types of alternative acceptor particles the transfer experiments were carried out from the crystalline resuspended nanoparticles of FS75/SGChigh. The drug transfer to the acceptor monoolein dispersions was very rapid and equilibrated after about 1.5 minutes (figure 4.29, table 4.9). The equilibrium values for both acceptors (vesicles and cubic particles) were close to the expected value of the equal distribution (more than 90%) (table 4.9).

Table 4.8: Retention of the acceptor Miglyol nanoemulsion and the acceptor monoolein/poloxamer nanodispersions on the ion exchange column, data were obtained with porphyrin loaded samples

Formula	Fraction retained (%)
Monoolein vesicles (5% amphiphile, 12% poloxamer, 95 nm/ –4.3 mV)	1.3 ± 0.25
Monoolein cubic particles (5% amphiphile, 12% poloxamer, 310 nm/ –3.5 mV)	1 ± 0.12
Miglyol nanoemulsion (5% Miglyol, 4% poloxamer 188, 113 nm/ –4.6 mV)	1.8 ± 0.42

The course of drug transfer from the donor particles to the two different monoolein dispersions was nearly the same (figure 4.29). The transfer rate constant and the final percent of drug transfer were very high in comparison with the “conventional” acceptor particles (unilamellar vesicles) (table 4.9). With the same molar ratio (1:25) and the same lipid concentration (about 50 mg/ml), the transfer rate constant and the final percent transferred from the resuspended crystalline lipid nanoparticles of FS75/SGChigh to the acceptor unilamellar vesicles were 0.09 min^{-1} and 55%, respectively, while with the acceptor monoolein/poloxamer vesicles they were 2.62 min^{-1} and 93%, respectively. The equilibration time was about 42 minutes with the acceptor unilamellar vesicles while it was only about 1.5 minutes with the acceptor monoolein/poloxamer nanodispersions (table 4.9).

These differences between the two acceptors may be attributed to the difference in the lipid composition of the two types of acceptor particles. In the case of monoolein, the hydrophilic lipophilic balance (HLB) is about 3.8 [92] while in the case of the acceptor unilamellar vesicles the HLB of EPC is about 9 [93-94]. This difference in the HLB between the two lipids indicates that monoolein is more hydrophobic than EPC. Monoolein has a small hydrophilic head group which may allow the penetration of the drug to the water interface inside the vesicles (high lipid water interface in which the drug can distribute). In other words, the high hydrophobicity of monoolein in comparison with EPC facilitates the diffusion of the drug molecules to the water interface inside the vesicles. While the HLB of EPC indicates that EPC has a relatively large hydrophilic head group which may either hinder the penetration or decrease the diffusion rate of porphyrin to the interface inside the vesicles.
These results are in agreement with previous observations [95], which indicate that cubic particles should be quite useful for a rapid uptake because they can rapidly absorb pollutants (e.g., for water treatment or cosmetic skin protection) and retain an amount determined by the solute partition coefficient.

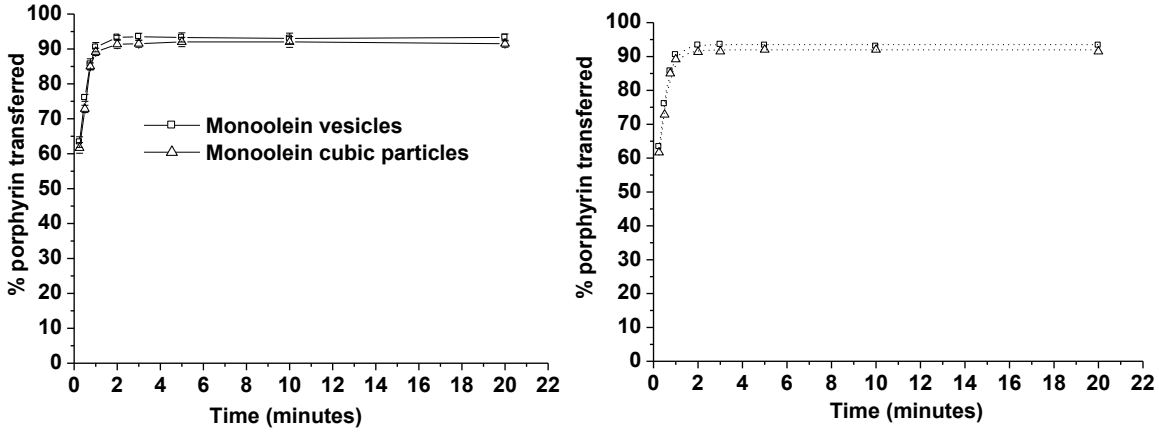

Figure 4.29: Porphyrin transfer (column method) from the resuspended crystalline donor particles of FS75/SGChigh to the acceptor monoolein dispersions prepared from 5% amphiphile and 12% poloxamer without autoclaving (vesicles) or with autoclaving (cubic particles) with a donor: acceptor molar ratio of 1:25, measurement results (left), fitted curve (right), n = 3.

Table 4.9: Results of the transfer studies with porphyrin from the crystalline resuspended nanoparticles of FS75/SGChigh to different acceptors obtained by the column method assuming transfer kinetics according to equation [1]

Acceptor	Molar ratio	Total lipid concentration (mg/ml)	Transfer rate constant K (min^{-1})	Final % transferred	Equilibrium time (minutes)
Monoolein vesicles	1:25	48	2.62 ± 0.16	93.3 ± 1.5	1.5
Monoolein cubic particles	1:25	48	2.5 ± 0.27	91.5 ± 1	1.5
Unilamellar vesicles*	1:25	50	0.09 ± 0.002	55 ± 1.1	42
Miglyol nanoemulsion	1:100	50	1.08 ± 0.091	85 ± 2.1	4

* Data from table 4.6

This rapid uptake of the pollutants by the monoolein cubic particles could be attributed to the sponge like structure of the cubic monoolein particles. This sponge like structure may lead to the high transfer rate and the complete drug transfer that was observed with the acceptor monoolein cubic particles. In addition to the low HLB value of monoolein and the sponge like structure of the cubic phase, the cubic bicontinuous phase has a unique structure where the monoolein bilayer (internal structure) is extending in three dimensions, with a high specific bilayer/water interfacial area (500-600 m^2/g lipid) [17]. As mentioned before [84], the interfacial area (lipid/water interface) plays an important role in the transfer of porphyrin to the different acceptor particles. This unique structure of the cubic particles facilitates the mobility of the drug molecules within the bilayer. All of these factors make the cubic phase a suitable candidate for receiving the porphyrin molecules from the donor particles. On the other hand, presence of cholesterol in the acceptor unilamellar vesicles increases the rigidity of the membrane surface and occupies a part from this surface and thus hinders the localization of the drug at the outer interface and decreases the rate of porphyrin diffusion to the interface inside the vesicles.

Figure 4.30 illustrates the transfer of porphyrin to the acceptor Miglyol nanoemulsion. Also with this acceptor, the drug transfer was very rapid (K = 1 min^{-1}) and the equilibrium value (85%) was obtained after 4 minutes (figure 4.30, table 4.9). As observed with the acceptor unilamellar vesicles, the final fraction of porphyrin transferred to the acceptor Miglyol nanoemulsion was lower than the expected value (99%) (table 4.9). The transfer rate to the acceptor Miglyol nanoemulsion was higher than to the acceptor unilamellar vesicles while the equilibrium amount was nearly the same. These results could be attributed to the difference in the lipid composition between the two acceptor particles. The transfer from the donor trimyristin (medium chain triglyceride) to the acceptor particles, which were also prepared from medium chain triglyceride (Miglyol), may be the reason for the difference between the two acceptors.

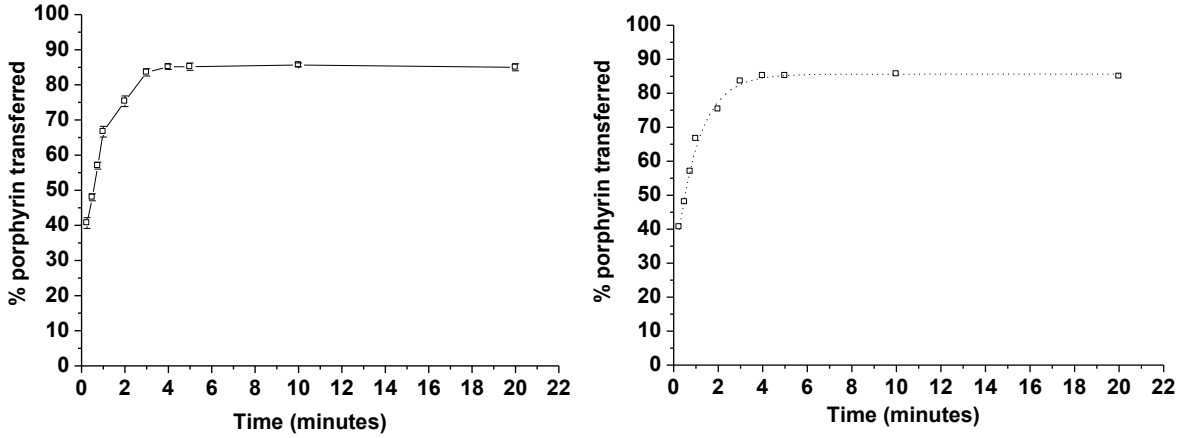

Figure 4.30: Porphyrin transfer (column method) from the resuspended crystalline donor particles of FS75/SGChigh to the acceptor Miglyol nanoemulsion prepared from 5% Miglyol and 4% poloxamer with a donor: acceptor molar ratio of 1:25, measurement results (left), fitted curve (right), n = 3.

4.3.5 Porphyrin affinity to monoolein dispersions and to unilamellar vesicles

Porphyrin was transferred to the different acceptor monoolein dispersions very rapidly and complete drug transfer (until equilibrium) was obtained with these acceptor particles. To explore the background of this phenomenon in more detail, especially in comparison with unilamellar phospholipid vesicles as acceptor particles, time dependent solubilization studies were carried out with the porphyrin. Already by visual observation (figure 4.31) the high affinity of porphyrin to the acceptor monoolein dispersions in the form of vesicles or cubic particles was obvious. The uptake of the porphyrin by the monoolein particles was much faster than by the unilamellar liposomes. It also reached a distinctly higher value within the time frame of the experiment as evident from the spectroscopic investigations (figure 4.31). With the monoolein acceptor particles, the saturation with porphyrin had almost been reached already after 5 minutes whereas uptake continued over many hours with the liposomes (figure 4.32). Obviously, the affinity of porphyrin to the acceptor monoolein dispersions is much higher than that to the phospholipid vesicles. Although the monoolein vesicles and monoolein cubic particles contain the same amount of porphyrin the monoolein vesicles appeared much darker than the cubic particles. This could be attributed to the difference in the appearance between the drug free monoolein vesicles and the monoolein cubic particles. The monoolein vesicles are translucent while the cubic particles have a milky appearance.

4.3.6 Transfer of DiI to the acceptor monoolein cubic particles

The transfer of porphyrin to the acceptor monoolein dispersions (vesicular and cubic nanoparticles) was characterized by a very rapid drug transfer and the equilibrium values were the same as the expected values (complete drug transfer). To further evaluate the suitability of monoolein dispersions as acceptor for very lipophilic substances, DiI, which is a

very lipophilic dye (more lipophilic than porphyrin), was used as a drug model to measure the drug transfer to the acceptor monoolein dispersions. As reported before [6], the transfer rate of DiI from lipid nanoparticles (2% D114 nanoparticles stabilized with 1.6% poloxamer 188) to large acceptor emulsion droplets (5% Miglyol 812 droplets stabilized with 3% polyvinyl alcohol, 8 µm) was very low. The amount of dye transferred in equilibrium was at most about 7%, which was far away from the calculated equilibrium value (~ 96%). The transfer of DiI to

Figure 4.31: Optical appearance of dispersions of unilamellar (PL) vesicles, monoolein cubic particles and monoolein (Mo) vesicles at different time points after mixing with excess porphyrin powder.

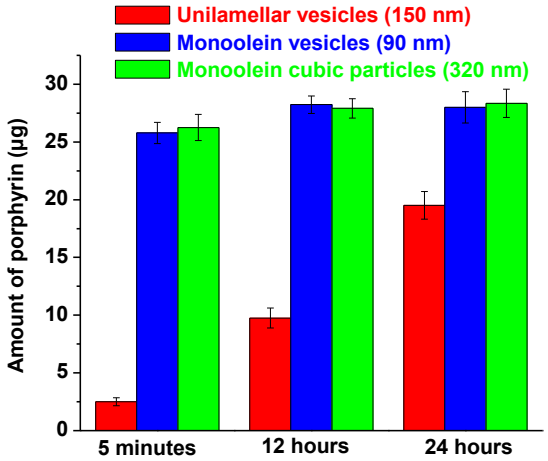

Figure 4.32: Amount of porphyrin incorporated with the different acceptors at different time points after mixing the acceptors with the excess porphyrin powder.

acceptor unilamellar vesicles was also very slow and only a very small fraction of the dye was transferred. Therefore, the transfer of DiI from FS75/SGChigh to the acceptor monoolein cubic particles was measured and compared to the previous results with the different acceptors and also compared with the transfer of porphyrin. In contrast to the transfer to the acceptor emulsion and unilamellar vesicles, most of DiI was transferred after 40 minutes of incubation with the acceptor monoolein cubic particles (figure 4.33). The amount transferred in equilibrium was about 82% and 67% with donor:acceptor molar ratios of 1:25 and 1:100, respectively (table 4.10). These equilibrium values were reached after about 40 minutes with the different molar ratios. The transfer of DiI was characterized by a very rapid initial dye transfer (burst release). More than 30% had been transferred after 2 minutes with a molar ratio of 1:25 and with a molar ratio of 1:100 more than 40% had been transferred after 2 minutes. The transfer rate constant was about 0.09 min^{-1} with no difference between the two molar ratios (table 4.10). The transfer rate constant to the acceptor monoolein cubic particles was much higher than the transfer rate constant to the acceptor emulsion (about 0.04 day^{-1}) [6]. These differences in the transfer of DiI between the two acceptors could be attributed to the differences in the particle size and the available lipid/water interfacial area between the two acceptors. The particle size of the cubic particles was 320 nm while the particle size of the acceptor emulsion droplets was 8 µm. The transfer rate and the transferred amount of DiI to the unilamellar vesicles were much lower than those observed with the cubic particles (table 4.10). These differences might be related to the difference in the lipophilicity between the two acceptors where monoolein cubic particles are more lipophilic than EPC unilamellar vesicles, which facilitate the transfer of DiI to the cubic particles. Although the transfer rate and transferred amount of DiI to the acceptor monoolein cubic particles was much higher in comparison to the acceptor emulsion the transfer was not complete (equilibrium values were less than the expected values) and the transfer rate constant was smaller than the transfer rate constant of porphyrin (table 4.10). These differences in the transfer rate constant and the transferred amount between porphyrin and DiI can be attributed to the difference in the lipophilicity of the two dyes. The results of DiI and porphyrin transfer to the acceptor monoolein dispersions indicate a high affinity of the different lipophilic dyes to the acceptor monoolein, which may be attributed to the high lipophilicity and the high bilayer/water interfacial area of the monoolein dispersions. This high interfacial area and lipophilicity make the monoolein dispersions a good candidate for the incorporation of the different lipophilic dyes inside the acceptor particles.

4.3.7 Practical considerations of the column method

To measure the transfer by the column method, it was important before each experiment to prepare the gel for filling the columns (about 30 columns for each experiment)

and after each experiment these columns had to be carefully cleaned and dried. Furthermore, since each column needs 1 ml of gel the method is not inexpensive. About 1 minute was needed to separate the donor and acceptor particles, which means that the time resolution of the method is not below 1 minute. Moreover, one of the two populations (donor or acceptor) should be charged and both should have a small particle size. This makes this method tedious and not easy to handle.

Table 4.10: Results of transfer studies of porphyrin and DiI obtained by the column method assuming transfer kinetics according to equation [1]

Donor	Acceptor	Molar ratio	Total lipid concentration (mg/ml)	Transfer rate constant K (min^{-1})	Final % transferred	Equilibrium time (minutes)
FS75/SGChigh (DiI)	Cubic particles	1:25	48	0.093 ± 0.002	67.2 ± 0.3	40
		1:100	45	0.098 ± 0.003	81.8 ± 0.26	40
	Unilamellar vesicles	1:100	50	$2.7 * 10^{-4}$ ± $0.27 * 10^{-4}$	3.8 ± 0.14	7200 (5 days)
FS75/SGChigh (porphyrin)	Cubic particles	1:25	48	2.5 ± 0.27	91.5 ± 1	1.5

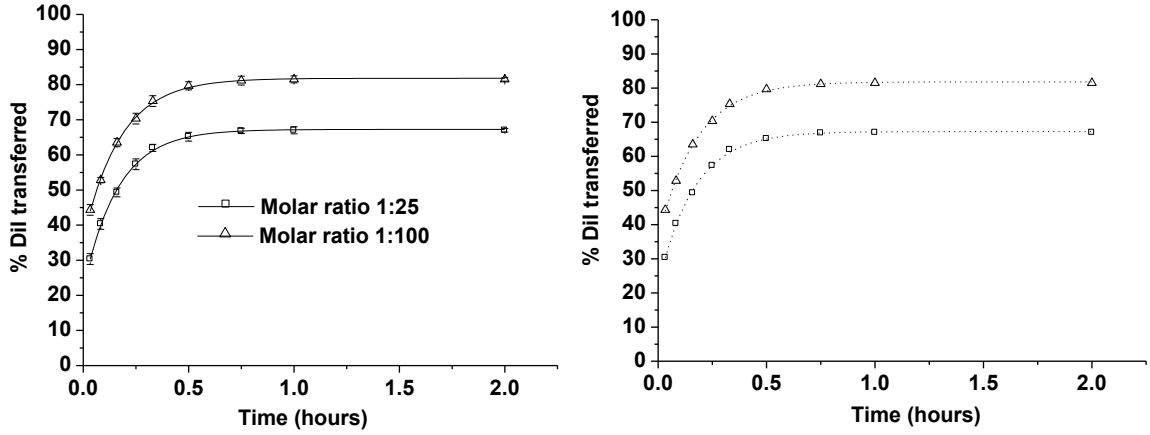

Figure 4.33: DiI transfer (column method) from the resuspended crystalline nanoparticles of FS75/SGChigh to the acceptor cubic particles (4.4% monoolein, 0.6% poloxamer, 320 nm), measurement results (left), fitted curve (right), n = 3.

4.4 Transfer studies with the centrifugation method

Another transfer method, which depends on centrifugation to separate the donor and acceptor particles, was used to measure the transfer kinetics of the three drug models. This method was chosen because it does not require the use of charged donor particles as with the ion exchange column technique. This advantage of the centrifugation method over the ion exchange made it possible to measure the transfer from Fpoloxamer/DCP, which had a low charge and cannot be measured by the column method.

4.4.1 Transfer of porphyrin to the different acceptors (MLV and emulsion)

Porphyrin transfer from the liquid lipid nanoparticles of FS75/SGClow, FS75/SGChigh, FS75 and Fpoloxamer/DCP to the acceptor MLV, which had a mean particle size of 10 µm, was investigated. The donor and acceptor particles were separated by centrifugation where the donor will appear in the supernatant layer and the acceptor MLV will be separated as pellets. To investigate the effect of the molar ratio between the donor and acceptor on the initial amount of drug transferred, amount of drug transferred in equilibrium and the rate of drug transfer, the transfer experiments were carried out with different molar ratios (1:25, 1:50 and 1:100). For a molar ratio of 1:100, the amount of drug transferred after 0.5 hour was 27, 23, 20 and 28% for FS75/SGClow, FS75/SGChigh, FS75 and Fpoloxamer/DCP, respectively (figure 4.34). The transfer of porphyrin to the acceptor MLV was slow and the equilibrium was obtained after several hours. The steady state concentration was reached after about 12 hours with all formulations at a molar ratio of 1:25 while the equilibrium was obtained after about 11 and 10 hours at molar ratios of 1:50 and 1:100, respectively (table 4.11). The transfer rate constant ranged from 0.005 and 0.0068 min^{-1} for the four formulations with the different molar ratios (1:25, 1:50 and 1:100). Obviously, the different molar ratios affect only the final fraction of drug transferred and have no significant effect on the transfer rate constant. There were virtually no differences in the final percent of drug transferred and the transfer rate constant between the four formulations, which were prepared with different emulsifier concentrations. With the centrifugation method, it was also possible to determine the fraction of porphyrin that was retained in the nanoparticles at different time points. The recovery of porphyrin (total of percentage transferred and retained) ranged between 95 and 103%, which was a good results. Porphyrin transfer from resuspended crystalline nanoparticles of FS75/SGChigh and the original crystalline nanoparticles of Fpoloxamer/DCP to the acceptor o/w emulsion, which had a mean particle size of 6 µm, was measured after separating the donor and acceptor by ultracentrifugation. Here, the crystalline donor will be separated as pellet and the acceptor emulsion will appear in the supernatant as a creamy emulsion layer. Contrary to the acceptor MLV, the drug transfer to the acceptor emulsion was very rapid and equilibrium was obtained after about 3 minutes with both donor formulations (figure 4.35, table 4.11). After 30 seconds, the drug transfer was about 15% for both formulations and at equilibrium about 33% had been transferred from both formulations. Although the final percent of drug transfer to the acceptor emulsion was nearly the same as with the acceptor MLV (at the same donor: acceptor molar ratio of 1:25), the transfer rate constant with the acceptor emulsion was much higher than with the acceptor MLV (table 4.11). The main reason for this large difference in the drug transfer rate between the two acceptors can be attributed to the difference in the composition and particle size of the two acceptors. The acceptor MLV particles were composed of multilayers and had a mean

particle size of about 11 µm. In contrast, the acceptor emulsion with a mean particle size of 6 µm was composed of a single droplet (no layers). This difference in the particle size means that higher number of acceptor emulsion particles was present in the transfer mixture in comparison with the acceptor MLV. Thus, a higher rate of porphyrin transfer to the acceptor emulsion was observed in comparison with the acceptor MLV. Additionally, the acceptor MLV was prepared from EPC with cholesterol, which increases the rigidity of the bilayer and thus decreases the rate of porphyrin transfer from layer to layer within the MLV multilayer. With both acceptors, the final percent of drug transferred was much lower than the expected

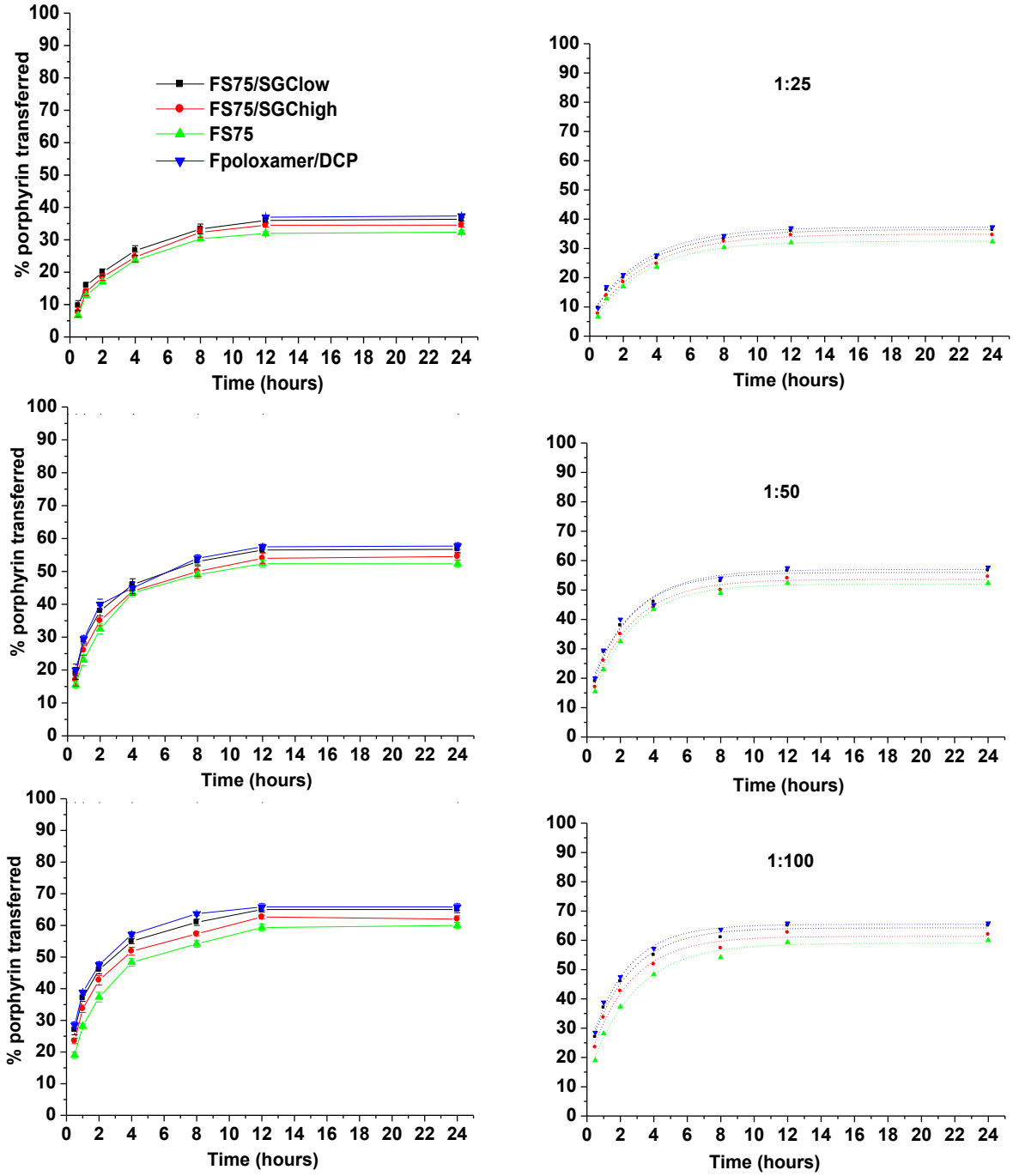

Figure 4.34: Porphyrin transfer (centrifugation method) from the resuspended liquid lipid nanoparticles of the four D114 formulations to the acceptor MLV; porphyrin transferred (left panel), fitted curves (right panel), n = 3.

values (table 4.11). The maximum amount of porphyrin transferred was between 35-70% for the three donor:acceptor ratios. The reason for this low equilibrium values might be the localization of porphyrin at the interface of the particles. Due to the limited size of the large acceptor particles, saturation might occur and thus probably the transfer stopped at a low level. In an attempt to check the effect of the stabilizer PVA on the transfer of the porphyrin, 3% PVA was added to the MLV acceptor (the same concentration that was used in the preparation of the acceptor emulsion). There was no difference in the rate and amount of porphyrin transfer to the acceptor MLV with and without the presence of PVA. The initial drug transfer after 0.5 hour was 22% and 19% for the acceptor MLV with and without PVA, respectively. Equilibrium was obtained after about 11 and 10 hours with an equilibrium amount of 60% and 65% for the acceptor MLV with and without PVA, respectively (figure 4.36, table 4.11). These results indicate that PVA has no effect on the transfer of porphyrin to the acceptor MLV.

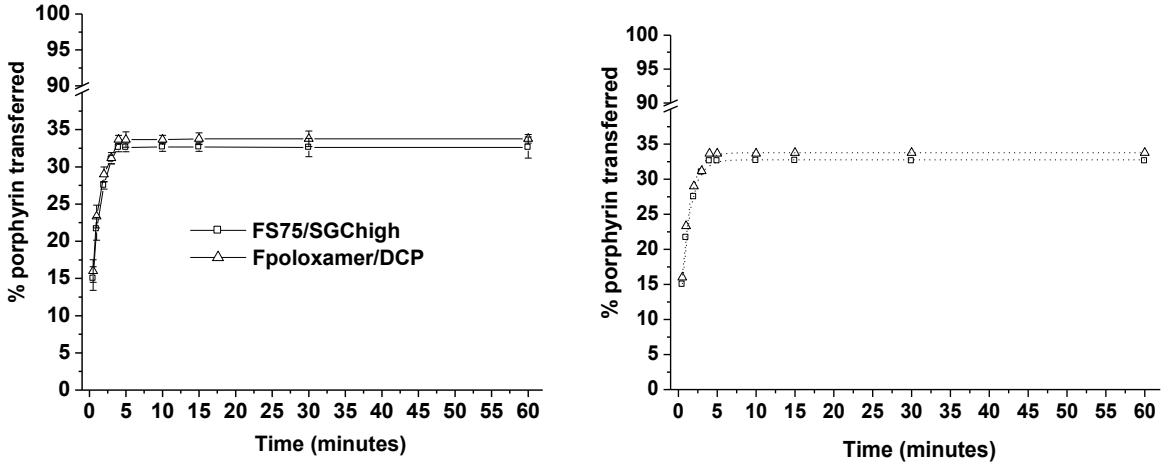

Figure 4.35: Porphyrin transfer (centrifugation method) from the resuspended crystalline lipid nanoparticles of FS75/SGChigh and the original crystalline lipid nanoparticles of Fpoloxamer/DCP to the acceptor o/w emulsion, molar ratio 1:25; measurement results (left), fitted curve (right), n = 3.

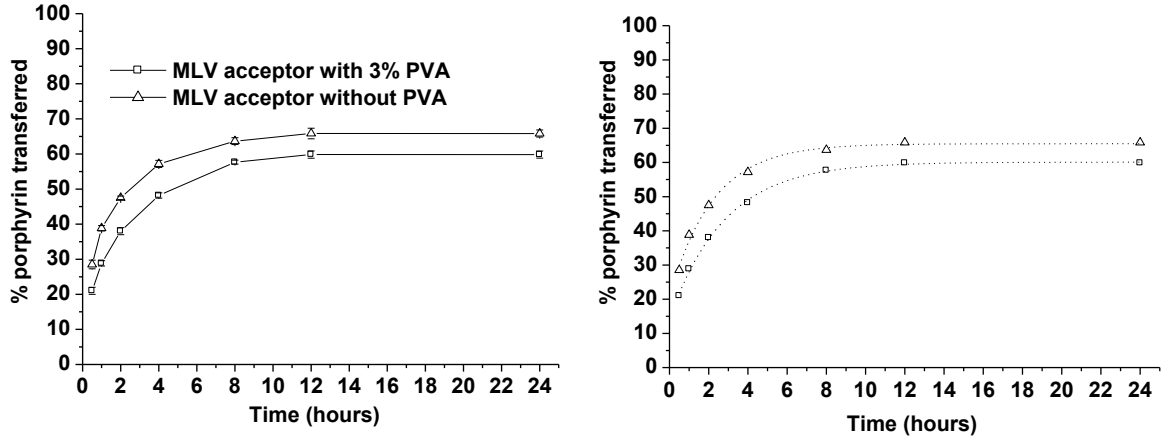

Figure 4.36: Porphyrin transfer (centrifugation method) from the resuspended liquid lipid nanoparticles of Fpoloxamer/DCP to the acceptor MLV with and without the presence of PVA, molar ratio 1:100; measurement results (left), fitted curve (right), n = 3.

Table 4.11: Results of the transfer studies with porphyrin obtained by the centrifugation technique assuming transfer kinetics according to equation [1]

Donor	Acceptor	Molar ratio	Transfer rate constant K (min^{-1})	Final % transferred	Equilibrium time
FS75/SGClow (liquid)	MLV	1:25	0.0054 ± 0.0003	36 ± 1.9	12.4 h
		1:50	0.0066 ± 0.0009	59 ± 1.57	10.5 h
		1:100	0.0068 ± 0.0016	64 ± 1	10 h
FS75/SGChigh (liquid)	MLV	1:25	0.005 ± 0.0005	34.5 ± 2.1	12.5 h
		1:50	0.0065 ± 0.001	53 ± 1.15	10.8 h
		1:100	0.0065 ± 0.0007	61 ± 1.7	10 h
FS75 (liquid)	MLV	1:25	0.0055 ± 0.0002	32 ± 1.6	12.4 h
		1:50	0.0066 ± 0.0003	52 ± 0.9	10.5 h
		1:100	0.006 ± 0.0011	59 ± 1.5	11 h
Fpoloxamer/DCP (liquid)	MLV	1:25	0.0055 ± 0.0009	37 ± 1	12.4 h
		1:50	0.0061 ± 0.0008	57 ± 1.57	11 h
		1:100	0.0068 ± 0.0004	65 ± 1.9	10 h
Fpoloxamer/DCP (liquid)	MLV (3% PVA)	1:100	0.006 ± 0.0005	60 ± 1.8	11 h
FS75/SGChigh (crystalline)	O/w emulsion	1:25	1.28 ± 0.15	32 ± 0.75	3 min
Fpoloxamer/DCP (crysrtalline)	O/w emulsion	1:25	1.38 ± 0.25	33 ± 1.9	3 min

4.4.2 Transfer of Nile red to MLV and emulsion droplets

In order to determine the effect of lipophilicity on the transfer, Nile red, which is less lipophilic than porphyrin, was used as a drug model. The transfer of Nile red from the resuspended lipid nanoparticles of FS75/SGChigh in the liquid or crystalline form to the different acceptor particles was studied with a molar ratio of 1:100. The liquid nanoparticles were used with the acceptor MLV while the crystalline nanoparticles were used with the acceptor emulsion. In contrast to porphyrin transfer, the transfer of Nile red to the different acceptor particles was complete and equivalent to the expected equilibrium value. The transfer of Nile red seemed to be completed after about 2 minutes (figure 4.37, table 4.12). Large differences were thus observed between the transfer of porphyrin and Nile red. Firstly, the porphyrin transfer reached an equilibrium value much lower than the expected one at a molar ratio of 1:100 while the Nile red transfer reached the expected equilibrium value.

The rate of porphyrin transfer was very low especially to the acceptor MLV and increased with the emulsion acceptor while the rate of Nile red transfer was nearly the same with the two acceptors (MLV and emulsion). As observed before for the porphyrin transfer, the transfer rate of Nile red to the acceptor MLV (1.9 min^{-1}) was lower than that to the acceptor o/w emulsion (3.3 min^{-1}). This might be due to the difference in the particle size of the two acceptors and thus the difference in the number of acceptor particles in the transfer mixture. The difference in the transfer between Nile red and porphyrin could be attributed to the difference in the lipophilicity between the two drug models. Nile red is less lipophilic than porphyrin, which allows the fast diffusion of Nile red molecules to the acceptor particles. Also this difference in the lipophilicity facilitates the rapid diffusion of Nile red from layer to layer within the MLV acceptor.

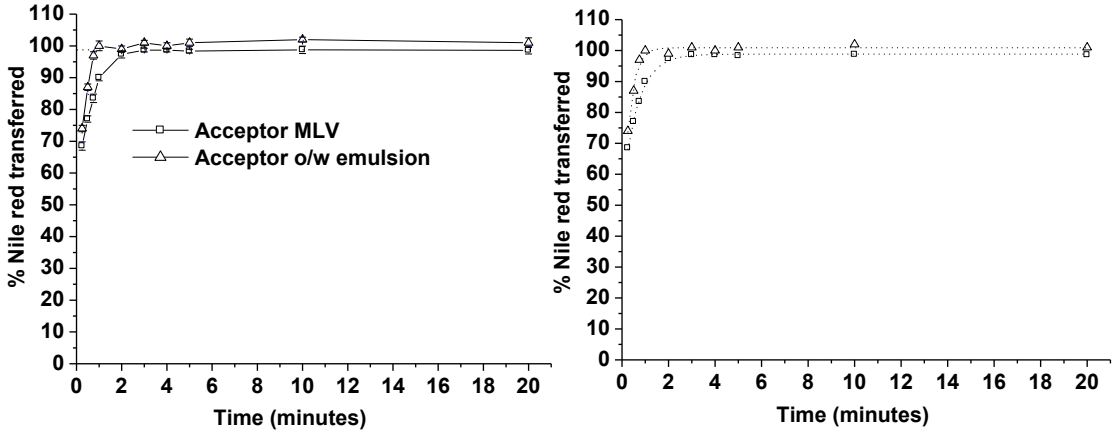

Figure 4.37: Nile red transfer (centrifugation method) from the resuspended lipid nanoparticles of FS75/SGChigh to the acceptor o/w emulsion and the acceptor MLV, molar ratio 1:100, measurement results (left), fitted curve (right), n = 3.

Table 4.12: Results of the transfer studies with Nile red obtained by the centrifugation technique at a molar ratio of 1:100, assuming transfer kinetics according to equation [1]

Donor	Acceptor	Transfer rate constant K (min^{-1})	Final % transferred	Equilibrium time (min)
FS75/SGChigh	MLV	1.9 ± 0.08	98 ± 1.8	2.5
	O/w emulsion	3.3 ± 0.37	101 ± 1.9	1

4.4.3 Transfer of different drug models to cubic monoolein particles

In order to measure the drug transfer to large acceptor particles other than the acceptor MLV and emulsion, cubic monoolein particles were used as acceptor particles. The transfer of porphyrin from the crystalline particles of FS75/SGChigh was studied to acceptor monoolein cubic particles with different sizes to investigate the effect of particle size on the

transfer rate. The acceptor cubic particles, which were prepared from 5 and 10% amphiphile (12% poloxamer) by autoclaving, were used in the transfer experiment. Ultracentrifugation was a successful method for the separation between the acceptor cubic particles (supernatant creamy emulsion layer) and the donor crystalline nanoparticles (pellets) (figure 4.38). Figure 4.38 gives a good illustration of the transfer of porphyrin from the crystalline particles to the acceptor cubic particles. As reflected in the pink color of the creamy acceptor layer and the white pellet layer, the drug was highly transferred to the acceptor cubic particles. The transfer was very rapid and after 1 minute about 94 and 90% had been transferred to the acceptor cubic particles with a particle size of 0.32 and 0.71 µm, respectively (figure 4.39). Equilibrium was obtained after about 1.5 minutes with both acceptors and the amount of porphyrin transferred at equilibrium was the same as the expected value. The transfer rate constant was 2.54 and 2.42 min^{-1} for the cubic particles with a particle size of 0.32 and 0.71 µm, respectively (table 4.13).

By comparing the transfer of porphyrin to the acceptor MLV, emulsion and cubic particles, it was found that porphyrin had a high affinity to monoolein cubic particles.

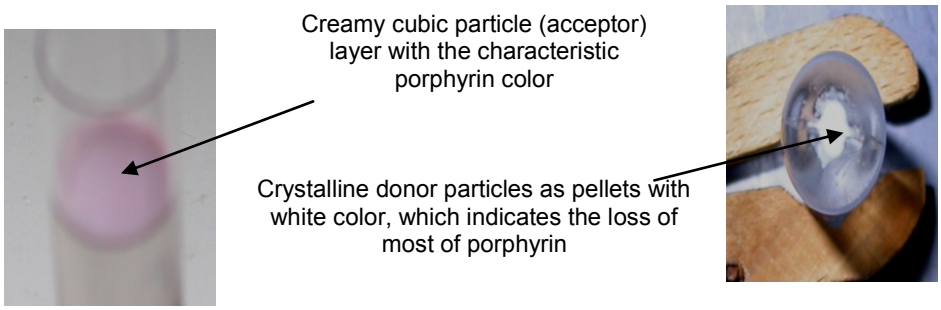

Figure 4.38: Optical appearance of supernatant and pellet after ultracentrifugation of the mixture of FS75/SGChigh and the cubic particles at 55000 rpm for 30 minutes Ultracentrifugation was carried out after 5 minutes of mixing the donor and acceptor with a molar ratio of 1:25

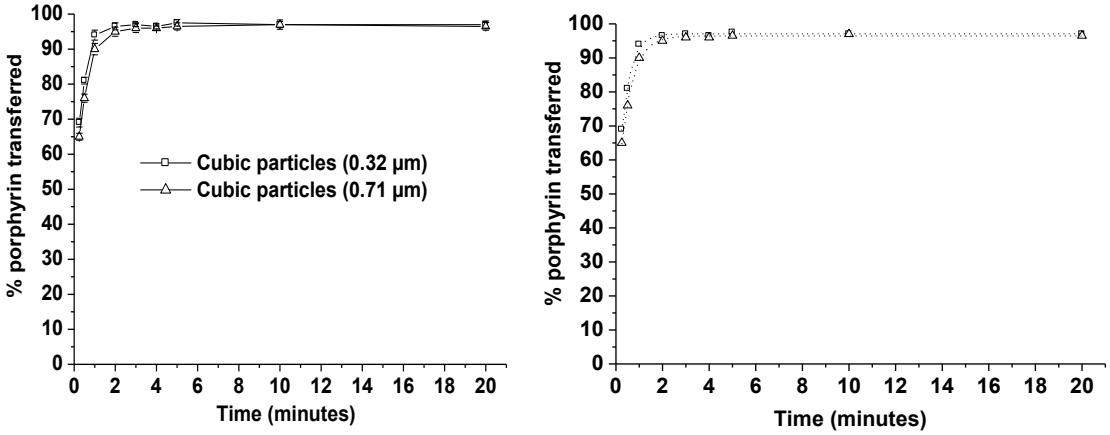

Figure 4.39: Porphyrin transfer (centrifugation method) from the crystalline donor particles of FS75/SGChigh to the acceptor cubic particles with different particle sizes, molar ratio 1:25, measurement results (left), fitted curve (right), n = 3.

Table 4.13: Results of the transfer studies with porphyrin and DiI obtained by the centrifugation technique assuming transfer kinetics according to equation [1]

Donor	Acceptor	Molar ratio	Transfer rate constant K (min^{-1})	Final % transferred	Equilibrium time (min)
Fpoloxamer/DCP (porphyrin)	Cubic particles (0.32 µm)	1:25	2.54 ± 0.35	97	1.5
	Cubic particles (0.71 µm)	1:25	2.42 ± 0.24	96.5	1.8
FS75/SGChigh (DiI)	Cubic particles (0.32 µm)	1:25	0.093 ± 0.006	69.8 ± 1.4	42
		1:100	0.09 ± 0.011	82.9 ± 1.6	43

Although the transfer rate to the acceptor cubic particles was nearly the same as to the acceptor emulsion, the amount transferred to the cubic particles was higher than to the emulsion. Compared with the acceptor MLV, the rate and amount of porphyrin transferred to the acceptor cubic particles were higher than to the acceptor MLV. These differences between the three acceptors might be attributed to the unique structure of the cubic particles where the monoolein bilayer (internal structure) is extending in three dimensions, with a high specific bilayer/water interfacial area (500-600 m^2/g lipid) [17]. This unique structure of the cubic particles facilitates the diffusion of porphyrin molecules within the bilayer. On the other hand, presence of cholesterol in the acceptor MLV increases the rigidity of the membrane surface and thus decreases the rate of porphyrin transfer to the internal bilayer. In addition, the cubic particles had a smaller particle size (0.32, 0.71 µm) than the emulsion (6 µm) and MLV (10 µm), which leads to a higher number of cubic particles in the transfer mixture.

Due to the high affinity and transfer rate that was observed with porphyrin to the acceptor monoolein dispersion, further transfer experiments were carried out with the more lipophilic drug model DiI to the monoolein acceptor. In contrast to the transfer to the acceptor emulsion [6] and unilamellar vesicles (column method), most of DiI was transferred after 40 minutes with donor:acceptor molar ratio of 1:100 (figures 4.40 and 4.41, table 4.13). The transfer experiments of DiI to the acceptor cubic particles with the ultracentrifugation method thus showed the same results as observed before with the column method. With both methods, the equilibrium amount was about 80% and 65% with molar ratios of 1:25 and 1:100, respectively, and these equilibrium amounts were reached after about 45 minutes with the different transfer methods and the different lipid ratios.

4.4.4 Practical considerations of the centrifugation method

Although the transfer experiments with the centrifugation method do not require the use of columns this method is more tedious than the column method because it requires longer

separation times between the donor and acceptor particles. For each time point in each transfer experiment, three samples (transfer mixture) should be diluted and centrifuged, which is very time consuming. Furthermore, after separation between the donor and acceptor particles, the pellets need to be scraped from the centrifugation tube and dissolved before measuring the drug concentrations. In the case of rapid transfer, each time point was performed as a separate experiment which makes the measurements of rapid transfer with this method very difficult. Moreover, the centrifugation time was 10 and 30 minutes with the acceptor MLV and emulsion or cubic particles, respectively, which means that the time resolution of the method is not below 10 minutes. Also during these long separation times the transfer can continue. In addition, one of the two populations (donor or acceptor) should be in a crystalline form and the other in a liquid form to be easily separated by centrifugation.

Figure 4.40: Supernatant containing the creamy acceptor cubic particles with the characteristic DiI color after ultracentrifugation at 45000 rpm for 30 minutes. Ultracentrifugation was carried out after 1 hour of mixing the donor FS75/SGChigh and acceptor cubic particles with a molar ratio of 1:100.

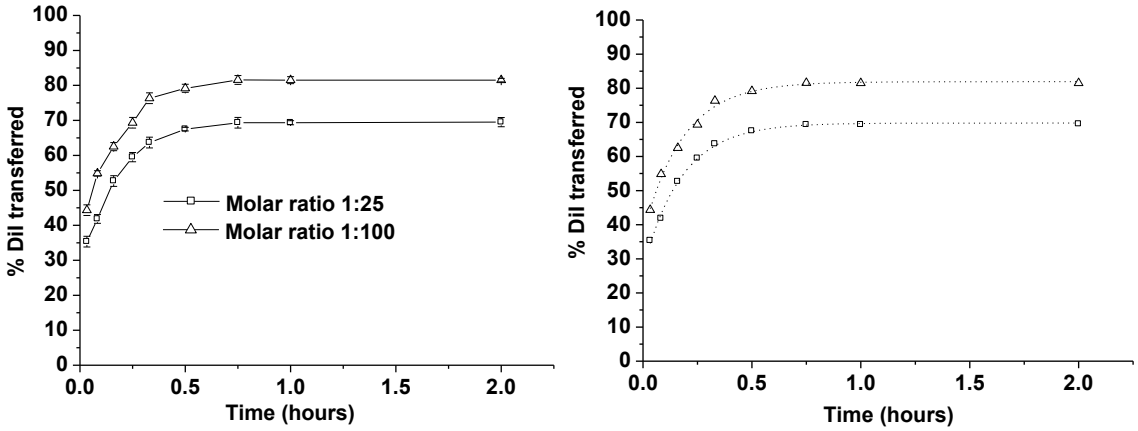

Figure 4.41: DiI transfer (centrifugation method) from the resuspended crystalline nanoparticles of FS75/SGChigh to the acceptor autoclaved monoolein cubic particles prepared from 5% amphiphile (320 nm) with different molar ratios, measurement results (left), fitted curve (right), n = 3.

4.5 Transfer studies with the flow cytometric method

Flow cytometry is mainly used for cell studies. It has also been used for the characterization and quantification of lipid particles like liposomes and emulsion droplets [59, 61, 96-98]. Recently, it has been used to investigate drug transfer between lipid particles [6]. In order to obtain more precise results for the rate of drug transfer, it is useful to work with the flow cytometric method, which is characterized by a very good time resolution and can detect large acceptor particles, which have a particle size of more than 1 µm [59-61].

4.5.1 Porphyrin transfer from trimyristin nanoparticles to MLV and emulsion

Porphyrin transfer studies from Fpoloxamer/DCP to the acceptor emulsion and MLV were carried out using the flow cytometric method with different molar ratios between the donor and acceptor (1:25, 1:50 and 1:100). With regard to the particle size, the detection limits of the flow cytometer used in this investigation are between 0.5 and 40 µm [6]. The acceptor particles with mean particle sizes of about 10 µm and 6 µm for the MLV and emulsion, respectively, fit into this size interval. The lower size detection limit of 0.5 µm indicates that a detection of the donor particles with a z-average diameter below 0.2 µm will not be possible and thus that these small particles will not disturb the measurements.

By comparing the drug transfer to the acceptor emulsion and MLV a large difference in the rate of drug transfer could be observed between the two types of acceptors (figures 4.42, 4.43 and 4.44). Equilibrium was obtained after about 4 or 5 minutes in case of the acceptor emulsion with all investigated lipid ratios while in the case of the MLV acceptor the equilibrium was obtained after about 12 hours with the all lipid ratios. The amount of drug transferred at equilibrium with the two acceptors was quite similar with the comparable lipid ratios (table 4.14). In the case of the MLV acceptor, the amount transferred from the liquid form of Fpoloxamer/DCP was 32, 45 and 59% for a molar ratio of 1:25, 1:50 and 1:100, respectively, while in the case of the acceptor emulsion it was 32, 46 and 62% for the three molar ratios. These results indicate that the difference between the MLV and emulsion acceptor was mainly in the rate of drug transfer but the final amount transferred was nearly the same. These observations confirm the results that were obtained by the centrifugation method with the acceptor MLV and emulsion. Also the equilibrium values were the same as with the centrifugation method, which were less than the expected equilibrium values.

With both acceptors and as expected, increasing the molar ratio from 1:25 to 1:50 and 1:100 led to an increase in the amount of drug transferred to the different acceptors. This increase in the drug transfer by increasing the molar ratio was due to the increase in the number of the acceptor particles in the transfer mixture. As observed previously with the acceptor unilamellar vesicles using the ion exchange column method, a slightly higher drug transfer was obtained from the crystalline donor particles than from the liquid particles (figure

4.43). This difference in drug transfer was most pronounced with a molar ratio of 1:100 between the donor and acceptor.

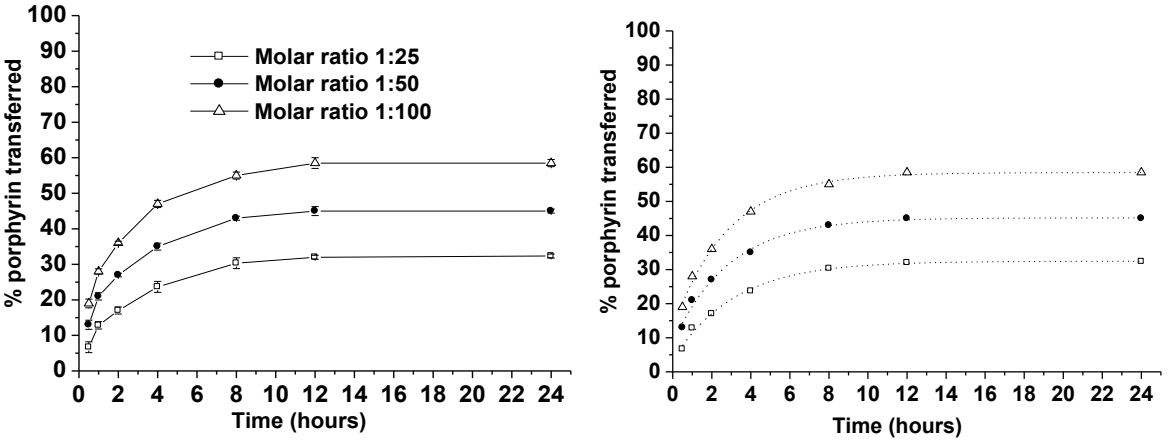

Figure 4.42: Porphyrin transfer (flow cytometry) from the liquid nanoparticles of Fpoloxamer/DCP to the acceptor MLV with different molar ratios, measurement results (left), fitted curves (right), n = 3.

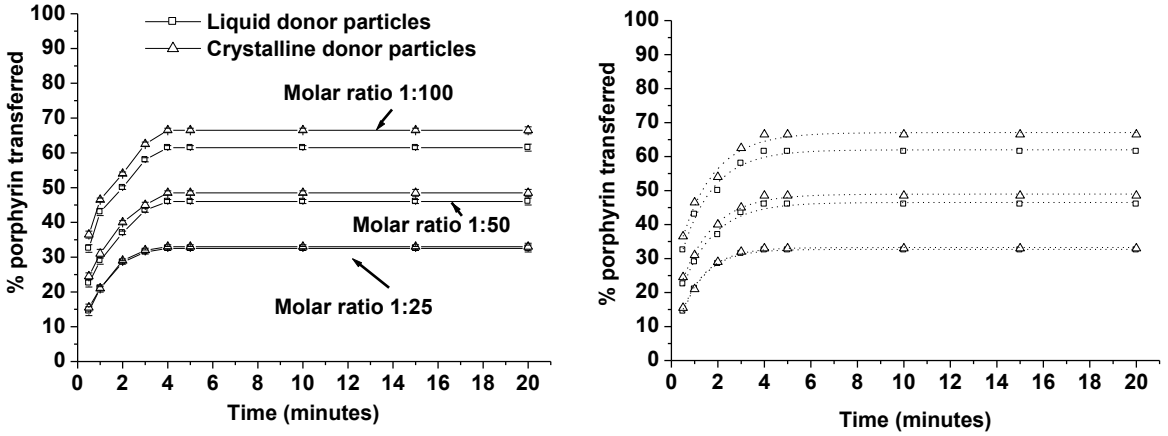

Figure 4.43: Porphyrin transfer (flow cytometry) from the liquid and crystalline nanoparticles of Fpoloxamer/DCP to the acceptor emulsion with different molar ratios, measurement results (left), fitted curves (right), n = 3.

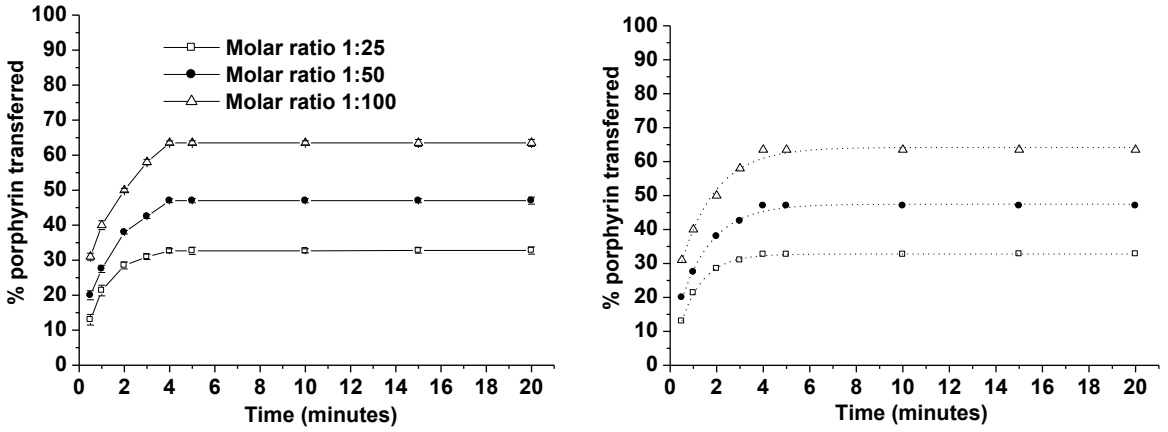

Figure 4.44: Porphyrin transfer (flow cytometry) from the resuspended crystalline nanoparticles of FS75/SGChigh to the acceptor emulsion with different molar ratios, measurement results (left), fitted curves (right), n = 3.

Table 4.14: Results of the transfer studies with porphyrin obtained by the flow cytometric technique assuming transfer kinetics according to equation [1]

Donor	Acceptor	Molar ratio	Transfer rate constant K (min^{-1})	Final % transferred	Equilibrium time
Fpoloxamer/DCP (liquid)	MLV	1:25	0.0053 ± 0.0002	32 ± 1.7	12.8 h
		1:50	0.0058 ± 0.0006	45 ± 1.5	11.8
		1:100	0.006 ± 0.0005	58.5 ± 1.9	11.9
Fpoloxamer/DCP (liquid)	O/w emulsion	1:25	0.9 ± 0.04	32.5 ± 1.5	4.2 min
		1:50	0.8 ± 0.07	46.5 ± 1.2	5 min
		1:100	0.9 ± 0.08	62 ± 1.6	4.9 min
Fpoloxamer/DCP (crystalline)	O/w emulsion	1:25	0.913 ± 0.06	33.5 ± 0.9	4.5 min
		1:50	0.8 ± 0.08	49 ± 1.9	5 min
		1:100	0.85 ± 0.06	67 ± 1.6	5.2 min
FS75/SGChigh (crystalline)	O/w emulsion	1:25	0.95 ± 0.03	33 ± 1.1	4.4 min
		1:50	0.85 ± 0.04	47 ± 0.9	5.4 min
		1:100	0.8 ± 0.07	65 ± 1.5	5.5 min

4.5.2 Porphyrin transfer from the Miglyol nanoemulsion to an o/w emulsion

Assuming an equal porphyrin distribution between the donor and acceptor, about 99% of the porphyrin was expected in the different acceptors (MLV, unilamellar vesicles and emulsion) at a molar ratio of 1:100 between the donor and acceptor. The maximum amount of porphyrin transferred to the different acceptors was, however, less than this expected value. To find the reason for this difference between the expected and the actual amount of drug transferred and to study the effect of drug affinity on the transfer, the transfer experiment was carried out from Miglyol nanoparticles loaded with porphyrin (donor) to the acceptor o/w emulsion, which was prepared also from Miglyol. As observed before in the transfer from the different donor particles to the acceptor emulsion, the transfer was very rapid and equilibrium was reached after 4 minutes (figure 4.45) with a transfer rate constant (K) of 1.07 min^{-1}. The equilibrium amount was about 68%, which was much less than the expected distribution equilibrium (99%) for the molar ratio of 1:100. According to these

results, the affinity to the matrix lipid was not the reason for the difference between the expected distribution value and the actual value because in this experiment the transfer was carried out by using acceptor and donor prepared from the same lipid (Miglyol oil) but still the equilibrium values were less than the expected one.

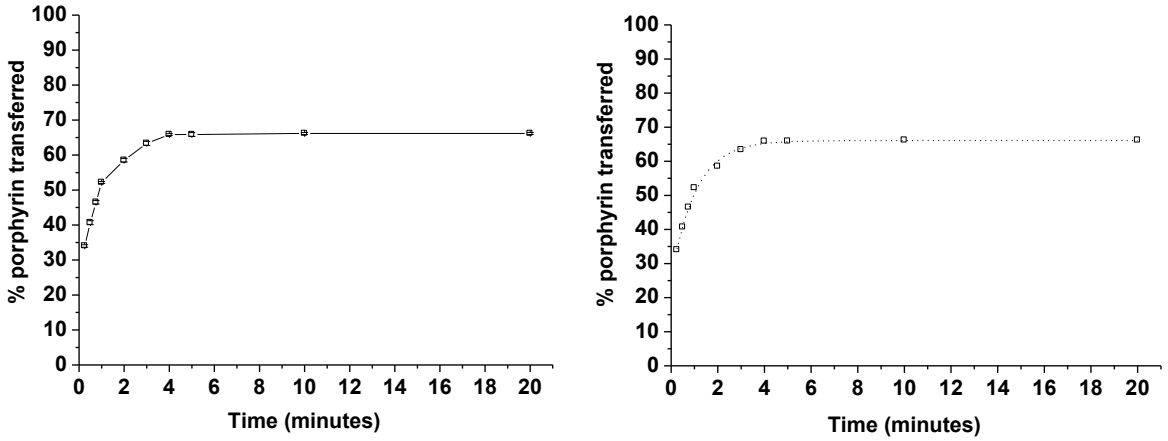

Figure 4.45: Porphyrin transfer (flow cytometry) from Miglyol nanoparticles prepared with 4% poloxamer to the acceptor o/w emulsion with a molar ratio of 1:100, measurement results (left), fitted curve (right), n = 3.

4.5.3 Transfer of porphyrin from tristearin nanoparticles to an o/w emulsion

The transfer of porphyrin from tristearin lipid nanoparticles in the different polymorphic forms (α and β form) to the acceptor o/w emulsion was studied using the flow cytometric technique with a molar ratio of 1:100. The rate of drug transfer (about 1 min^{-1}) observed with the tristearin (D118) nanoparticles was nearly the same as observed before with trimyristin (D114) (figure 4.46, table 4.15).

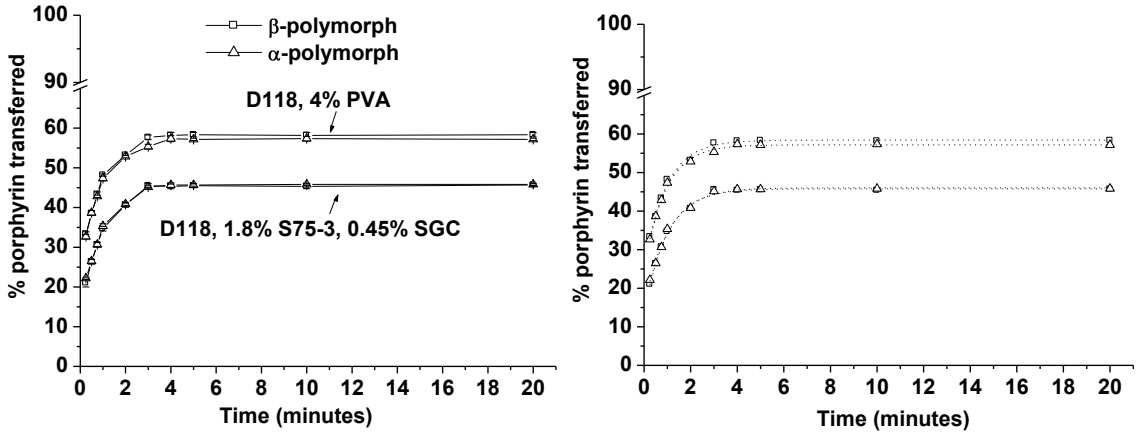

Figure 4.46: Porphyrin transfer (flow cytometry) from the tristearin (D118) nanoparticles stored at 4°C (α-polymorph) or at 23°C after heating to 50°C for 8 hours (β-polymorph) to the acceptor emulsion with a molar ratio of 1:100, measurement results (left), fitted curve (right), n = 3.

Table 4.15: Results of transfer studies of porphyrin from the D118 lipid nanoparticles to the acceptor o/w emulsion with a molar ratio of 1:100 obtained by the flow cytometric technique assuming transfer kinetics according to equation [1]

Donor	Transfer rate constant K (min^{-1})	Final % transferred	Equilibrium time (minutes)
5% D118, 4% PVA (α-form) [a]	1.1 $\pm$ 0.087	57%	3.5
5% D118, 4% PVA (β-form) [b]	1.1 $\pm$ 0.09	58%	3.8
5% D118, 1.8% S75-3, 0.45% SGC (α-form) [a]	1.1 $\pm$ 0.06	45%	4
5% D118, 1.8% S75-3, 0.45% SGC (β-form) [b]	1 $\pm$ 0.07	46%	4.1

[a] stored at 4°C
[b] stored at 23°C after shaking at 50°C for 8 hours

There was no difference in the course of porphyrin transfer between the nanoparticles in the two different polymorphic forms. For D118 nanoparticles stabilized with different stabilizers, equilibrium was obtained after a few minutes with an equilibrium amount transferred of about 45% and 58% for D118 particles stabilized with 1.8% S75-3/0.45% SGC and 4% PVA, respectively (figure 4.46, table 4.15). The rate of drug transfer was nearly the same in the differently stabilized dispersions but the equilibrium amount in case of S75-3/SGC stabilized nanoparticles was much lower than for the PVA stabilized nanoparticles. This low equilibrium amount might be due to the formation of a rigid phospholipid shell by the stabilizer S75-3 surrounding the triglyceride core of the nanoparticles [65-66].

4.5.4 Porphyrin and DiI transfer to the acceptor cubic particles

Complete porphyrin transfer within few minutes was observed with the acceptor cubic particles using the centrifugation and the ion exchange column methods. In order to obtain more precise results in the amount and rate of drug transfer, it is useful to work with the flow cytometric method. As observed before with the other methods (centrifugation and column method) porphyrin transfer to the acceptor cubic particles detected by flow cytometry was very rapid and completed within 3 minutes (figure 4.47, table 4.16). The transfer rate constant was 1.6 and 1.5 min^{-1} and the final percentage of drug transferred was 98 and 97.5% for the cubic particles with the particle size of 1.2 and 2.1 µm, respectively. These results obtained from flow cytometry confirm the results that were obtained with centrifugation and the column method. They indicate that porphyrin transfer to the different acceptor cubic particles was very rapid and complete (the drug transfer at equilibrium was about the same as the expected value). By comparing these results of porphyrin transfer to the acceptor cubic particles with the results of porphyrin transfer to the other acceptors

(emulsion, MLV and unilamellar vesicles) with the different transfer methods, it could be observed that complete porphyrin transfer was only observed with the acceptor cubic particles, while in the case of the other acceptors porphyrin transfer at equilibrium was not the same as the expected value. As mentioned before, the cubic phase is characterized by an extremely high membrane area to which the drug can be transferred and this explains the complete porphyrin transfer that was observed with the acceptor cubic particles in comparison with the other acceptors. By comparing the transfer rate constant of porphyrin to the acceptor monoolein dispersions using the three different techniques (ion exchange column, centrifugation and flow cytometry) it could be observed that the transfer rate constant of porphyrin using the flow cytometric technique (about 1.5 min^{-1}) was lower than the transfer rate constant derived from the centrifugation and ion exchange techniques (about 2.5 min^{-1}). This difference can be attributed to the difference in the time resolution. Column and centrifugation technique require the separation of the donor and acceptor particles and during the time required for separation the transfer can continue. Thus, column and centrifugation technique lead to an overestimation of the transfer rate constant. The best technique to measure the rapid porphyrin transfer to the cubic particles was the flow cytometric one, which has a very good time resolution and does not require the critical step separating the donor and acceptor.

The results of DiI transfer using the flow cytometric technique confirmed the results that were obtained from the centrifugation and column technique (figure 4.48, table 4.16). For the transfer of DiI, there were no differences between the three techniques (ion exchange column, centrifugation and flow cytometry). This can be explained by the moderate transfer rate of DiI for which the time resolution is not a critical factor.

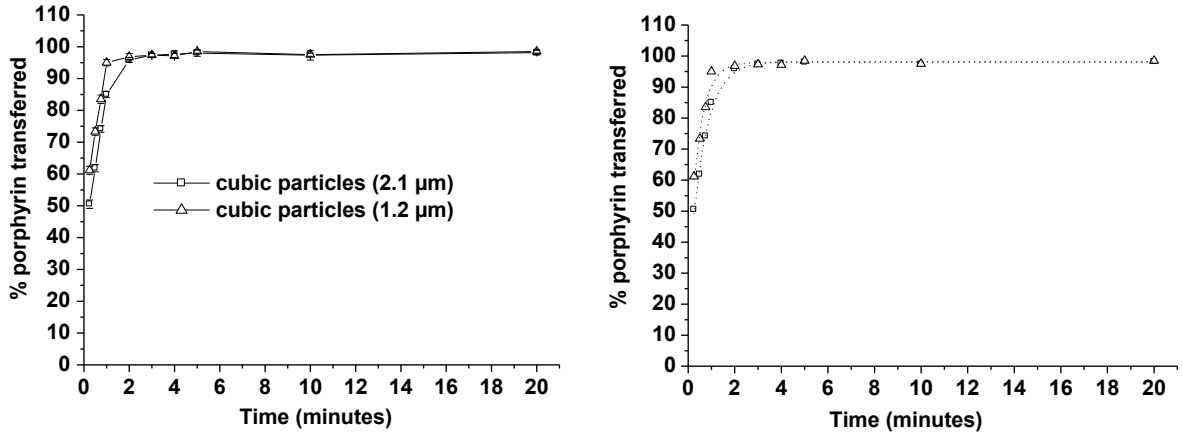

Figure 4.47: Porphyrin transfer (flow cytometry) from the crystalline donor particles of Fpoloxamer/DCP to the acceptor cubic particles with different particle sizes at a molar ratio of 1:25, measurement results (left), fitted curve (right), n = 3.

Table 4.16: Results of the transfer studies with porphyrin and DiI obtained by the flow cytometric technique assuming transfer kinetics according to equation [1]

Donor	Acceptor	Molar ratio	Transfer rate constant K (min^{-1})	Final % transferred	Equilibrium time (min)
Fpoloxamer/DCP (porphyrin)	Cubic particles (1.2 µm)	1:25	1.6 ± 0.21	98 ± 1.8	2.8
	Cubic particles (2.1 µm)	1:25	1.5 ± 0.15	97.5 ± 2.4	3
FS75/SGChigh (DiI)	Cubic particles (2.1 µm)	1:25	0.105 ± 0.003	64 ± 1.5	40
		1:100	0.1 ± 0.004	82 ± 1.7	40

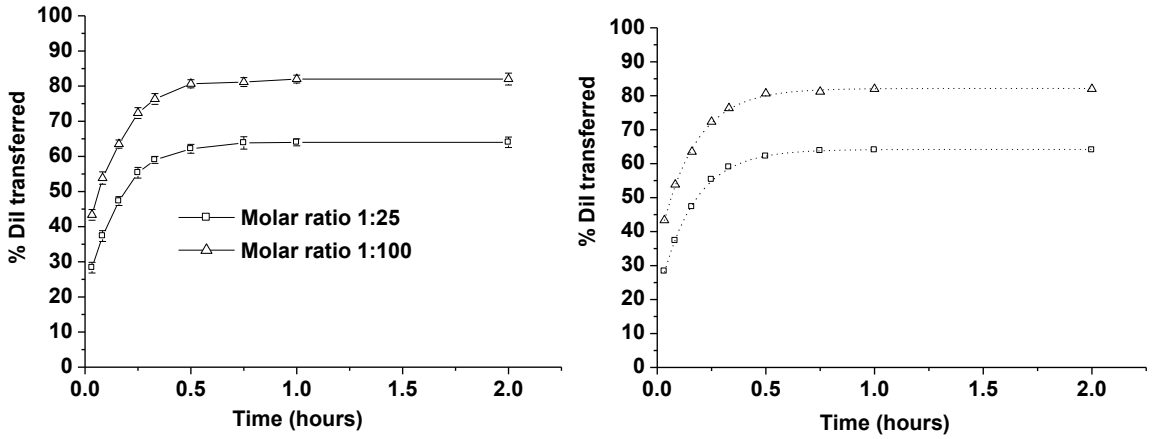

Figure 4.48: DiI transfer (flow cytometry) from the resuspended crystalline nanoparticles of FS75/SGChigh to the acceptor monoolein cubic particles prepared from 15% amphiphile (particle size 2.1 µm) with different molar ratios, measurement results (left), fitted curve (right), n = 3.

4.5.5 Porphyrin transfer from the donor monoolein dispersions to an o/w emulsion

The transfer experiments from the monoolein/poloxamer dispersions (vesicles and cubic particles) to the acceptor emulsion with the flow cytometric method were carried out to confirm the affinity of porphyrin to the monoolein dispersions. At a donor:acceptor ratio of 1:100, the rate of drug transfer was low (about 0.7 h^{-1}) and the final percent transferred was about 50% with both types of donor particles (figure 4.49, table 4.17). Equilibrium was obtained after about 6 hours. In contrast, the transfer from D114 donor lipid nanoparticles to the same acceptor emulsion equilibrated after about 3 minutes. The transfer from the donor monoolein dispersion was thus very slow in comparison with the donor D114 lipid nanoparticles. By using these monoolein dispersions as acceptor particles, rapid and almost complete drug transfer was observed and by using them as donor particles, the drug transfer was very low. The results of the monoolein dispersions as acceptor particles in one experiment and as donor in the other experiments indicate the high affinity of porphyrin to monoolein dispersions.

Table 4.17: Results of the transfer studies with porphyrin from the monoolein dispersions to the acceptor emulsion droplets at a molar ratio of 1:100 obtained by the flow cytometric technique assuming transfer kinetics according to equation [1]

Donor	Transfer rate constant K (min^{-1})	Final % transferred	Equilibrium time (h)
Monoolein vesicles	0.012 ± 0.008	54 ± 0.5	5.7
Monoolein cubic particles	0.011 ± 0.005	52 ± 0.3	6

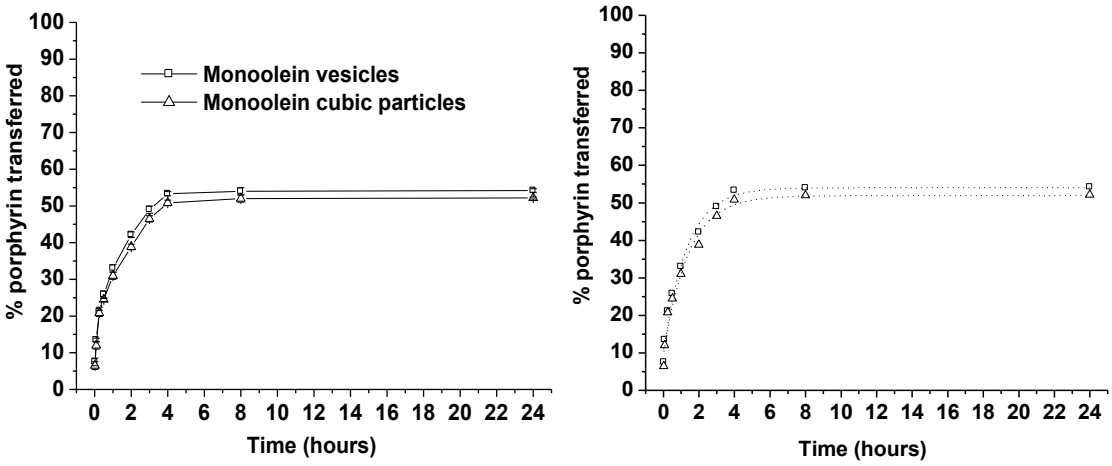

Figure 4.49: Porphyrin transfer (flow cytometry) from the donor monoolein/poloxamer dispersions (vesicles or cubic particles) to the acceptor Miglyol emulsion with a molar ratio of 1:100, measurement results (left), fitted curve (right), n = 3.

4.5.6 Nile red transfer to the acceptor MLV and o/w emulsion

The transfer of Nile red, which is a less lipophilic dye than porphyrin, was very rapid and equilibrated after few minutes as observed by the column and centrifugation method. In order to calculate the transfer rate constant and also to obtain results from a method that has an even better time resolution, experiments were performed with the flow cytometric method. The transfer results of Nile red to the acceptor emulsion and MLV are illustrated in figure 4.50. The transfer of Nile red seemed to be completed after about 3 minutes with the different acceptors (as observed in the transfer experiments with the centrifugation and column method). After 15 seconds, the percentage of drug transferred was 53 and 47% for the acceptor emulsion and MLV, respectively, and after 1 minute more than 75% of the drug had been transferred with both formulations. The amount of Nile red transferred at equilibrium was the same as the expected value, which indicates that all of the Nile red must have transferred from the donor particles to the different acceptors. The transfer rate constant was 1.9 and 1.05 min^{-1} for the acceptor emulsion and MLV, respectively (table 4.18). When comparing the transfer rate constant of Nile red to the acceptor MLV and emulsion obtained

by the centrifugation and flow cytometric technique (table 4.18), it is obvious that the transfer rate constant to both acceptors derived from the centrifugation technique was higher than the transfer rate constant obtained from the flow cytometric technique. As discussed before, this difference in the transfer rate constant can be attributed to the rapid drug transfer of Nile red and the long separation time between the donor and the acceptor resulting in an overestimation of the transfer rate constant by the centrifugation method.

4.5.7 Practical considerations of the flow cytometric method

Since the flow cytometric method does not require a separation between the donor and acceptor particles, it is considered as the easiest method compared to the other methods (column and centrifugation method). Although this advantage of the flow cytometric technique it requires the use of fluorescent substances as drug model and large acceptor particles which can be recognized by a flow cytometer. This means that the transfer to the acceptor unilamellar vesicles and monoolein vesicles cannot be measured using this technique.

Table 4.18: Results of the transfer studies from the resuspended nanoparticles of FS75/SGChigh with Nile red at a molar ratio of 1:100 assuming transfer kinetics according to equation [1]

Transfer method	Acceptor	Transfer rate constant K (min^{-1})	Final % transferred	Equilibrium time (min)
Flow cytometry	MLV	1.05 ± 0.07	100.5 ± 1.5	4
	O/W emulsion	1.9 ± 0.05	100 ± 1.15	2.5
Centrifugation	MLV	1.9 ± 0.08	98 ± 1.8	2.5
	O/W emulsion	3.3 ± 0.37	101 ± 1.9	1

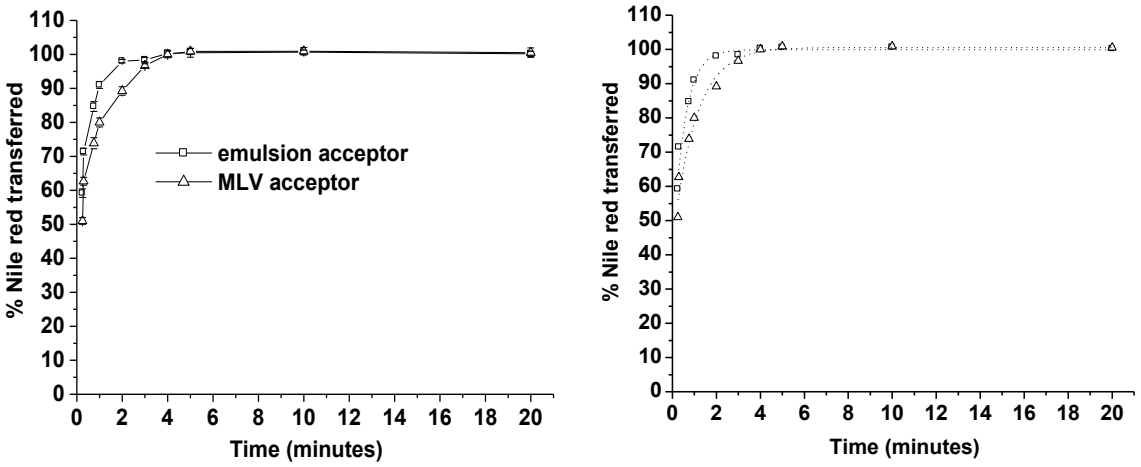

Figure 4.50: Nile red transfer (flow cytometry) from the resuspended crystalline lipid nanoparticles of FS75/SGChigh to different acceptor particles with a molar ratio of 1:100, measurement results (left), fitted curve (right), n = 3.

Chapter 5: Final discussion

The aim of this study was to measure the transfer of different drug models from lipid nanoparticles to different lipophilic acceptors and to determine the factors affecting this transfer. Transfer measurements to different lipophilic acceptor compartments were used instead of measuring the drug release into the aqueous phase to better mimic the environment encountered by the drug in the body. In addition to these transfer measurements, a comparison between three different techniques, which were used to measure the transfer, was an important goal of this study. Lipid nanoparticles were chosen as donor particles due to their advantages, which include their small particle size, toxicological safety and the possibility of large-scale production. Lipid nanoparticles from trimyristin were prepared by using different concentrations of S75, SGC and poloxamer as stabilizers. To eliminate a potential influence of additional colloidal structures, the lipid nanoparticles were separated from the excess liposomes, which were formed during homogenization. Ultracentrifugation was a good technique to separate the lipid nanoparticles from the liposomes but a small amount of the lipid nanoparticles was lost due to the centrifugation procedure. Trimyristin nanoparticles can exist in two different physical states, depending on storage conditions after preparation by melt-homogenization. After cooling to room temperature, the nanoparticles are present in the form of emulsion droplets whereas storage at lower temperatures, e.g. in a refrigerator, will lead to crystallization of the matrix lipid.

Many factors affecting the drug transfer from the lipid nanoparticles were studied such as the physical state of the nanoparticles, particle size of the acceptors, molar ratio between the donor and acceptor, the type of the acceptor lipid, the total lipid concentration in the transfer mixture and the lipophilicity of the drug model. During the crystallization of the nanoparticles, expulsion of the drug to the surface of the nanoparticles took place, which made the transfer from the crystalline nanoparticles slightly higher than the liquid one [6]. Increasing the acceptor to donor ratio led to an increase in the available surface area of the acceptor and thus increased the amount of drug transferred. On the other hand, increasing the total lipid concentration in the transfer mixture led to a decrease in the distance between the donor and acceptor particles in the transfer mixture which in turn increased the transfer rate of the drug.

The effect of the type of the lipid that was used in the preparation of the acceptor particles was demonstrated by comparing the transfer of porphyrin to the acceptor monoolein vesicles and the unilamellar vesicles, which were prepared from EPC and cholesterol. Although both are vesicles and nearly have the same size the transfer to the acceptor monoolein vesicles was faster than to the vesicles, which were prepared from EPC and cholesterol. In addition to this faster transfer, the transfer to the acceptor monoolein vesicles was complete while the

transfer to the acceptor EPC vesicles was incomplete. Monoolein is more hydrophobic than EPC, which may explain the high affinity of the lipophilic porphyrin to the acceptor monoolein vesicles. In addition, the acceptor EPC vesicles contain cholesterol, which increases the rigidity of the vesicles bilayer and thus may decrease the rate of porphyrin transfer to the acceptor EPC vesicles. The transfer of porphyrin to the acceptor emulsion was very rapid with a transfer rate constant nearly the same as for the acceptor monoolein dispersions. Similar results were previously reported for the transfer of porphyrin from trimyristin lipid nanoparticles to the acceptor emulsion [6]. Although the acceptor MLV had the same composition as the acceptor unilamellar vesicles the transfer of porphyrin to the acceptor MLV was slower than to the acceptor unilamellar vesicles, which might be attributed to the differences in the particle size and lamellarity of the two acceptors. The large particles size of the acceptor MLV decreased the number of the acceptor particles in transfer mixture as compared with the acceptor unilamellar vesicles which had a small particle size and thus a higher number of acceptor particles in the transfer mixture.

The lipophilicity of the drug model was another factor, which affected the drug transfer and this factor was studied by measuring the transfer of different drug models with different degrees of lipophilicity. The transfer of Nile red, which is the least lipophilic drug model, was very rapid and complete to the different acceptors due to its rapid diffusion to the acceptor particles and also the rapid diffusion from layer to layer within the acceptor particles (MLV). The transfer of porphyrin, which is more lipophilic than Nile red, occurred at the lipid water interface [6, 84]. By increasing the lipid water interface as in case of the acceptor cubic particles, complete and very rapid drug transfer was observed. In contrast to the acceptor cubic particles, porphyrin transfer to the other acceptors (MLV, emulsion and unilamellar vesicles) was incomplete which confirmed the fact that porphyrin transfer was limited to the lipid water interface and saturation of this interface led to termination of the transfer at values less than the expected values. Furthermore, porphyrin appears to have a higher affinity to apolar lipids than Nile red which explains the less pronounced transfer from the donor lipid nanoparticles as compared with Nile red [99]. This high affinity to apolar lipids explains also the high transfer rate and amount of porphyrin to the acceptor monoolein dispersions because monoolein is more lipophilic than the other acceptor lipids. The transfer of DiI, which is the drug model with the highest lipophilicity, was very slow and the transfer stopped at very low values except with the acceptor monoolein dispersions.

The transfer rate is a very important parameter in the transfer experiments. In some transfer experiments, the transfer was very rapid and the equilibrium was obtained after few minutes. The centrifugation and the ion exchange column technique were not suitable to measure this very rapid transfer in an undistorted way because in both techniques a separation between the donor and acceptor was required. This separation took time and during this time the

transfer can continue which led to an overestimation of the transfer rate constant. This is considered as the most important disadvantage of both methods, which was overcome with the flow cytometric technique. The flow cytometry was the best technique to measure these very rapid transfer rates because it does not need the separation step between the donor and acceptor. Thus the transfer rate that was obtained from the flow cytometric technique was more precise than the transfer rate constant that was obtained from the centrifugation and column technique for rapid drug transfer. In addition to the inaccurate transfer rate constant that was calculated from the centrifugation and ion exchange column technique, other disadvantages were observed with both techniques. In case of the centrifugation technique one of the two populations (donor or acceptor) should be in the liquid state while the other should be in the crystalline form to be easily separated from each other. The acceptor MLV particles are neither crystalline nor liquid but they were prepared with a highly concentrated sucrose solution in order to be easily separated as pellet after centrifugation. With the ion exchange column technique one of the two populations should be charged and the other should be neutral and both populations should be of small particle size to avoid blockage of the column. These requirements were not needed in the flow cytometric technique but the flow cytometric technique depends on the use of fluorescent substances as drug model and large acceptor particles which can be recognized by a flow cytometer. This means that the transfer to the acceptor unilamellar vesicles and monoolein vesicles cannot be measured using this technique. Concerning the performance of the three techniques, the centrifugation technique is a tedious technique because it needs a long time to separate the donor and acceptor particles and after this separation the pellets and the supernatant should be dissolved to measure the drug concentration. In contrast, the flow cytometry is the easiest technique because it does not need the separation between the donor and acceptor particles, which allows the direct measurement of the transfer mixture.

Many conclusions can be derived from this study, first each technique has its own advantages and disadvantages and the choice of the technique that can be used to measure the transfer depends on several factors such as the physicochemical properties of both populations (donor and acceptor particles) and the type of the drug. Second, compared to commonly applied release methods, the transfer to the different lipophilic acceptor compartments is better than the commonly applied release methods relative to the conditions in the blood. Finally, monoolein dispersions containing cubic particles or vesicles can very successfully be used as a new lipophilic acceptor compartment to measure the drug transfer from lipid nanoparticles. In addition to providing a good affinity for the lipophilic drug models under investigation the properties of the monoolein particles can be adapted to be used in all three transfer study techniques.

Chapter 6: Summary

Many methods have been described to investigate the in vitro drug release of lipid nanoparticles, which appear to be of limited suitability due to the use of aqueous release media. In this study, in order to better mimic the environment encountered by the drug after administration, many lipophilic compartments were used to which the transfer of different drug models was measured. The detection of the substances transferred from lipid nanoparticles into the different lipophilic compartments was performed using the three different techniques centrifugation, ion exchange and flow cytometry.

Different lipid donor nanoparticles were prepared using trimyristin and medium chain triglycerides as matrix lipids. Ultracentrifugation was carried out on the trimyristin nanoparticles to separate the nanoparticles from the excess phospholipid used as emulsifier. The nanoparticles were loaded with the three different drug models porphyrin, Nile red and DiI. Differential scanning calorimetry (DSC), ^{31}P NMR spectroscopy, cryo transmission electron microscopy (cryo-TEM) and high performance liquid chromatography of the donor lipid nanoparticles showed that the ultracentrifugation process did not only lead to the separation between the lipid nanoparticles and the excess S75 emulsifier but also to the loss of a small amount of the nanoparticles. The mean particle size of the different donor particles was less than 150 nm.

Different lipophilic acceptor compartments were used in this study. Egg phosphatidyl choline and cholesterol were chosen for the preparation of acceptor multilamellar and unilamellar vesicles since they represent an unsaturated and uncharged bilayer that is similar to many physiological membranes. O/w emulsion droplets, which were prepared from Miglyol 812, were also used as acceptor particles. Monoolein dispersions (in the form of lyotropic liquid crystalline cubic particles or vesicles) were introduced as a new lipophilic acceptor compartment for drug transfer studies. Six monoolein dispersions were prepared with different concentrations of monoolein and poloxamer in order to obtain large cubic particles to be suitable for the use with the flow cytometric transfer technique. Monoolein dispersions were also applicable as acceptor particles for the transfer experiments with the other two techniques.

A large difference was observed in the transfer of porphyrin to the different acceptors where the transfer was moderate to the acceptor MLV and rapid to the acceptor unilamellar vesicles. With monoolein dispersions and emulsions as acceptor, the transfer was very rapid and equilibrium was obtained after a few minutes. In case of the acceptor MLV, unilamellar vesicles and emulsion the transfer was not complete and the transfer stopped at concentrations lower than the expected values. This may be due to the saturation of the surface of the acceptor particles. In contrast, the transfer to the acceptor monoolein

dispersions was complete which means that the equilibrium values were the same as the expected values. The porphyrin transfer from the crystalline nanoparticles was slightly higher than from the liquid nanoparticles especially at a high acceptor/donor ratio.

The transfer of Nile red, which is less lipophilic than porphyrin, was very rapid to all different acceptors employed (MLV, unilamellar vesicles and emulsion) with an equilibrium amount transferred that was nearly the same as the expected values. This was attributed to the ability of Nile red to diffuse and distribute within the acceptor particles. The transfer of DiI, which is more lipophilic than porphyrin, to the acceptor monoolein cubic particles was slower than that of porphyrin and incomplete. Also the transfer rate and amount of DiI to the acceptor unilamellar vesicles was very low. The transferred amount of the different drug models highly depended on the acceptor to donor ratio and by increasing this ratio the amount of transferred drug increased.

The transfer rate constant of porphyrin to the acceptor monoolein dispersions and emulsion derived from the centrifugation and ion exchange column technique was higher than the transfer rate constant obtained from the flow cytometric technique. This can be attributed to the rapid transfer of porphyrin to these acceptors and the inability of the two techniques (centrifugation and ion exchange column) to accurately measure the rapid transfer because they require the separation between the donor and acceptor particles and during this separation time the transfer can continue. The flow cytometric technique does not require this separation and thus it gives more accurate transfer rate constant than the other two techniques. The same was observed with the transfer of Nile red to the different acceptors because the transfer of Nile red was very rapid. Since the transfer of DiI was slower than the transfer of porphyrin to the acceptor monoolein dispersions and o/w emulsion and also slower than the transfer of Nile red to the different acceptors, the three techniques showed the same transfer results (transfer rate and amounts) of DiI to the acceptor cubic particles. In conclusion, this study shows that the transfer depends on several factors such as the physical state of the nanoparticles, particle size of the acceptors, molar ratio between the donor and acceptor, the type of the lipid that is used in the preparation of the acceptors, the total lipid concentration in the transfer mixture and the lipophilicity of the drug model. All three techniques studied are suitable to investigate the transfer of DiI while the flow cytometric technique is the best one to measure the very rapid transfer of porphyrin and Nile red. Finally, monoolein dispersions in the form of cubic particles or vesicles are very useful as acceptor particles for transfer studies with lipophilic drugs.

Zusammenfassung

Es sind viele Methoden beschrieben, um die in vitro-Freisetzung aus Lipidnanopartikeln zu untersuchen. Allerdings sind diese aufgrund der Verwendung von wässrigen Freisetzungsmedien nur bedingt in dieser Arbeit geeignet. Um eine bessere Annäherung an in vivo-Zustände zu erreichen, wurden viele lipophile Kompartimente verwendet, in die hinein der Transfer verschiedener Arzneistoffmodelle gemessen wurde. Durch die drei unterschiedlichen Methoden Zentrifugation, Ionenaustausch und Durchflusszytometrie wurde der Transfer der unterschiedlichen Substanzen aus Lipidnanopartikeln in die verschiedenen lipophilen Kompartimente detektiert.

Verschiedene Donor-Lipidnanopartikel wurden unter Verwendung von Trimyristin und mittelkettigen Triglyceriden als Matrixmaterialien hergestellt. Trimyristin-Nanopartikel wurden ultrazentrifugiert, um die Nanopartikel vom Überschuss der als Emulgator eingesetzten Phospholipide zu trennen. Die Nanopartikel wurden mit drei verschiedenen Arzneistoffmodellen beladen, Porphyrin, Nilrot und DiI. Differentialthermoanalyse (DSC), ^{31}P-NMR-Spektroskopie und Kryotransmissionselektronenmikroskopie (Kryo-TEM) sowie Hochleistungs-Flüssigchromatographie an den Donorpartikeln zeigten, dass die Ultrazentrifugation der Lipidnanopartikel nicht nur zur Trennung der Lipidnanopartikel vom Überschuss des S75-Emulgators führte, sondern auch den Verlust einer kleinen Menge der Nanopartikel verursachte. Die mittlere Teilchengröße der verschiedenen Donorpartikel betrug weniger als 150 nm. In dieser Studie wurden unterschiedliche lipophile Akzeptor-Kompartimente verwendet. Zur Herstellung des MLV-Akzeptors und der unilamellaren Akzeptor-Vesikel wurden Ei-Phosphatidylcholin und Cholesterol eingesetzt, da sie eine ungesättigte und ungeladene Doppelschicht bilden, die vielen physiologischen Membranen ähnlich ist. Als Akzeptorpatikel sind ebenfalls o/w Emulsionspartikel aus Miglyol angewendet worden. Monoolein-Dispersionen (in Form von lyotrop-kubischen flüssigkristallinen Partikeln oder Vesikeln) wurden als neue lipophile Akzeptorkompartimente eingeführt. Sechs Monoolein-Dispersionen mit verschiedenen Konzentrationen von Monoolein und Poloxamer wurden hergestellt, um große kubische Partikel zu erhalten, die für die durchflusszytometrische Transfer-Technik geeignet sind. Für die beiden anderen Transfermethoden waren Monoolein-Dispersionen als Akzeptoren ebenfalls geeignet.

Es wurden große Unterschiede im Transferverhalten von Porphyrin zu den verschiedenen Akzeptoren beobachtet. Die Übertragung auf den MLV-Akzeptor war mäßig, die auf die unilamellaren Akzeptor-Vesikeln hingegen schnell. Mit Monoolein-Dispersionen und Emulsionen als Akzeptor war der Transfer sehr schnell, und das Gleichgewicht war nach wenigen Minuten erreicht. Im Falle der MLV, unilamellaren Vesikel und Emulsion als Akzeptor kam der Transfer bei Konzentrationen unterhalb der erwarteten Werte zum

Stillstand, was wahrscheinlich auf die Sättigung der Partikeloberfläche des Akzeptors zurückzuführen ist. Im Gegensatz dazu war der Transfer zu den Akzeptorpartikeln aus Monoolein vollständig, d. h. die erwarteten Gleichgewichtswerte wurden erreicht. Der Porphyrin-Transfer aus den kristallinen Nanopartikeln war höher als der aus flüssigen Nanopartikeln, vor allem bei einem hohen Akzeptor / Donor-Verhältnis. Der Transfer von Nilrot, das weniger lipophil ist als Porphyrin, zu allen untersuchten Akzeptoren (MLV, unilamellare Vesikel und Emulsion) war sehr schnell. Die im Gleichgewicht übertragene Menge stimmte mit den erwarteten Werten fast überein. Dies könnte auf die Fähigkeit des Nilrots, sich in den Akzeptor-Teilchen zu verteilen, zurückzuführen sein. Es wurde eine geringe Übertragung des DiI zu den unilamelaren Akzeptor-Vesikeln beobachtet. Die transferierte Menge der verschiedenen Wirkstoffmodelle war stark abhängig vom Akzeptor-zu-Donor-Verhältnis. Durch eine Erhöhung dieses Verhältnisses wurde die Menge des übertragenen Wirkstoffs erhöht. Die Geschwindigkeitskonstanten des Porphyrin-Transfers auf die Akzeptoren aus Monoolein und die Emulsionspartikel, die mit der Zentrifugations und Ionenaustauschmethode erhalten wurden, waren höher als die Geschwindigkeitskonstanten aus der Durchflusszytometrie. Dies kann auf die sehr schnelle Übertragung des Porphyrins zu diesen Akzeptoren zurückgeführt werden. Die beiden Methoden Zentrifugation und Ionenaustauschersäule sind nicht in der Lage, den raschen Transfer genau zu messen, weil sie auf einer Trennung zwischen den Donor- und Akzeptorteilchen beruhen und während des Trennungsvorgangs der Transfer fortgesetzt werden kann. Die Durchflusszytometrie benötigt keine Trennung, wodurch genauere Transferkonstanten erhalten werden können. Die gleichen Beobachtungen wurden für den Transfer des Nilrots zu den verschiedenen Akzeptoren, der ebenfalls sehr schnell war, gemacht. Da der Transfer von DiI zu den Monoolein-Dispersionen und O/W-Emulsionen langsamer war als der des Porphyrins und ebenso langsamer war als der Transfer vom Nilrot zu den verschiedenen Akzeptoren, ergaben die drei Detektionsmethoden die gleichen Ergebnisse für den Transfer von DiI zu den Akzeptoren aus kubischen Teilchen. In dieser Arbeit konnte gezeigt werden, dass der Wirkstofftransfer von verschiedenen Faktoren abhängt, wie dem Aggregatzustand der Donor-Nanopartikel, der Partikelgröße der Akzeptoren, dem Mengenverhältnis zwischen Donor und Akzeptor, der Art des Lipids, das für die Herstellung der Akzeptoren verwendet wurde, der Lipidgesamtkonzentration in der Untersuchungsmischung und der Lipophilie des Modellwirkstoffs. Alle drei in dieser Studie eingesetzten Transfermethoden sind für die Untersuchung des DiI-Transfers geeignet, während die Durchflusszytometrie die beste Methode zur Messung des schnellen Transfers von Porphyrin und Nilrot ist. Schließlich können Monoolein-Dispersionen in Form von kubischen Teilchen oder Vesikeln vorteilhaft als Akzeptor-Partikel für Transferuntersuchungen mit lipophilen Wirkstoffen eingesetzt werden.

References

1 G. M. Lanza, X. Yu, P. M. Winter, D. R. Abendschein, K. K. Karukstis, M. J. Scott, L. K. Chinen, R. W. Fuhrhop, D. E. Scherrer and S. A. Wickline, *Targeted antiproliferative drug delivery to vascular smooth muscle cells with a magnetic resonance imaging nanoparticle contrast agent implications for rational therapy of restenosis.* Circulation, 2002. **106**(22): p. 2842-2847

2 B. Magenheim, M. Y. Levy and S. Benita, *A new in-vitro technique for the evaluation of drug-release profile from colloidal carriers - ultrafiltration technique at low-pressure.* Int J Pharm, 1993. **94**(1-3): p. 115-123

3 A. Fahr, P. van Hoogevest, S. May, N. Bergstrand and M. L. S. Leigh, *Transfer of lipophilic drugs between liposomal membranes and biological interfaces: Consequences for drug delivery.* Eur J Pharm Sci, 2005. **26**(3-4): p. 251-265

4 A. Fahr and X. Liu, *Utilization of liposomes for studying drug transfer and uptake.* Methods Mol Biol, 2010. **606**: p. 1-10

5 J. A. Shabbits, G. N. C. Chiu and L. D. Mayer, *Development of an in vitro drug release assay that accurately predicts in vivo drug retention for liposome-based delivery systems.* J Control Release, 2002. **84**(3): p. 161-170

6 S. Petersen, A. Fahr and H. Bunjes, *Flow cytometry as a new approach to investigate drug transfer between lipid particles.* Mol Pharmaceut, 2010. **7**(2): p. 350–363

7 W. Mehnert and K. Mäder, *Solid lipid nanoparticles - production, characterization and applications.* Adv Drug Deliver Rev, 2001. **47**(2-3): p. 165-196

8 E. Merisko-Liversidge, P. Sarpotdar, J. Bruno, S. Hajj, L. Wei, N. Peltier, J. Rake, J. M. Shaw, S. Pugh, L. Polin, J. Jones, T. Corbett, E. Cooper and G. G. Liversidge, *Formulation and antitumor activity evaluation of nanocrystalline suspensions of poorly soluble anticancer drugs.* Pharm Res, 1996. **13**(2): p. 272-278

9 D. B. Vieira and A. M. Carmona-Ribeiro, *Synthetic bilayer fragments for solubilization of amphotericin B.* J Colloid Interf Sci, 2001. **244**(2): p. 427-431

10 J. T. Kumpulainen and J. T. Salonen, *Natural antioxidants and food quality in atherosclerosis and cancer prevention*. Royal Society of Chemistry Information Service, Cambridge, UK, 1996.

11 K. N. Prasad, L. Santamaria and R. M. Williams, *Nutrients in cancer prevention and treatment*. Humana Press, Totowa, NJ, 1995.

12 R. H. Müller, K. Mäder and S. Gohla, *Solid lipid nanoparticles (SLN) for controlled drug delivery - a review of the state of the art.* Eur J Pharm Biopharm, 2000. **50**(1): p. 161-177

13 S. A. Wissing, O. Kayser and R. H. Müller, *Solid lipid nanoparticles for parenteral drug delivery.* Adv Drug Deliver Rev, 2004. **56**(9): p. 1257-1272

14 G. Storm and D. J. A. Crommelin, *Liposomes: Quo vadis?* Pharm Sci Technol To, 1998. **1**(1): p. 19-31

15 M. Budai and M. Szogyi, *[liposomes as drug carrier systems. Preparation, classification and therapeutic advantages of liposomes].* Acta Pharm Hung, 2001. **71**(1): p. 114-118

16 K. Larsson, *Cubic lipid-water phases - structures and biomembrane aspects.* J Phys Chem, 1989. **93**(21): p. 7304-7314

17 S. Engström, T. P. Norden and H. Nyquist, *Cubic phases for studies of drug partition into lipid bilayers.* Eur J Pharm Sci, 1999. **8**(4): p. 243-254

18 G. Wörle, B. Siekmann, M. H. J. Koch and H. Bunjes, *Transformation of vesicular into cubic nanoparticles by autoclaving of aqueous monoolein/poloxamer dispersions.* Eur J Pharm Sci, 2006. **27**(1): p. 44-53

19 D. Yang, B. Armitage and S. R. Marder, *Cubic liquid-crystalline nanoparticles.* Angew Chem Int Edit, 2004. **43**(34): p. 4402-4409

20 L. S. Helledi and L. Schubert, *Release kinetics of acyclovir from a suspension of acyclovir incorporated in a cubic phase delivery system.* Drug Dev Ind Pharm, 2001. **27**(10): p. 1073-1081

21 S. Engström, B. Ericsson and T. Landh, *A cubosome formulation for intravenous administration of somatostatin.* Proc Int Symp Control Rel Bioact Mater, 1996. **23**: p. 382-383

22 J. Gustafsson, H. Ljusberg-Wahren, M. Almgren and K. Larsson, *Cubic lipid-water phase dispersed into submicron particles.* Langmuir, 1996. **12**(20): p. 4611-4613

23 P. T. Spicer, K. L. Hayden, M. L. Lynch, A. Ofori-Boateng and J. L. Burns, *Novel process for producing cubic liquid crystalline nanoparticles (cubosomes).* Langmuir, 2001. **17**(19): p. 5748-5756

24 C. J. Drummond and C. Fong, *Surfactant self-assembly objects as novel drug delivery vehicles.* Curr Opin Colloid Interface Sci, 1999. **4**(6): p. 449-456

25 J. Gustafsson, H. Ljusberg-Wahren, M. Almgren and K. Larrson, *Submicron particles of reversed lipid phases in water stabilized by a nonionic amphiphilic polymer.* Langmuir, 1997. **13**(26): p. 6964-6971

26 L. C. Collins-Gold, R. T. Lyons and L. C. Bartholow, *Parenteral emulsions for drug delivery.* Adv Drug Deliver Rev, 1990. **5**(3): p. 189-208

27 E. Elbaz, A. Zeevi, S. Klang and S. Benita, *Positively charged submicron emulsions - a new-type of colloidal drug carrier.* Int J Pharm, 1993. **96**(1-3): p. R1-R6

28 R. H. Müller and S. Heinemann, *Fat emulsions for parenteral-nutrition .IV. Lipofundin MCT/LCT regimens for total parenteral-nutrition (TPN) with high electrolyte load.* Int J Pharm, 1994. **107**(2): p. 121-132

29 S. Venkataram, W. M. Awini, K. Jordan and Y. E. Rahman, *Pharmacokinetics of 2 alternative dosage forms for cyclosporine - liposomes and Intralipid.* J Pharm Sci, 1990. **79**(3): p. 216-219

30 R. J. Prankerd and V. J. Stella, *The use of oil-in-water emulsions as a vehicle for parenteral drug administration.* J Parent Sci Technol, 1990. **44**(3): p. 139-149

31 A. Wretlind, *Development of fat emulsions.* J Parenter Enter Nutr, 1981. **5**(3): p. 230-235

32 R. H. Müller, W. Mehnert, J. S. Lucks, C. Schwarz, A. zur Mühlen, H. Weyhers, C. Freitas and D. Rühl, *Solid lipid nanoparticles (SLN) - an alternative colloidal carrier system for controlled drug delivery.* Eur J Pharm Biopharm, 1995. **41**(1): p. 62-69

33 V. Venkateswarlu and K. Manjunath, *Preparation, characterization and in vitro release kinetics of clozapine solid lipid nanoparticles.* J Control Release, 2004. **95**(3): p. 627-638

34 A. zur Mühlen, C. Schwarz and W. Mehnert, *Solid lipid nanoparticles (SLN) for controlled drug delivery - drug release and release mechanism.* Eur J Pharm Biopharm, 1998. **45**(2): p. 149-155

35 K. Westesen, *Novel lipid-based colloidal dispersions as potential drug administration systems - expectations and reality.* Colloid Polym Sci, 2000. **278**(7): p. 608-618

36 K. Westesen and H. Bunjes, *Do nanoparticles prepared from lipids solid at room-temperature always possess a solid lipid matrix?* Int J Pharm, 1995. **115**(1): p. 129-131

37 S. Benita, D. Friedman and M. Weinstock, *Pharmacological evaluation of an injectable prolonged release emulsion of physostigmine in rabbits.* J Pharm Pharmacol, 1986. **38**(9): p. 653-658

38 S. Benita, D. Friedman and M. Weinstock, *Physostigmine emulsion - a new injectable controlled release delivery system.* Int J Pharm, 1986. **30**(1): p. 47-55

39 K. Westesen and B. Siekmann, *Investigation of the gel formation of phospholipid-stabilized solid lipid nanoparticles.* Int J Pharm, 1997. **151**(1): p. 35-45

40 K. Manjunath, J. S. Reddy and V. Venkateswarlu, *Solid lipid nanoparticles as drug delivery systems.* Method Find Exp Clin, 2005. **27**(2): p. 127-144

41 K. Westesen, H. Bunjes and M. H. J. Koch, *Physicochemical characterization of lipid nanoparticles and evaluation of their drug loading capacity and sustained release potential.* J Control Release, 1997. **48**(2-3): p. 223-236

42 H. Bunjes, M. H. J. Koch and K. Westesen, *Effect of particle size on colloidal solid triglycerides.* Langmuir, 2000. **16**(12): p. 5234-5241

43 R. Lander, W. Manger, M. Scouloudis, A. Ku, C. Davis and A. Lee, *Gaulin homogenization: A mechanistic study.* Biotechnol Progr, 2000. **16**(1): p. 80-85

44 B. J. Boyd, *Characterisation of drug release from cubosomes using the pressure ultrafiltration method.* Int J Pharm, 2003. **260**(2): p. 239-247

45 F. Cui, K. Shi, L. Q. Zhang, A. J. Tao and Y. Kawashima, *Biodegradable nanoparticles loaded with insulin-phospholipid complex for oral delivery: Preparation, in vitro characterization and in vivo evaluation.* J Control Release, 2006. **114**(2): p. 242-250

46 M. Demirel, Y. Yazan, R. H. Müller, F. Kilic and B. Bozan, *Formulation and in vitro-in vivo evaluation of piribedil solid lipid micro- and nanoparticles.* J Microencapsulation, 2001. **18**(3): p. 359-371

47 F. Q. Hu, H. Yuan, H. H. Zhang and M. Fang, *Preparation of solid lipid nanoparticles with clobetasol propionate by a novel solvent diffusion method in aqueous system and physicochemical characterization.* Int J Pharm, 2002. **239**(1-2): p. 121-128

48 S. S. D'Souza and P. P. DeLuca, *Methods to assess in vitro drug release from injectable polymeric particulate systems.* Pharm Res, 2006. **23**(3): p. 460-474

49 P. I. Lelkes and H. B. Tandeter, *Studies on the methodology of the carboxyfluorescein assay and on the mechanism of liposome stabilization by red blood cells in vitro.* Biochim Biophys Acta, 1982. **716**(3): p. 410-419

50 S. S. D'Souza and P. P. DeLuca, *Development of a dialysis in vitro release method for biodegradable microspheres.* AAPS Pharmscitech, 2005. **6**(2): p. E323-E328

51 M. Y. Levy and S. Benita, *Drug release from submicronized o/w emulsion - a new invitro kinetic evaluation model.* Int J Pharm, 1990. **66**(1-3): p. 29-37

52 C. Washington, *Drug release from microdisperse systems: A critical review.* Int J Pharm, 1990. **58**(1): p. 1-12

53 C. Washington, *Evaluation of non-sink dialysis methods for the measurement of drug release from colloids - effects of drug partition.* Int J Pharm, 1989. **56**(1): p. 71-74

54 R. Margalit, R. Alon, M. Linenberg, I. Rubin, T. J. Roseman and R. W. Wood, *Liposomal drug delivery - thermodynamic and chemical kinetic considerations.* J Control Release, 1991. **17**(3): p. 285-296

55 C. Washington and F. Koosha, *Drug release from microparticulates - deconvolution of measurement errors.* Int J Pharm, 1990. **59**(1): p. 79-82

56 L. R. McLean and M. C. Phillips, *Mechanism of cholesterol and phosphatidylcholine exchange or transfer between unilamellar vesicles.* Biochemistry, 1981. **20**(10): p. 2893-2900

57 J. A. Hellings, H. H. Kamp, K. W. A. Wirtz and L. I. Vandeene, *Transfer of phosphatidylcholine between liposomes.* Eur J Biochem, 1974. **47**(3): p. 601-605

58 A. M. H. P. van den Besselaar, G. M. Helmkamp and K. W. A. Wirtz, *Kinetic model of protein-mediated phosphatidylcholine exchange between single bilayer liposomes.* Biochemistry, 1975. **14**(9): p. 1852-1858

59 M. Hai, K. Bernath, D. Tawfik and S. Magdassi, *Flow cytometry: A new method to investigate the properties of water-in-oil-in-water emulsions.* Langmuir, 2004. **20**(6): p. 2081-2085

60 A. P. R. Johnston, A. N. Zelikin, L. Lee and F. Caruso, *Approaches to quantifying and visualizing polyelectrolyte multilayer film formation on particles.* Anal Chem, 2006. **78**(16): p. 5913-5919

61 K. Sato, K. Obinata, T. Sugawara, I. Urabe and T. Yomo, *Quantification of structural properties of cell-sized individual liposomes by flow cytometry.* J Biosci Bioeng, 2006. **102**(3): p. 171-178

62 R. Bonnett, *The porphyrins, structure and synthesis.* Academic Press, New York, Part A, 1978. **1**: p. 1-27

63 P. Greenspan, E. P. Mayer and S. D. Fowler, *Nile red: A selective fluorescent stain for intracellular lipid droplets.* J Cell Biol, 1985. **100**(3): p. 965-973

64 F. Rashid and R. W. Horobin, *Interaction of molecular probes with living cells and tissues.2. A structure-activity analysis of mitochondrial staining by cationic probes,*

and a discussion of the synergistic nature of image-based and biochemical approaches. Histochemistry, 1990. **94**(3): p. 303-308

65 H. Bunjes and M. H. J. Koch, *Saturated phospholipids promote crystallization but slow down polymorphic transitions in triglyceride nanoparticles.* J Control Release, 2005. **107**(2): p. 229-243

66 H. Bunjes, F. Steiniger and W. Richter, *Visualizing the structure of triglyceride nanoparticles in different crystal modifications.* Langmuir, 2007. **23**(7): p. 4005-4011

67 K. M. Rosenblatt and H. Bunjes, *Poly(vinyl alcohol) as emulsifier stabilizes solid triglyceride drug carrier nanoparticles in the alpha-modification.* Mol Pharmaceut, 2009. **6**(1): p. 105-120

68 A. Fahr and J. Seelig, *Liposomal formulations of cyclosporin A: A biophysical approach to pharmacokinetics and pharmacodynamics.* Crit Rev Ther Drug, 2001. **18**(2): p. 141-172

69 J. Barauskas, M. Johnsson, F. Johnson and F. Tiberg, *Cubic phase nanoparticles (cubosome): Principles for controlling size, structure, and stability.* Langmuir, 2005. **21**(6): p. 2569-2577

70 J. Drew, A. Liodakis, R. Chan, H. Du, M. Sadek, R. Brownlee and W. H. Sawyer, *Preparation of lipid emulsions by pressure extrusion.* Biochem Int, 1990. **22**(6): p. 983-992

71 J. Ferezou, N. T. Lai, C. Leray, T. Hajri, A. Frey, Y. Cabaret, J. Courtieu, C. Lutton and A. C. Bach, *Lipid-composition and structure of commercial parenteral emulsions.* BBA Lipid Lipid Met, 1994. **1213**(2): p. 149-158

72 M. Rotenberg, M. Rubin, A. Bor, D. Meyuhas, Y. Talmon and D. Lichtenberg, *Physicochemical characterization of intralipid emulsions.* Biochim Biophys Acta, 1991. **1086**(3): p. 265-272

73 K. Westesen, M. Drechsler and H. Bunjes, *Colloidal dispersions based on solid lipids.* In: Dickinson E., Miller R. (Hrg.), Food Colloids: Fundamentals of Formulation, Roy Soc Ch, Cambridge, 2001. p. 103-115

74 S. C. de Araujo, A. C. de Mattos, H. F. Teixeira, P. M. Coelho, D. L. Nelson and M. C. de Oliveira, *Improvement of in vitro efficacy of a novel schistosomicidal drug by incorporation into nanoemulsions.* Int J Pharm, 2007. **337**(1-2): p. 307-315

75 H. Bunjes and T. Unruh, *Characterization of lipid nanoparticles by differential scanning calorimetry, x-ray and neutron scattering.* Adv Drug Deliver Rev, 2007. **59**(6): p. 379-402

76 T. Unruh, H. Bunjes, K. Westesen and M. H. J. Koch, *Observation of size-dependent melting in lipid nanoparticles.* J Phys Chem B, 1999. **103**(47): p. 10373-10377

77 T. Unruh, H. Bunjes, K. Westesen and M. H. J. Koch, *Investigations on the melting behaviour of triglyceride nanoparticles.* Colloid Polym Sci, 2001. **279**(4): p. 398-403

78 E. Esposito, M. Fantin, M. Marti, M. Drechsler, L. Paccamiccio, P. Mariani, E. Sivieri, F. Lain, E. Menegatti, M. Morari and R. Cortesi, *Solid lipid nanoparticles as delivery systems for bromocriptine.* Pharm Res, 2008. **25**(7): p. 1521-1530

79 K. Westesen and T. Wehler, *Physicochemical characterization of a model intravenous oil-in-water emulsion.* J Pharm Sci, 1992. **81**(8): p. 777-786

80 K. Westesen and T. Wehler, *Investigation of the particle-size distribution of a model intravenous emulsion.* J Pharm Sci, 1993. **82**(12): p. 1237-1244

81 K. M. Rosenblatt, D. Douroumis and H. Bunjes, *Drug release from differently structured monoolein/poloxamer nanodispersions studied with differential pulse polarography and ultrafiltration at low pressure.* J Pharm Sci, 2007. **96**(6): p. 1564-1575

82 G. Wörle, M. Drechsler, M. H. J. Koch, B. Siekmann, K. Westesen and H. Bunjes, *Influence of composition and preparation parameters on the properties of aqueous monoolein dispersions.* Int J Pharm, 2007. **329**(1-2): p. 150-157

83 G. Wörle, B. Siekmann and H. Bunjes, *Effect of drug loading on the transformation of vesicular into cubic nanoparticles during heat treatment of aqueous monoolein/poloxamer dispersions.* Eur J Pharm Biopharm, 2006. **63**(2): p. 128-133

84 A. Wiehe, Y. M. Shaker, J. C. Brandt, S. Mebs and M. O. Senge, *Lead structures for applications in photodynamic therapy. Part 1: Synthesis and variation of m-thpc (temoporfin) related amphiphilic a(2)bc-type porphyrins.* Tetrahedron, 2005. **61**(23): p. 5535-5564

85 X. Y. Liu, Q. Yang, N. Kamo and J. Miyake, *Effect of liposome type and membrane fluidity on drug-membrane partitioning analyzed by immobilized liposome chromatography.* J Chromatogr A, 2001. **913**(1-2): p. 123-131

86 K. Jores, A. Haberland, S. Wartewig, K. Mäder and W. Mehnert, *Solid lipid nanoparticles (SLN) and oil-loaded SLN studied by spectrofluorometry and Raman spectroscopy.* Pharm Res, 2005. **22**(11): p. 1887-1897

87 V. Jenning, M. Schäfer-Korting and S. Gohla, *Vitamin A-loaded solid lipid nanoparticles for topical use drug release properties.* J Control Release, 2000. **66**(2-3): p. 115-126

88 E. Yang and W. H. Huestis, *Mechanism of intermembrane phosphatidylcholine transfer: Effects of pH and membrane configuration.* Biochemistry, 1993. **32**(45): p. 12218-12228

89 L. C. Haynesa and M.J. Cho, *Mechanism of nile red transfer from o/w emulsions as carriers for passive drug targeting to peritoneal macrophages in vitro.* Int J Pharm, 1988. **45**(1-2): p. 169-177

90 M. C. Doody, H. J. Pownall, Y. J. Kao and L. C. Smith, *Mechanism and kinetics of transfer of a fluorescent fatty acid between single-walled phosphatidylcholine vesicles.* Biochemistry, 1980. **19**(1): p. 108-116

91 M. A. Roseman and T. E. Thompson, *Mechanism of the spontaneous transfer of phospholipids between bilayers.* Biochemistry, 1980. **19**(3): p. 439-444

92 R. Pichot, F. Spyropoulos and I. T. Norton, *Mixed-emulsifier stabilised emulsions: Investigation of the effect of monoolein and hydrophilic silica particle mixtures on the stability against coalescence.* J Colloid Interface Sci, 2009. **329**(2): p. 284-291

93 H. Chung, T. W. Kim, I. C. Kwon and S. Y. Jeong, *Stability of the oil-in-water type triacylglycerol emulsions.* Biotechnol Bioprocess Eng, 2001. **6**(4): p. 284-288

94 P. Kan, Z. B. Chen, R. Y. Kung, C. J. Lee and I. M. Chu, *Study on the formulation of o/w emulsion as carriers for lipophilic drugs.* Colloid Surface B, 1999. **15**(2): p. 117-125

95 A. Ribier and B. Biatry, *Oily phase in an aqueous phase dispersion stabilized by cubic gel particles and method of making*. Eur Pat Appl, 2001. (L'Oreal, Fr)

96 N. K. Childers, S. M. Michalek, J. H. Eldridge, F. R. Denys, A. K. Berry and J. R. McGhee, *Characterization of liposome suspensions by flow cytometry.* J Immunol Methods, 1989. **119**(1): p. 135-143

97 M. Hai and S. Magdassi, *Investigation on the release of fluorescent markers from w/o/w emulsions by fluorescence-activated cell sorter.* J Control Release, 2004. **96**(3): p. 393-402

98 K. Vorauer-Uhl, A. Wagner, N. Borth and H. Katinger, *Determination of liposome size distribution by flow cytometry.* Cytometry, 2000. **39**(2): p. 166-171

99 Y. N. Konan, R. Gurny and E. Allemann, *State of the art in the delivery of photosensitizers for photodynamic therapy.* J Photochem Photobiol B, 2002. **66**(2): p. 89-106

A.1 Calibration curves of the different drug models in the different solvents

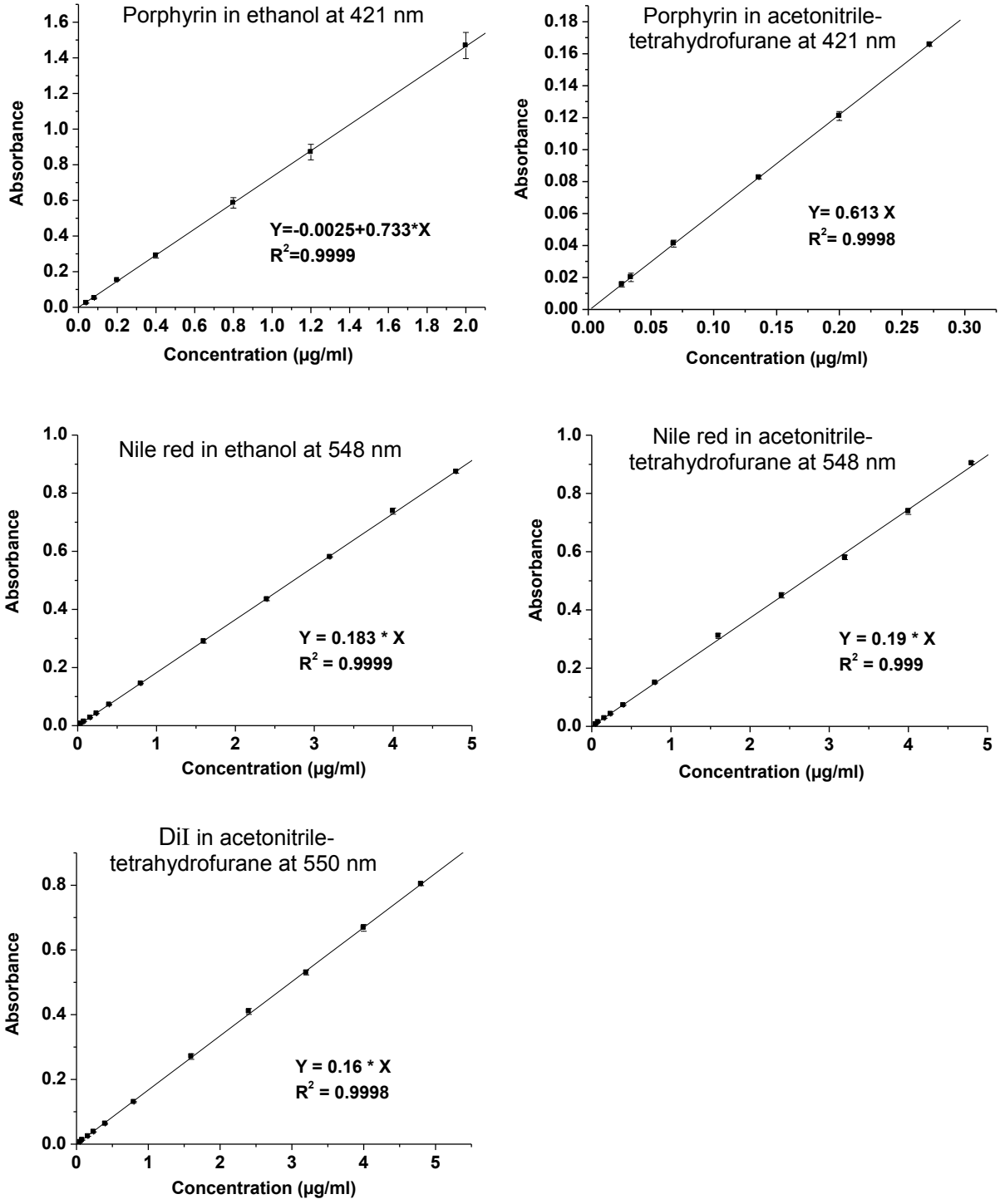

Figure A.1: Calibration curves of the different drug models in the different solvents

A.2 Calibration curves of the different drug models using flow cytometer

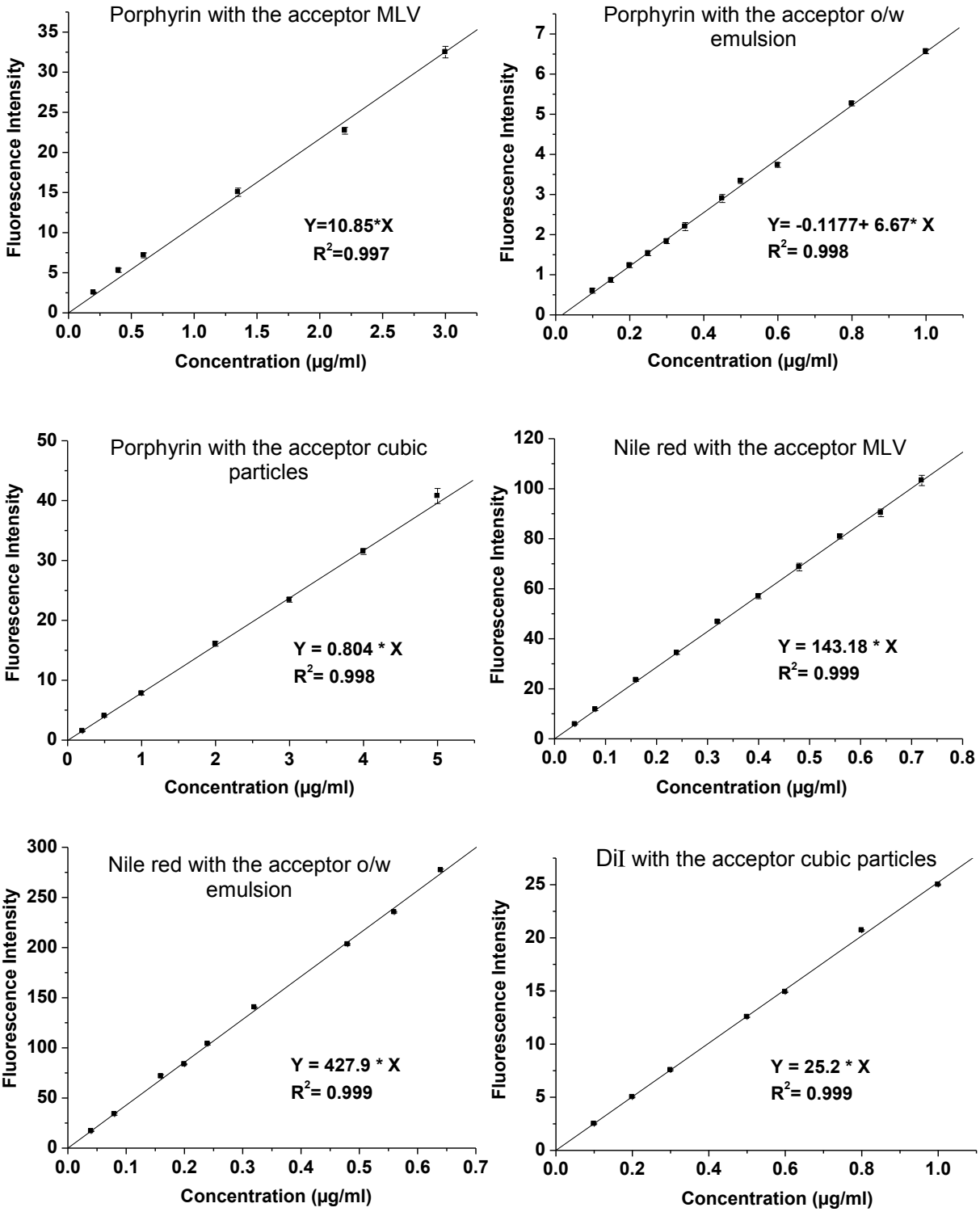

Figure A.2: Calibration curves of the different drug models using flow cytometer

Lebenslauf

Name: Dawou, Mohamed

Geburtsdatum: 18.2.1976

Geburtsort: Kairo, Ägypten

Familienstand: verheiratet

Ausbildung

9.1983-6.1987	Grundschule Abdel Aziz Gawish , Nasr city, Kairo, Ägypten
9.1986-6.1994	Nasr city Gymnasium, Kairo, Ägypten
Abschluss	Ägyptische Abschlussprufung (Thanaweya Ama, Durchschnitt 90%)
9.1994-6.1999	Pharmaceutische Fakultät, Helwan Universität, Kairo, Ägypten
Abschluss	Bachelor
1.2000-12.2001	Diplomarbeit an der Abteilung fur Pharmaceutische Technologie pharmazeutischen Fakultät Helwan, Ägypten
1.2002-12.2004	Magisterarbeit in Pharmaceutischer Technologie an der Abteilung pharmazeutische Fakultät, Helwan, Ägypten

Beruf

1.2000-10.2006	Assistententatigkeit an der Abteilung fur Pharmazeutische Technologie der Pharmazeutischen Fakultät, Helwan Universität, Ägypten
seit 11.2006	Doktorarbeit am Institut fur Pharmazeutische Technologie der, Biologisch-Pharmazeutischen Fakultät, Friedrich Schiller Universität Jena

Publications

M. Dawoud, A. Fahr, H. Bunjes, Liquid crystalline cubic particles as a new lipophilic acceptor compartment to investigate drug transfer from lipid particles, (in preparation).

M. Dawoud, A. Fahr, H. Bunjes, Comparison of drug transfer from lipid nanoparticles to lipophilic acceptor compartments using centrifugation and flow cytometric techniques, (in preparation).

M. Dawoud, A. Fahr, H. Bunjes, Investigation on the transfer of lipophilic model drugs from lipid nanoparticles to lipophilic acceptor compartments, (in preparation).

Presentation

M. Dawoud, A. Fahr, H. Bunjes, Transfer of a lipophilic drug model from lipid nanoparticles to liposomes studied with two different methods, Controlled Release Society German Chapter Annual Meeting, Halle (Saale) 2009.

Posters

M. Dawoud, A. Fahr, J. Kuntsche, H. Bunjes, Investigations on the transfer of porphyrin from o/w emulsion droplets to liposomes with two different methods, Controlled Release Society German Chapter Annual Meeting, Braunschweig 2008.

M. Dawoud, A. Fahr, H. Bunjes, Comparison of drug transfer from lipid nanoparticles into different types of acceptor particles, Jahrestagung der Deutschen Pharmazeutischen Gesellschaft (DPhG), Jena 2009.

Selbstständigkeitserklärung

Hiermit erkläre ich, die eingereichte Arbeit selbstständig angefertigt und keine anderen Hilfsmittel und Quellen als die angegebenen benutzt zu haben.
Diese Arbeit ist weder identisch noch teilidentisch mit einer Arbeit, welche an der Friedrich-Schiller-Universität Jena oder einer anderen Hochschule zur Erlangung eines akademischen Grades oder als Prüfungsleistung vorgelegt worden ist.
Die Promotionsordnung der Biologisch-Pharmazeutischen Fakultät der Friedrich-Schiller-Universität Jena ist mir bekannt.

Mohamed Dawoud

Jena, den 11.10.2010